AD-A243 426

ESL-TR-89-12

VAPOR-PHASE CATALYTIC OXIDATION OF MIXED VOLATILE ORGANIC COMPOUNDS

DR H.L. GREENE

UNIVERSITY OF AKRON
CHEMICAL ENGINEERING DEPARTMENT
AKRON OH 44325

SEPTEMBER 1989

FINAL REPORT

SEPTEMBER 1985 — SEPTEMBER 1988

AIR FORCE ENGINEERING & SERVICES CENTER
ENGINEERING & SERVICES LABORATORY
TYNDALL AIR FORCE BASE, FLORIDA 32403

NOTICE

PLEASE DO NOT REQUEST COPIES OF THIS REPORT FROM HQ AFESC/RD (ENGINEERING AND SERVICES LABORATORY). ADDITIONAL COPIES MAY BE PURCHASED FROM:

NATIONAL TECHNICAL INFORMATION SERVICE
5285 PORT ROYAL ROAD
SPRINGFIELD, VIRGINIA 22161

FEDERAL GOVERNMENT AGENCIES AND THEIR CONTRACTORS REGISTERED WITH DEFENSE TECHNICAL INFORMATION CENTER SHOULD DIRECT REQUESTS FOR COPIES OF THIS REPORT TO:

DEFENSE TECHNICAL INFORMATION CENTER
CAMERON STATION
ALEXANDRIA, VIRGINIA 22314

UNCLASSIFIED
SECURITY CLASSIFICATION OF THIS PAGE

REPORT DOCUMENTATION PAGE

Form Approved OMB No. 0704-0188

1a. REPORT SECURITY CLASSIFICATION: UNCLASSIFIED	1b. RESTRICTIVE MARKINGS: N/A
2a. SECURITY CLASSIFICATION AUTHORITY: N/A	3. DISTRIBUTION/AVAILABILITY OF REPORT: Approved for Public Release Distribution Unlimited
2b. DECLASSIFICATION/DOWNGRADING SCHEDULE: N/A	
4. PERFORMING ORGANIZATION REPORT NUMBER(S):	5. MONITORING ORGANIZATION REPORT NUMBER(S): ESL-TR-89-12
6a. NAME OF PERFORMING ORGANIZATION: University of Akron; 6b. OFFICE SYMBOL (If applicable):	7a. NAME OF MONITORING ORGANIZATION: Air Force Engineering & Services Center
6c. ADDRESS (City, State, and ZIP Code): Chemical Engineering Department, Akron OH 44325	7b. ADDRESS (City, State, and ZIP Code): HQ AFESC/RDVW, Tyndall AFB FL 32403-6001
8a. NAME OF FUNDING/SPONSORING ORGANIZATION: See Block 16; 8b. OFFICE SYMBOL (If applicable): RDVW	9. PROCUREMENT INSTRUMENT IDENTIFICATION NUMBER: USAF MIPR NO. FY8952-85-10013
8c. ADDRESS (City, State, and ZIP Code): US EPA AEERL, Air Toxics Branch, MD-61, Research Triangle Park NC 27711	10. SOURCE OF FUNDING NUMBERS: PROGRAM ELEMENT NO. 62601F; PROJECT NO. 1900; TASK NO 70; WORK UNIT ACCESSION NO. 32
11. TITLE (Include Security Classification): Vapor-Phase Catalytic Oxidation of Mixed Volatile Organic Compounds (U)	
12. PERSONAL AUTHOR(S): Howard L. Greene, PhD	
13a. TYPE OF REPORT: Final; 13b. TIME COVERED: FROM Sep 85 TO Sep 88; 14. DATE OF REPORT (Year, Month, Day): September 1989; 15. PAGE COUNT	
16. SUPPLEMENTARY NOTATION: US Environmental Protection Agency Air Energy and Engineering Research Laboratory (US EPA AEERL) and block 7a co-funded this project. Availability of this report is specified on reverse of the front cover.	

17. COSATI CODES			18. SUBJECT TERMS (Continue on reverse if necessary and identify by block number)
FIELD	GROUP	SUB-GROUP	
07	01		Catalytic Oxidation; Chlorinated VOCs; Transition Metal Oxide Catalyst
07	04		

19. ABSTRACT (Continue on reverse if necessary and identify by block number)

An initial 3 year study was undertaken to develop efficient low-temperature catalysts for selective oxidation of chlorinated VOCs (chiefly methylene chloride and trichloroethylene) to benign products. An organized screening process for choosing and evaluation catalyst candidates (catalyst development methodology) was formulated. Principal catalyst selection criteria were: activity, selectivity, and stability. Thermodynamic limitations on chlorinated VOC destruction were checked at reaction temperatures (~ 500°C), and found to favor products consisting of CO_2, HCl, Cl_2, and H_2O, with negligible chlorinated hydrocarbons remaining. Nine catalyst systems, containing one or more supported transition metal oxides (three primary, six secondary), were formulated and tested using this methodology with a monolithic reactor system. Analytical techniques for reactant and product stream determinations (largely carried out by gas chromatography/mass spectrometry methods) showed improvement during the study with reactor mole balances on chlorine and carbon rising from ~65 percent in early runs to ~90+ percent in more recent experiments.

(continued on reverse side)

20. DISTRIBUTION/AVAILABILITY OF ABSTRACT: ☒ UNCLASSIFIED/UNLIMITED ☐ SAME AS RPT. ☐ DTIC USERS	21. ABSTRACT SECURITY CLASSIFICATION: UNCLASSIFIED
22a. NAME OF RESPONSIBLE INDIVIDUAL: EDWARD G. MARCHAND, 1Lt, USAF, BSC	22b. TELEPHONE (Include Area Code): (904) 283-2942; 22c. OFFICE SYMBOL: HQ AFESC/RDVW

DD Form 1473, JUN 86 — Previous editions are obsolete.

19. Abstract (continued).

Thermal stability studies at 500°C in an HCl-air environment using a KCl/CuO catalyst demonstrated 50± fold improvements in catalyst lifetime by formation of a mixed melt catalyst on the support surface. This technology was subsequently used to develop a new supported liquid phase (SLP) catalyst (KCl/V_2O_5). For the catalyst systems studied, it was found that activity and selectivity correlate with catalyst composition at reaction conditions. Thus, transition metal catalysts remaining in the oxide form catalyze largely towards deep oxidation products by an electrophilic mechanism. Transition metal catalysts which tend to form chloride salts (often volatile) usually facilitate unwanted oxychlorination reactions by a nucleophilic mechanism. Based on stated criteria, the three primary catalysts can be ranked as follows:

Activity:	$Cr_2O_3 > KCl/V_2O_5 > KCl/CuO$
Selectivity:	$Cr_2O_3 > KCl/V_2O_5 > KCl/CuO$
Stability:	$KCl/V_2O_5 > Cr_2O_3 > KCl/CuO$

Chlorinated VOC conversions of 95+ percent should be possible in commercial reactors suing either the Cr_2O_3 or KCl/V_2O_5 catalysts. However, with the strong catalyst development program now in place, further improvements in VOC catalyst development can be expected.

EXECUTIVE SUMMARY

Groundwater contamination caused by past spillage of organic solvents, fuels, and degreasers (many of which are highly chlorinated) is of concern at a number of Air Force sites. Technology has previously been developed to air-strip these contaminants from aquifers via pump-and-treat methods, but effective methods for treatment of the resulting humid air streams, which contain mixed volatile organic compounds (VOCs) in low concentrations, has not yet been reduced to practice.

A rapid low temperature process for destruction of chlorinated VOCs would be highly desirable because it would significantly reduce energy costs and nitrous oxides (NOx) formation rates from those experienced with high temperature thermal incineration methods.

The objectives of this reserarch are to develop and test viable low temperature catalytic systems constructed from monolithic type ceramic supports which have been impregnated with one or more catalytic agents. Monolithic type supports have been chosen for all test catalytic systems because they offer minimal flow resistance (pressure drop), are widely available, and are passive (stationary) during operation. Catalytic agents are chosen primarily from the transition metal oxides (TMOs) based on their potential for selectively oxidizing chlorinated VOCs commonly found in the contaminated groundwater, and to form benign products at temperatures of 500 ^{o}C or less. Other criteria are the potential for catalyst activity above 95 percent and the resistance to thermal or chemical deactivation for at least 6-12 months at reaction conditions.

This report presents results from a thermodynamic study (Section II) which is designed to determine preferred oxidation products of chlorinated VOCs at temperatures near 500 ^{o}C. It is found that the ultimate selectivity (at equilibrium) favors formation of the desired deep oxidation products, including carbon dioxide (CO_2), water (H_2O), hydrochloric acid (HCl), and chlorine (Cl_2). Formation of higher chlorinated compounds, as well as NOx, is not favored in this temperature range.

This report also documents completed research on nine catalyst systems (three primary, six secondary) to determine their ability for conversion of typical VOCs (usually methylene chloride (CH_2Cl_3)) to more benign products, which include CO_2, H_2O, and HCl. The most common mode of failure for the catalysts selected is found to be conversion of the TMO to the corresponding transition metal chloride (TMCl) at reaction conditions. Most TMCls are subsequently volatilized and lost from the support surface or, if they remain, tend to catalyze unwanted oxychlorination reactions which form higher chlorinated products such as carbon tetrachloride (CCl_4) and perchloroethylene (C_2Cl_4).

Three types of primary catalyst systems (KCl/CuO, KCl/V_2O_5, Cr_2O_3) are studied in detail by evaluating their potential activity, selectivity, and stability at 500 ^{o}C. The KCl/CuO catalyst is chosen because of its reported resistance to volatilization in the chloride form, accomplished by forming a

low volatility melt on the support surface. The process of forming a supported liquid phase (SLP) catalyst is often quite effective in improving stability, but this particular catalyst has poor selectivity, yielding substantial oxychlorination products. Details are given in Sections III and IV.

A new SLP catalyst (KCl/V_2O_5) has been developed (and an invention disclosure duly filed) which shows excellent stability and much improved selectivity toward deep oxidation products (CO_2, HCl, H_2O) over the previous KCl/CuO system. Evaluation of this catalyst is discussed in Section V.

As described in Section IV, a Cr_2O_3 catalyst system, previously known for its deep oxidation ability, was also formulated and evaluated. It appears to be the most active of the three, and its selectivity to deep oxidation products is acceptable. Unfortunately, it shows a tendency to form chlorine (Cl_2) over HCl and its stability at reactor conditions is somewhat poorer than KCl/V_2O_5.

In conclusion, it is apparent that no single catalyst studied to date meets all criteria for decomposition of chlorinated VOCs. However, a strong foundation is laid for the systematic development and testing of new catalyst candidates as outlined in the Introduction (Section I). This foundation is expected to yield further improvements in chlorinated VOC catalyst technology in the near future.

PREFACE

This report presents and discusses research performed under US EPA Cooperative Agreement CR-812449, by designated faculty and graduate students from the Department of Chemical Engineering at the University, Akron OH 44325. This report summarizes work done between September 1985 and September 1988. HQ AFESC/RDVW project officer was Capt Richard A. Ashworth.

This report summarizes collective efforts of several individuals in addition to the authors, each of whom contributed in terms of experimentation, data analysis, and analytical methodology. This recognition is extended to R. Danals, A. Saraf, and S. Vimawala, who were graduate students at the University of Akron during the tenure of the investigation. Both Norton Company and Corning Glass Works donated refractory supports used in the study.

Mention of trademarks and trade names of material and equipment does not constitute endorsement or recommendation for use by the Air Force, nor can the report be used for advertising the product.

This report has been reviewed by the Public Affairs Office (PA) and is releasable to the National Technical Information Service (NTIS). At NTIS, it will be available to the general public, including foreign nationals.

This technical report has been reviewed and is approved for publication.

Edward J Marchand for

RICHARD A. ASHWORTH, Capt, USAF, BSC
Project Officer

F. THOMAS LUBOZYNSKI, Maj, USAF, BSC
Chief, Environics Division

Douglas C Downey

DOUGLAS C. DOWNEY, GS-13
Chief, Environmental Engineering
Branch

James R. VanOrman

JAMES R. VAN ORMAN
Deputy Director
Engineering and Services Laboratory

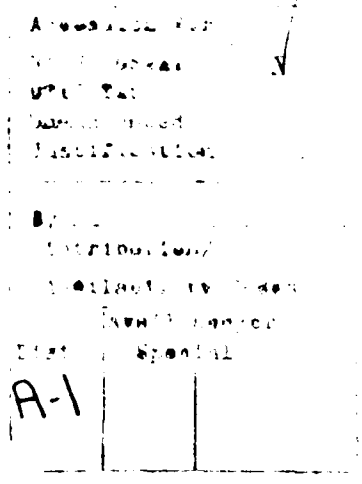

(The reverse of this page is blank.)

TABLE OF CONTENTS

TABLE OF CONTENTS
(Concluded)

LIST OF FIGURES

LIST OF FIGURES
(Continued)

LIST OF FIGURES
(Continued)

LIST OF FIGURES
(Continued)

LIST OF FIGURES
(Concluded)

LIST OF TABLES

SECTION I

INTRODUCTION

A. OBJECTIVES

The primary objective of this research was to develop catalyst/support systems capable of deep oxidation of low molecular weight chlorinated hydrocarbons at moderate temperature.

Three criteria have been established to determine the potential for any catalyst candidate: activity (are conversion levels sufficiently high?), selectivity (are products of low toxicity predominantly formed?) and stability (is catalyst lifetime sufficiently long under reaction conditions?).

Three secondary objectives are also required: (1) evaluate state of the art in catalytic dehalogenation processes; (2) develop an understanding of the primary catalytic dechlorination mechanisms; (3) assemble necessary analytical equipment and methods to obtain reliable experimental data.

B. BACKGROUND

Highly stable chlorinated hydrocarbons which have found widespread use in numerous industrial processes pose a significant environmental threat because of their carcinogenic and other toxicological properties. The deep oxidation of these fugitive compounds (to form benign products) as a means of abating pollution hazards has been of interest for some time.

Of primary interest is the problem of groundwater contamination from spillage of fuels, solvents, paint strippers, and degreasers, many of which are chlorinated. Air stripping of these pollutants from groundwater can effectively remove them from the liquid phase, but additional treatment is required to break down these largely stable compounds before their discharge to the environment.

High-temperature thermal incineration (1000–1500°C), the most widely studied method for the destruction of chlorinated hydrocarbons, has a major disadvantage of being highly expensive and energy intensive. Formation of oxides of nitrogen (NO_x) is also favored at these high temperatures. Low-temperature catalytic combustion (400–600°C) appears to be a more efficient and selective method for the destruction of these organic contaminants, potentially at a lower cost.

C. SCOPE

1. Catalyst Development Methodology

Successful catalyst development requires significant theoretical and experimental effort. A comprehensive workplan shown schematically in Figure 1, has been established and is now being utilized for careful and methodical evaluation of each candidate catalyst and support. Many candidate catalysts are discarded early in the evaluation procedure because of unsatisfactory activity, selectivity, or stability as described in later sections.

As shown in Figure 1, catalyst development and testing proceeds in an orderly fashion. Candidate catalysts are initially identified, based on various factors including: heat of oxygen chemisorption, number of unpaired d-electrons, tendency to melt, volatilize, sublime or form chlorides, and knowledge of prior state of the art (both in-house and from the literature). Once identified, the catalyst is formulated and combined with a support, usually by the method of incipient wetness. The monolithic reactor is used for initial evaluation because of simplicity and minimal analytical difficulty when conversions are held to less than 50 percent. Simultaneously, the catalyst is characterized as to surface area and, if the reactor tests are positive, it is checked for resistance to long-term exposure to HCl vapors.

If a catalyst shows promise (high activity, good selectivity, and stability), it is reformulated on the multicell reactor supports by incipient wetness methods and studied under high-conversion conditions. If results continue positive, runs are also made using prototype low-concentration chlorinated VOC feeds (~100 ppm) and analyzed by established trapping techniques. With continued promise, additional data may be warranted: long-term stability, resistance to specific poisons, toxicity of trace products from published data, potential for scale-up to commercial size reactors.

2. Reported Results

Section II of this report covers theoretical calculations of product distribution at conditions of thermodynamic equilibrium for the decomposition of specific chlorinated hydrocarbons. Regardless of the catalyst chosen, equilibrium product compositions represent the best that can be theoretically attained. Fortunately, all thermodynamic results to date point to a favorable equilibrium product mix composed primarily of CO_2, H_2O, HCl, and Cl_2.

Section II also describes the experimental apparatus and methods used to obtain catalytic oxidation results,

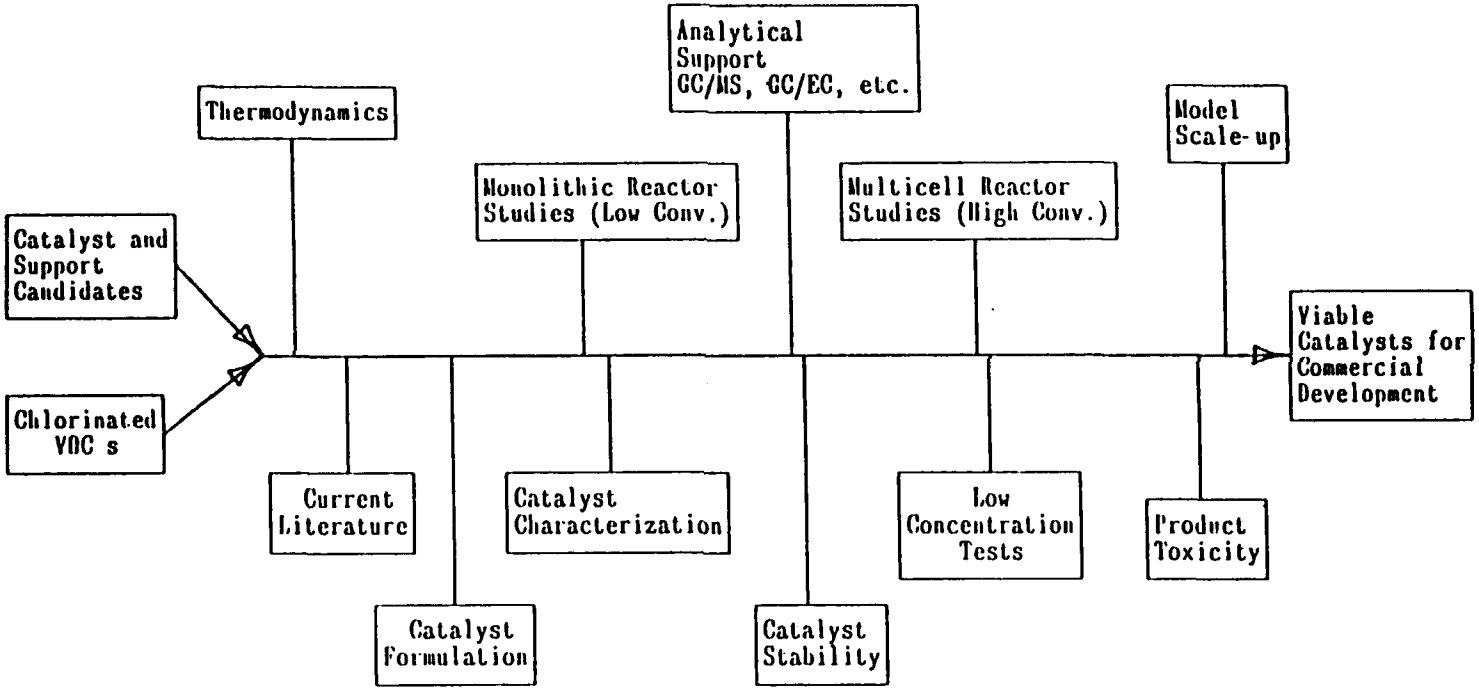

Figure 1. Work Plan for Catalyst Development

including choice and preparation of catalyst, selection of chlorinated VOCs, run procedures, and analytical determination of activity and selectivity.

Section III details the thermal studies of catalyst stability under conditions where HCl concentrations are high, as expected in an actual reactor. The KCl/CuO catalyst is used as a model to which other catalysts are compared.

Sections IV and V cover work completed on the development and testing of the three primary catalyst systems: KCl/CuO, Cr_2O_3, and KCl/V_2O_5, all supported on low surface area (LSA) silica monoliths. Pertinent literature is reviewed as appropriate for comparison. Chlorinated hydrocarbons used include CH_2Cl_2, $CHCl_3$, CCl_4, and C_2HCl_3. Results demonstrate the wide differences in oxychlorination tendency (to form higher chlorinated compounds) versus deep oxidation tendency (to form CO_2, H_2O, HCl, Cl_2) for the catalysts chosen. Ranking the catalysts according to relative activity, selectivity to deep oxidation products, and stability is generally as follows:

Activity:	$Cr_2O_3 > KCl/V_2O_5 > KCl/CuO$
Selectivity:	$Cr_2O_3 \geq KCl/V_2O_5 > KCl/CuO$
Stability:	$KCl/V_2O_5 > Cr_2O_3 > KCl/CuO$

Addition of water vapor and/or H_2S to the catalyst systems can significantly change these results, however.

SECTION II

CATALYTIC OXIDATION METHODOLOGY

A. INTRODUCTION

Open flame thermal incineration of many chlorinated hydrocarbons has been studied (References 1–7) to a considerable extent in the past and a number of reports are available on the subject. Unfortunately, due to the competitive and proprietary nature of the results, open literature on the catalytic oxidation of these compounds is scarce.

Musick, et al. (Reference 8) have investigated the catalytic decomposition of 19 halogenated hydrocarbons, associated with submarine burners, using a hopcalite catalyst. Bond, et al. (Reference 9) have studied the destruction of certain chloromethanes and chloroethenes over Pt/Al_2O_3 catalysts on which propane (used as a hydrocarbon fuel) is oxidized.

Pope, et al. (References 10,11) have evaluated cobalt oxide and platinum–honeycomb catalysts for the elimination of low concentrations of malodorous air pollutants. Johnston (Reference 12) claims to have developed a chromium–impregnated supported catalyst for catalytic oxidation of chlorinated compounds. Unfortunately, selectivity is primarily to Cl_2, not HCl, as desired. Lavanish, et al. (References 13,14) have developed a low temperature method for the catalytic oxidation of C_2–C_4 halogenated hydrocarbons in the presence of hydrated nickel oxide and cobalt oxide catalysts.

Among the recent work, an externally pumped recycle fluid bed catalytic reactor using a commercially available chromia on alumina catalyst has been studied by Manning (Reference 15) for the disposal of chlorocarbons. Weldon, et al. (Reference 16) have studied the kinetics of the oxidation of methylene chloride in air over a commercially available Cr_2O_3/Al_2O_3 catalyst.

The spectrum of products (selectivity) from any practical detoxification process is of paramount importance to a catalyst's overall effectiveness. Despite this significance, reliable data on the identity and concentration of the reaction products after treatment are not commonly reported in the literature. Senser, et al. (Reference 17) indicate that it is the lack of such data that has adversely affected public opinion on the use of incineration for hazardous waste disposal.

The practical importance of the Deacon reaction (oxidation of HCl) for the production of Cl_2 has generated considerable interest (References 18–20) in the study of copper–based catalyst systems.

Aglulin, et al. (Reference 21) and Bakshi, et al. (Reference 22) have studied the kinetics of the oxychlorination of chloromethanes and their destructive oxidation on a supported $CuCl_2$–KCl catalyst. Bakshi, et al. suggest that the oxychlorination reactions occur in two successive steps that proceed almost independently. The two steps, claimed to occur on separate active centers, are oxidation of HCl (Deacon reaction), and the substitutive chlorination of CH_4. The kinetic patterns of side reactions during deep oxidation of CH_4 and chloromethanes were ascertained and the reactivity of chloromethanes toward Cl_2 was found to be in the order CH_3Cl > CH_2Cl_2 > $CHCl_3$ > CCl_4. Muganlinskii, et al. (Reference 23) studied the effect of the nature of the support on rates of chlorination and oxidation in oxychlorination reactions. It was found that carriers (supports) that do not possess the active acidic centers (as on Al_2O_3) responsible for deep oxidation reaction show better results in the oxychlorination process.

This study investigates three primary and six secondary catalyst systems with potential application to catalytic oxidation of chlorinated hydrocarbons. The basic principles and methodology of catalytic oxidation and experimental protocols related to the three primary catalyst systems will be discussed in this section.

B. THERMODYNAMIC CONSIDERATIONS

1. Introduction

The thermodynamic equilibrium compositions for the reactor feeds, at temperatures studied experimentally, were calculated to verify that no undesirable products such as the chlorinated methanes, which contain residual carbon–chlorine bonds, were thermodynamically favored. It was also necessary to verify that there would not be any shift to favor these compounds as water was added to the reactor feed, thus decreasing both the C:H and C:O ratios. Verification of insignificant NO_x formation at reactor temperatures was also of interest. In addition, effects of temperature on the equilibrium composition required quantification. In all cases, results were generally positive under reaction conditions with only small amounts of phosgene and smaller amounts of the chloromethanes present at thermodynamic equilibrium.

2. Methodology

The calculations were performed by minimizing the Gibbs free energy of the system using the method of Lagrange multipliers. The JANAF Thermochemical Tables (Reference 24) were used as the source of thermochemical data. The calculations were programmed on an IBM PC using STSC APL*PLUS. A typical computation took between 2 and 10 minutes on the PC.

Equilibrium will not be obtained experimentally; the computations merely provide an indication of the expected final products. The results were checked against examples found in Smith and Van Ness (Reference 25), with results obtained from the ASPEN process simulation package, and with the results on similar systems published by Senken et al. (Reference 26); the correlation was good.

The object of the computation is to minimize the Gibbs free energy, $\left[G^t\right]_{T,P} = G(n_1, n_2, \ldots, n_N)$, and in so doing find the set of mole numbers, {n}, present at thermodynamic equilibrium for a given temperature and pressure. The procedure is begun by writing the material balance equations for conservation of the elements present.

$$\sum_{i=1}^{N} n_i a_{ik} = A_k \ , \ k=1, \ 2,\ldots,W \qquad [1]$$

Where a_{ik} is the number of atoms of element k in component i and A_k is the number of atoms (in moles) of element k present in the system. Next, a new objective function is defined,

$$F = G^t + \sum_{k=1}^{W} \lambda_k \left[\sum_{i=1}^{N} n_i a_{ik} - A_k\right] \qquad [2]$$

where the $\{\lambda_k\}$ are the Lagrange multipliers. It is apparent that $F = G^t$, but $\frac{\partial F}{\partial n_k} \neq \frac{\partial G^t}{\partial n_k}$. The purpose of defining F is to force not only minimization of G^t, but also satisfaction of the material balance constraints. Clearly, since $F = G^t$, their minima coincide and F can be used as the objective function. The minimization is accomplished in the usual fashion by setting the first derivative of F with respect to the mole numbers equal to zero. After making appropriate thermodynamic substitutions for the chemical potential and setting the fugacity coefficient equal to unity, the following equations result:

$$\Delta G^o_{fi} + RT \cdot \ln(y_i P) + \sum_{k=1}^{W} \lambda_k a_{ik} = 0, \ i=1,2\ldots N \qquad [3]$$

and

$$\sum_{i=1}^{N} n_i a_{ik} - A_k = 0, \quad k=1,2,\ldots,W \qquad [4]$$

which constitutes N+W nonlinear equations in N+W unknowns; the N mole numbers, $\{n\}$, and the W Lagrange multipliers, $\{\lambda_k\}$. Here ΔG^o_{fi} is the standard Gibbs free energy of formation of species i, y_i is the mole fraction of species i, and P is the pressure. For convenience, ΔG^o_{fi} was fit to the following equation.

$$\Delta G^o_{fi}(T) = \sum_{n=-1}^{4} a_{n+1,i} \cdot T^n \qquad [5]$$

This system of equations was solved using a Newton–Raphson procedure with a numerically evaluated Jacobian.

3. Results

For these calculations, a concentration of CH_2Cl_2 of 1 mole percent (or 10,000 ppm) in dry or moist air was used as the "feed". The effect of varying the H_2O:CH_2Cl_2 ratio was examined. Also, the effect of varying the temperature over the range from 100 to 900°C was studied. A large spectrum of possible products was used including: O_2, N_2, H_2O, CO_2, CO, HCl, Cl_2, HOCl, CH_4, CH_3Cl, CH_2Cl_2, $CHCl_3$, CCl_4, $COCl_2$, and NO.

The mole ratio of water to CH_2Cl_2 was varied from zero to 10 in these calculations. The major constituents of the equilibrium mixture, excluding O_2 and N_2, were H_2O, HCl, Cl_2, and HOCl. The variation of these with H_2O:CH_2Cl_2 ratio is depicted in Figure 2. The major effect of increasing H_2O is to increase the proportion of Cl atoms present as HCl compared to Cl_2. The equilibrium shifts from slightly more Cl_2 than HCl at a H_2O:CH_2Cl_2 ratio of zero, to the opposite situation (more HCl than Cl_2) for the rest of the range examined, ending with approximately seven times as much HCl as Cl_2 at H_2O:CH_2Cl_2 ratio of 10:1. Since HCl can probably be removed more efficiently than Cl_2 in a water scrub following the reactor, the presence of water is a positive factor. Also, the amount of HOCl present at equilibrium increases moderately as the H_2O:CH_2Cl_2 ratio increases. The chlorinated carbon–containing species (CH_3Cl, CH_2Cl_2, $CHCl_3$, CCl_4, and $COCl_2$) are present in much lower concentrations at equilibrium. There is, however, some effect on them as the H_2O:CH_2Cl_2 ratio is varied. This is depicted in

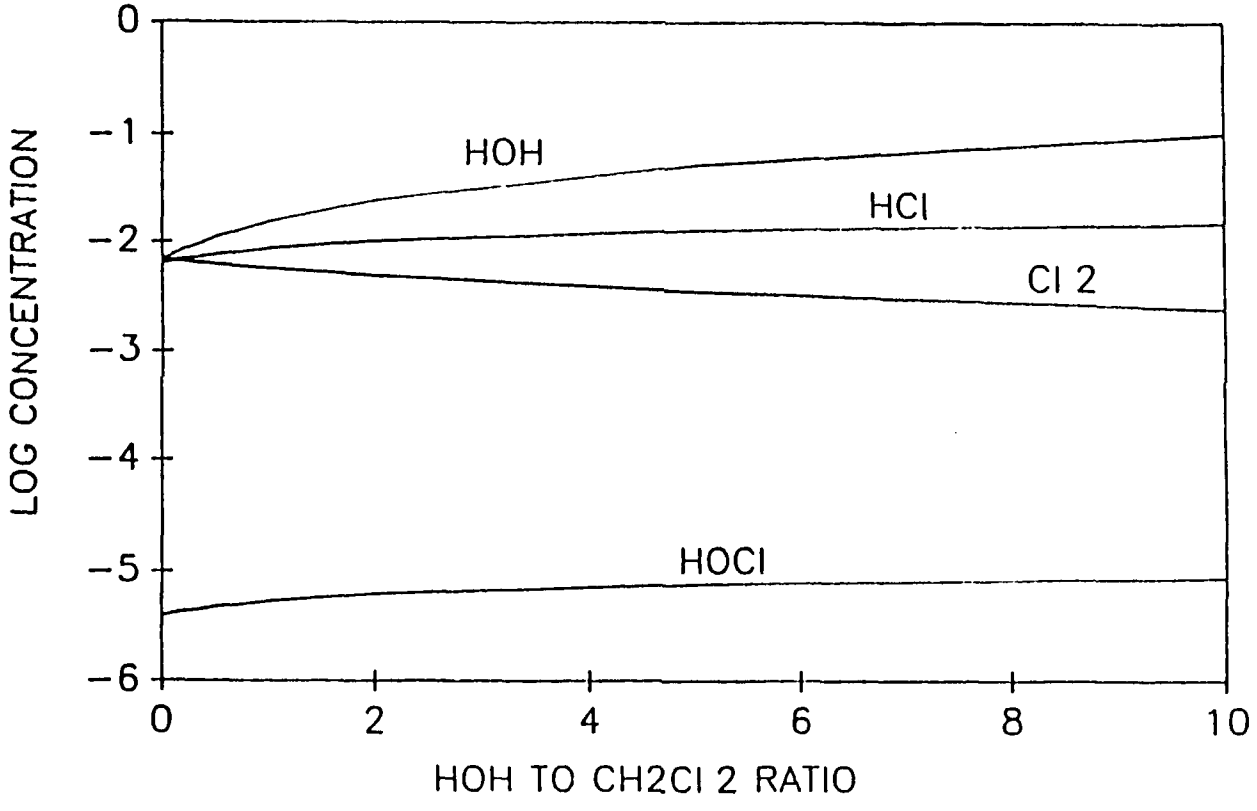

Figure 2. Major Products at 500°C as a Function of HOH to CH_2Cl_2 Ratio

Figure 3 for the $H_2O:CH_2Cl_2$ range from 0:1 to 10:1 and in Figure 4 for the expanded $H_2O:CH_2Cl_2$ range from 0:1 to 2:1. There is initially a fairly sharp change in the concentrations as water is added. The concentration of CH_3Cl drops while the concentration of CH_2Cl_2 is largely unaffected and the concentration of $CHCl_3$, CCl_4, and $COCl_2$ increase. After this initial concentration adjustment, the concentration of each of the species gradually declines as the $H_2O:CH_2Cl_2$ ratio increases beyond 2:1. This may be primarily from the dilution effect of adding water to the system.

The equilibrium temperature for a 1 mole percent CH_2Cl_2 (99 mole percent air) was varied from 100 to 900°C. The behavior of the major products: CO_2, HCl, H_2O and Cl_2 (excluding O_2 and N_2) is depicted in Figure 5. As the temperature increases the amount of HCl present increases while the amount of CO_2 varies only slightly. The behavior of the intermediate concentration products CO, $COCl_2$, NO, and HOCl is depicted in Figure 6. As the temperature increases, the concentrations of all of these components increase, although the concentration never exceeds 10 ppm for any of them. The CO concentration seems to peak at 800°C and declines above that. The behavior of the minor constituents ($CHCl_3$, CH_2Cl_2, CH_3Cl, and CCl_4) is depicted in Figure 7. The concentrations of all of these components rise with temperature over the range examined, but the equilibrium concentrations are very small (below a ppb).

C. EXPERIMENTAL PROTOCOL

1. Catalytic Oxidation Experiments

The experimental setup is shown in Figure 8. The primary part of this apparatus was a vertical Pyrex® tube, 28 millimeter outside diameter and 1 meter in length, which passed through two tube furnaces. The lower furnace served as a preheater; the upper furnace heated the reactor section.

A glass bubbler containing the chlorinated hydrocarbon reactant (usually methylene chloride or trichloroethylene) in the liquid form was connected to the bottom of the reactor setup as shown in Figure 8. The reactant was introduced into the reactor by passing dry grade air (2–10 cc/minute at RTP: 23°C and one atmosphere) through the glass bubbler maintained at 0°C using an ice–water bath. The low–temperature bath was required to achieve low concentrations, particularly for methylene chloride (2000 to 4000 ppm), in the reactor. Dry grade air (400–500 cc/minute at RTP), required for the oxidation process, was introduced through an adjacent port. Gas flow rates were controlled using Porter rotameters and mass flow controllers; furnace temperatures were controlled using Omega temperature indicating controllers. A laboratory–scale vacuum pump

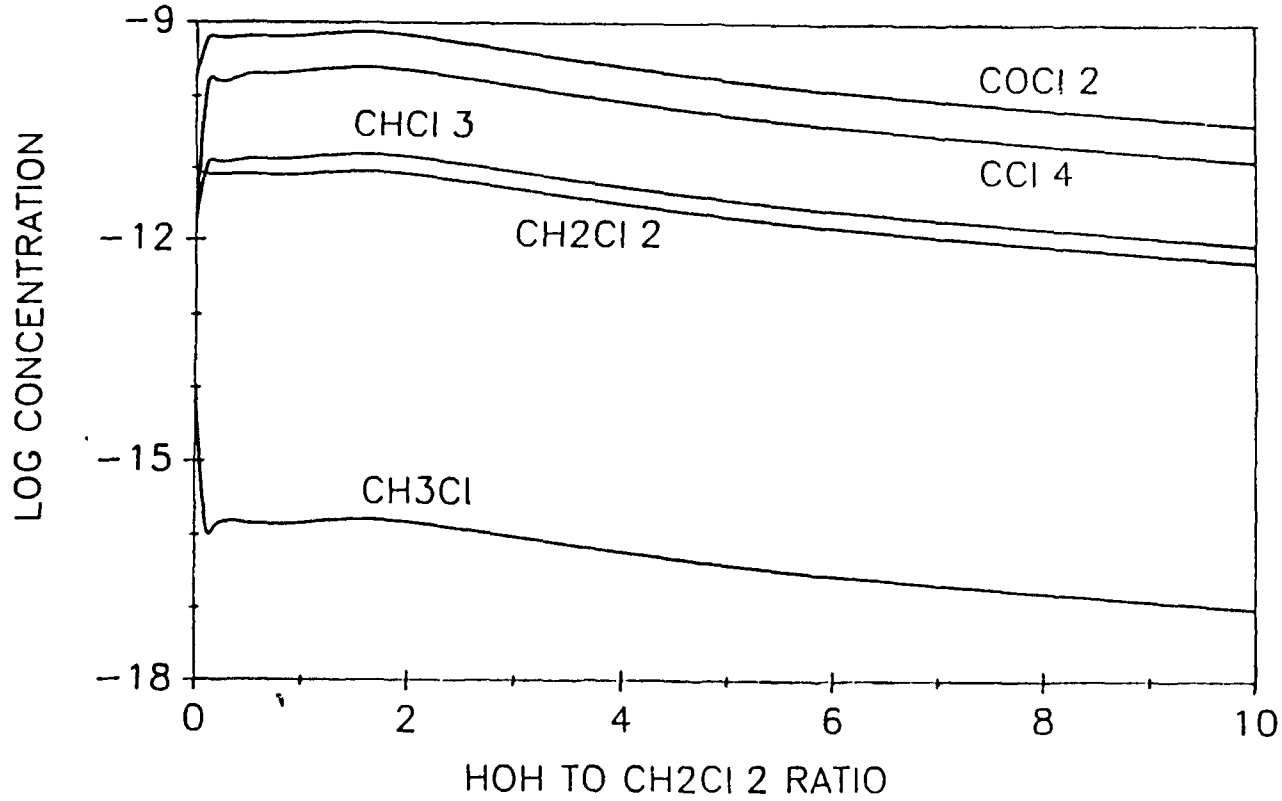

Figure 3. Minor Products at 500°C as a Function of HOH to CH_2Cl_2 Ratio

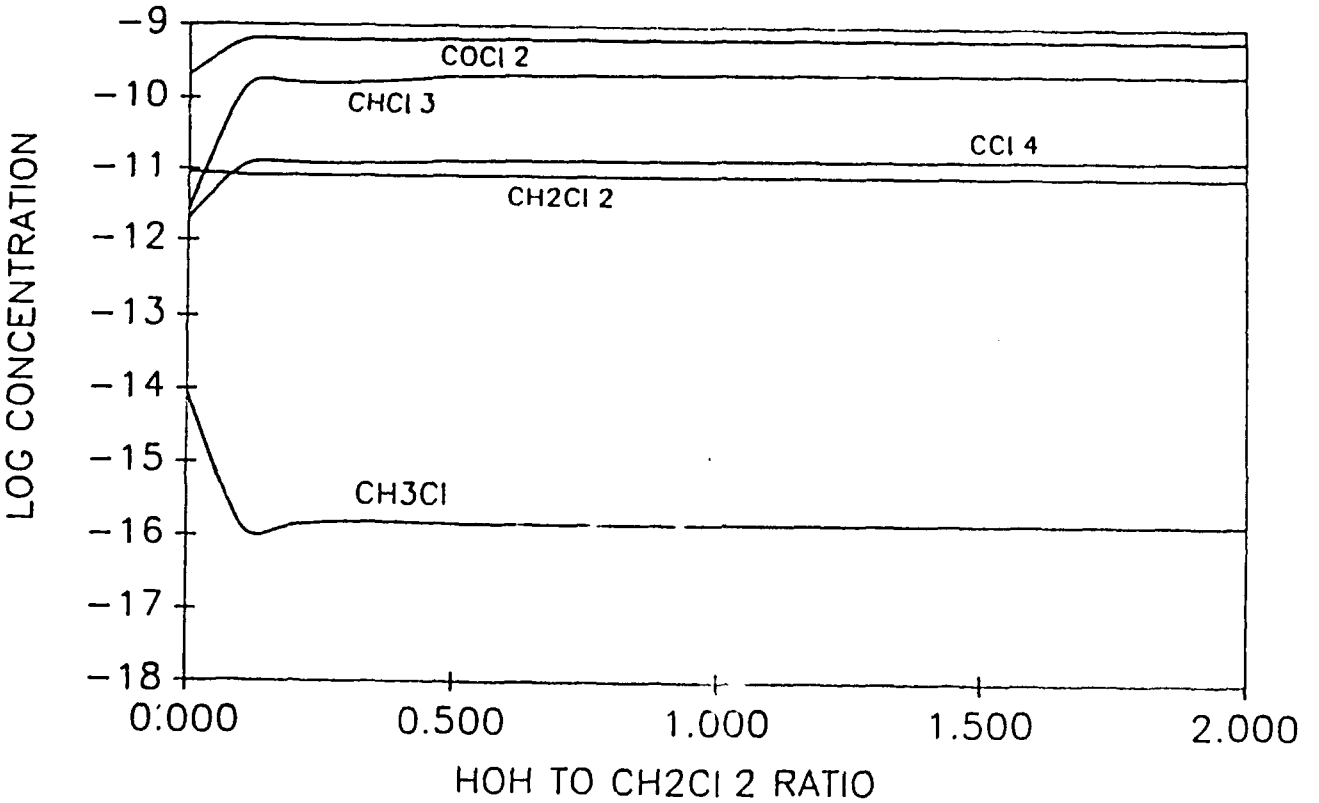

Figure 4. Minor Products, 500°C, Expanded Scale

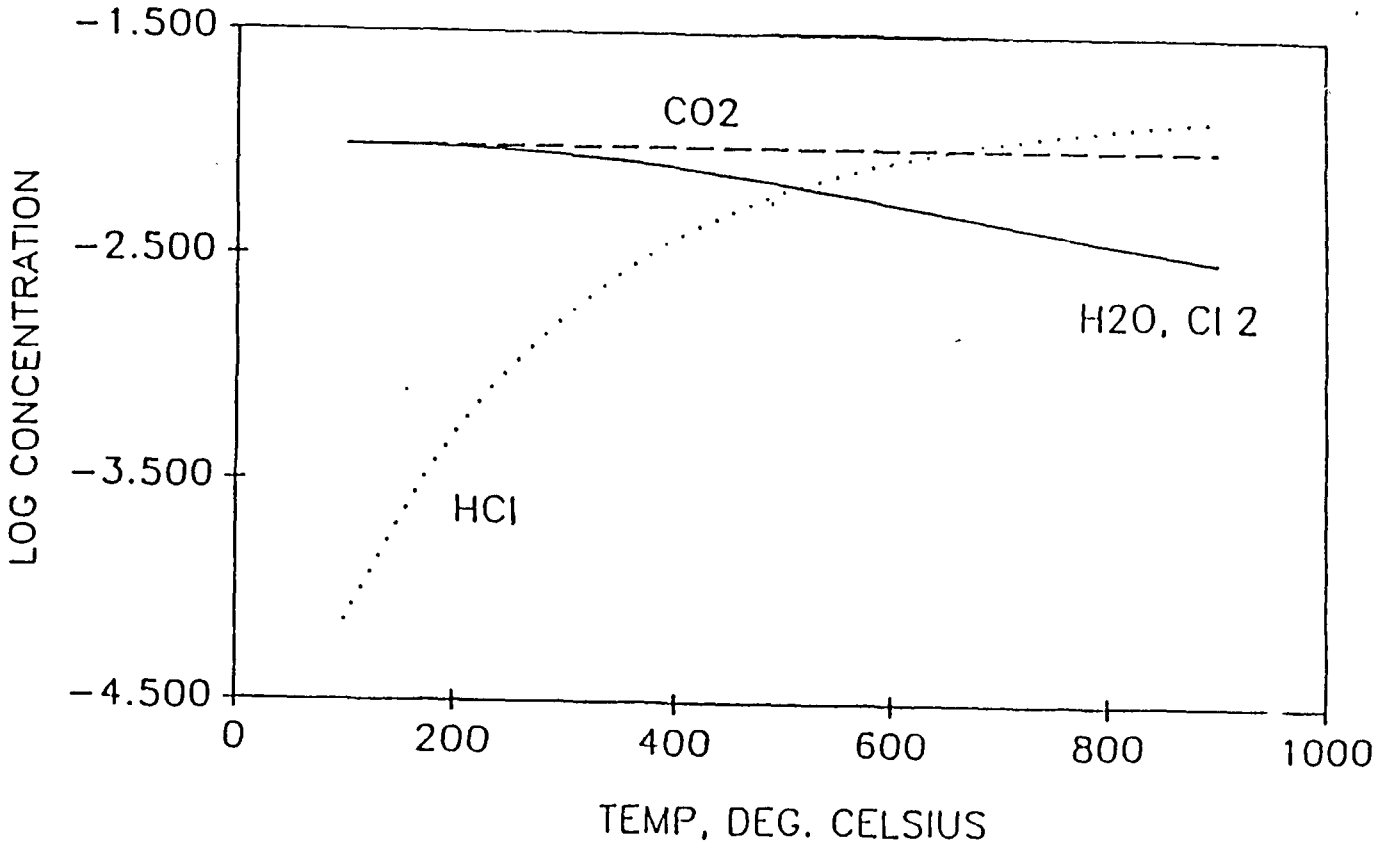

Figure 5. Major Products from 1 Percent CH_2Cl_2 in Air

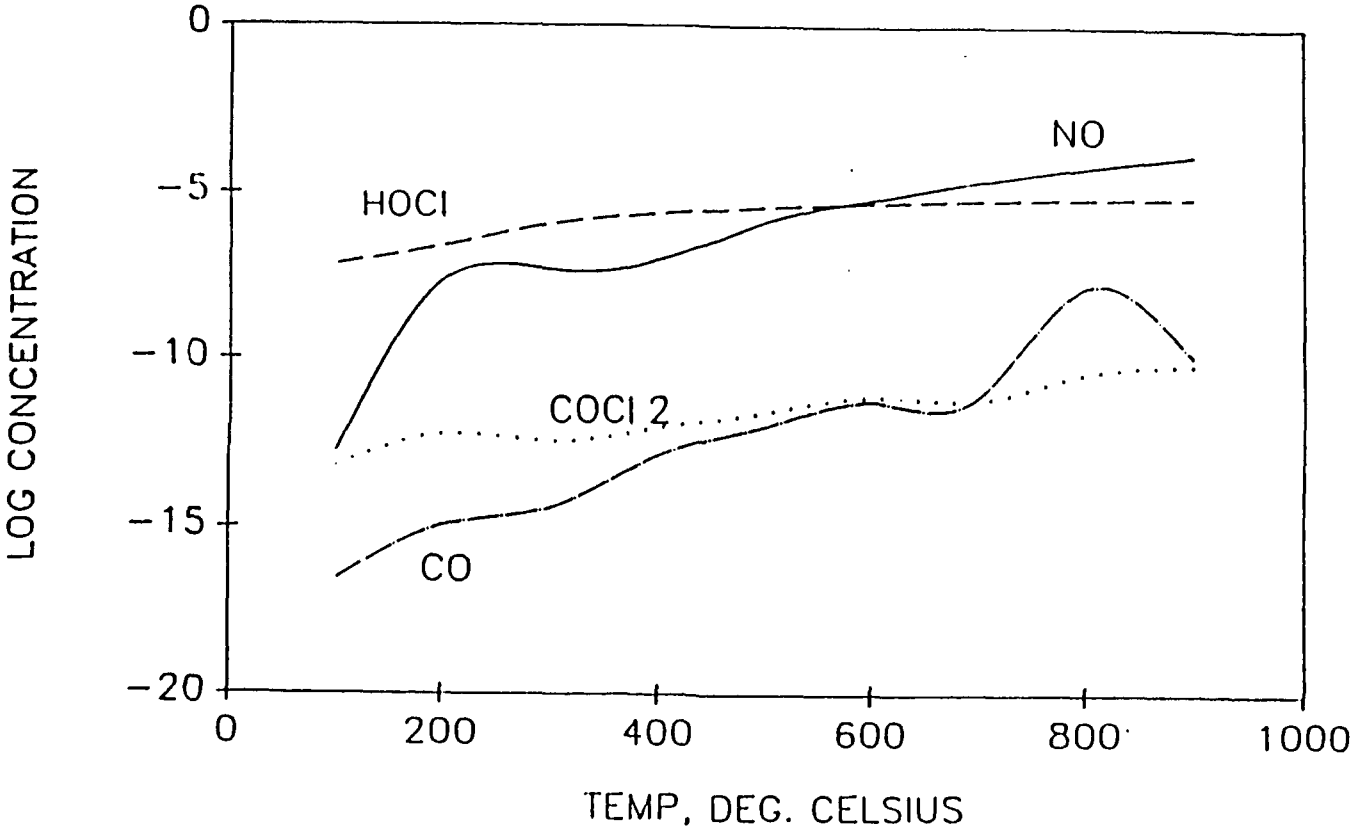

Figure 6. Intermediate Concentration Products from 1 Percent CH_2Cl_2 in Air

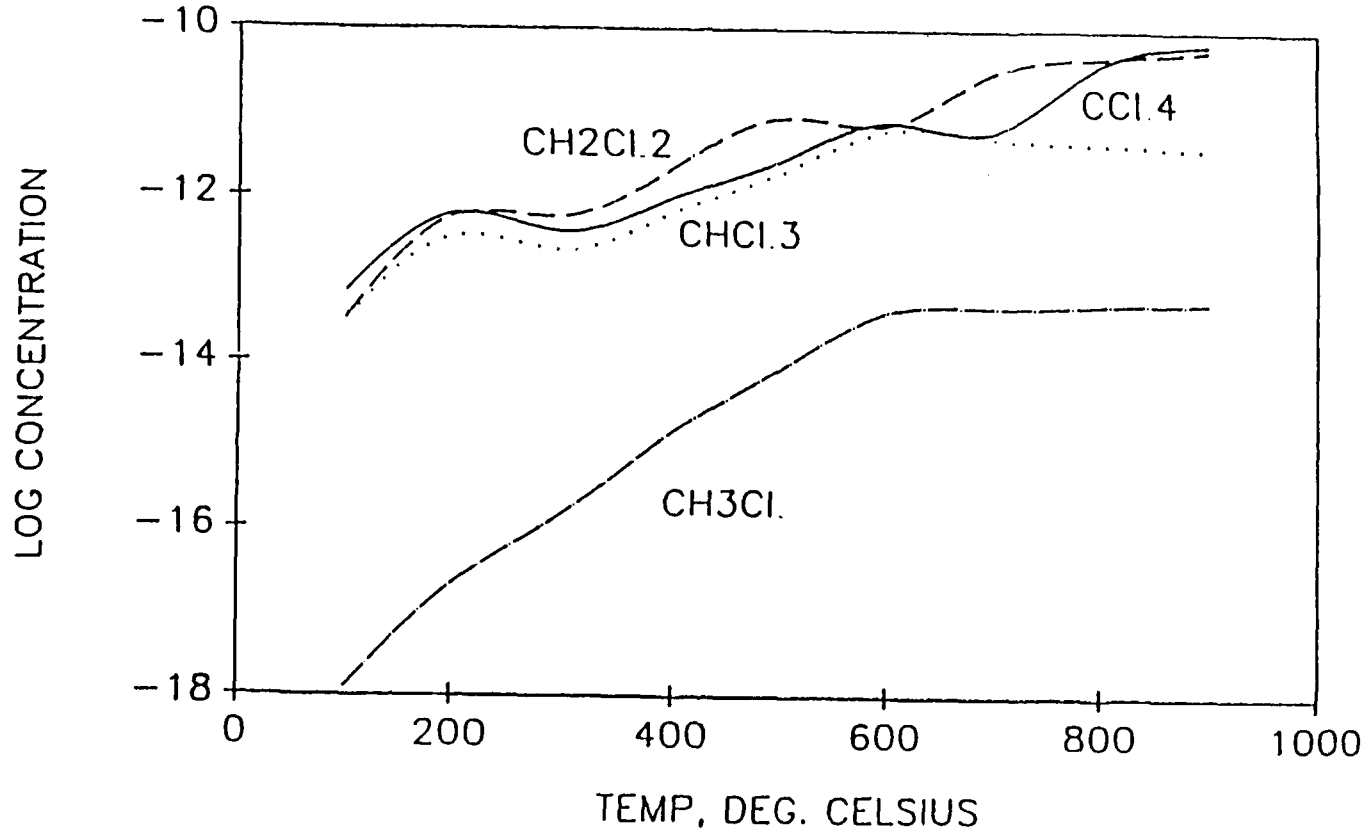

Figure 7. Chloromethane, Products from 1 Percent CH_2Cl_2 in Air

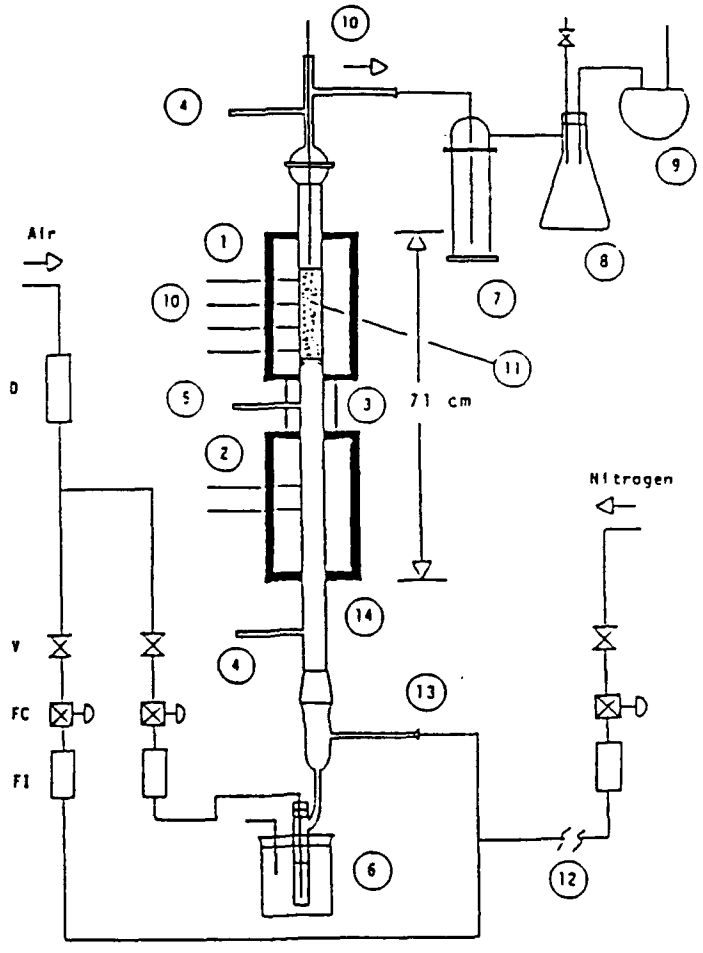

1. Reactor section
2. Preheater section
3. Heat tape and insulation
4. Sample port
5. Manometer tap
6. Chlorinated VOC bubbler
7. HCl trap
8. Surge tank
9. Vacuum pump
10. Thermocouple
11. Supported catalyst
12. Hydrogen source line
13. Main air flow inlet
14. 28 mm Pyrex tube

V: Valve
FC: Flow controller
FI: Flow indicator
D: Drier

Figure 8. Schematic of the Catalytic Oxidation Reactor

(Thomas Industries) was required to pull the gases through the water bubbler and to maintain atmospheric pressure inside the reactor.

2. Analytical Techniques

Vapor samples were obtained using a gas-tight syringe from the gas stream before and after the reactor section and analyzed in the GC/MS (Hewlett-Packard 5890 gas chromatograph with a 25 meter long, 0.2 millimeter in diameter capillary column with a 5 percent crosslimked phenyl methyl silicone coating and HP 5970B mass spectrometer) for carbon dioxide, methylene chloride, chloroform, carbon tetrachloride, trichloroethylene, perchloroethylene and phosgene content.

Chlorine measurements were made using detector tubes (Mine Safety Appliance Co.) for concentrations below 100 ppm. Also, a Varian 3300 gas chromatograph equipped with an electron capture detector and a 1.8 meter long, 3.2 millimeter in diameter column, packed with 10 percent SP-2100 on Supelcoport was used for concentrations above 100 ppm.

Relative standard deviations for GC/MS calibrations were usually less than 5 percent for any point on the calibration curve. However, errors in accuracy arise from the difficulties in measuring the small volumes required (in microliters) for the preparation of calibration standards, adding to the potential error in the accurate measurement of the reactor inlet and outlet content.

Relative standard deviations for GC/MS samples for each measured component in actual runs were usually 1 or 2 percent larger than the relative standard deviation for the calibration because it was a cumulative measure of reactor flow fluctuations as well as sampling errors. Since most of each run's relative standard deviation could be accounted for by the errors in sampling of vapors from the reactor and GC/MS, small reactor flow or conversion fluctuations probably contributed little to the error. Primarily due to these analysis errors, material balances for carbon and chlorine atoms in the range of 85 to 115 percent were considered acceptable.

The effluent gases from the top of the reactor were scrubbed in a water-containing bubbler trap. The HCl gas was removed from the gas stream by absorption and the remainder of the stream was vented. The solution from this trap was titrated for hydrochloric acid using a standard solution of sodium hydroxide and phenolphthalein as the endpoint indicator. Errors in HCl data can be caused by errors in titration of samples (inaccuracies in buret readings or in aliquots of NaOH added to each HCl sample) and time variations in reactor flow rate.

3. Halogenated Organics

Chlorinated hydrocarbons used in this study as a single component and/or as mixtures include CH_2Cl_2, $CHCl_3$, CCl_4, C_2HCl_3, C_2Cl_4.

4. Catalyst Preparation Techniques

The catalysts used in this study were prepared by the incipient wetness technique. For example, with the KCl/CuO catalyst, a saturated solution was prepared with an equimolar amount of copper nitrate and potassium chloride. The solution was injected onto a silica monolith tube. Then it was dried at 200°C for one hour, and calcined for 10 hours at 550°C to decompose the copper nitrate and drive off nitrogen dioxide. The resulting catalyst contained 2.7 percent total weight of copper oxide and potassium chloride in a 1:1 mole ratio.

D. CATALYSTS

Nine catalyst systems were prepared, tested, and evaluated for their activity and selectivity. The activity is defined as the percentage of inlet feed reacted, while selectivity is defined as the moles of the species formed divided by the moles of that species which could have been formed. For example, in the catalytic oxidation of one mole of CH_2Cl_2, the selectivity for HCl would be the moles of HCl actually formed divided by 2 (the moles of HCl that could have been formed if all available chlorine had produced HCl).

1. Hydrated Nickel Oxide

This catalyst was found to be unsuitable for the oxidation of methylene chloride, as conversion was limited to 10 percent at 250°C. Temperatures higher than this tended to dehydrate the catalyst, resulting in a reduction of catalyst activity. Also, required residence times were about 10 seconds, rendering the catalyst uneconomical for this project.

2. Nickel Oxide

Deactivation was found to be a major problem with this catalyst. Initial conversion of about 53 percent for methylene chloride dropped to 17 percent in approximately 8 hours. The catalyst can be easily regenerated, but deactivation occurs within a matter of minutes.

3. Hopcalite

This mineral, containing primarily CuO and MnO_2, was shown effective as a low temperature catalytic agent for systems where trace amounts of chlorinated species are present. With

higher concentration of VOCs at 500°C, the catalyst forms volatile $CuCl_2$ and rapidly deactivates.

4. Potassium Chloride/Copper Oxide

The catalyst literature suggests that addition of KCl to the CuO catalytic agent during initial preparation may cause formation of a mixed melt with resultant lower volatility and hence less tendency for vaporization. An optimum mixture of KCl to CuO is necessary for the catalyst to have reasonable stability and activity. From experiments carried out, the ratio of 1:1 CuO/KCl was found to be acceptable. More details about this catalyst appear in Sections III and IV.

5. Vanadium Pentoxide

Vanadium pentoxide was found to have stability problems during the destruction of methylene chloride. The formation of free chlorine appears to cause chlorination of the vanadium pentoxide, which results in the formation of volatile vanadyl oxytrichloride ($VOCl_3$).

6. Potassium Chloride/Vanadium Pentoxide

This catalyst possesses superior qualities, such as activity, selectivity and stability. More details about this catalyst appear in Section V.

7. Chromium Oxide

This catalyst does not appear to be as stable as the KCl/V_2O_5, but it shows somewhat better activity. More details about this catalyst appear in Section IV.

8. Copper/Palladium

A catalyst formed from CuO/PdO was briefly investigated, but appeared to form volatile metal chloride salts which were subsequently lost from the catalyst surface.

9. Platinum/palladium

This noble metal catalyst (0.08 percent each Pt and Pd) showed good initial activity and selectivity towards breaking the carbon–chlorine bond. However, with time on stream it was deactivated by forming volatile metal chlorides. It also suffers from being very expensive.

E. SUPPORTS

A low surface area support is desired to keep conversions low, thereby providing quantifiable concentrations of the

products of incomplete oxidation. The composition of the silica monolith tube (Norton Co.) and the cordierite multicell (Corning) are shown in Table 1.

TABLE 1. SUPPORT COMPOSITIONS

	Cordierite Multicell	Silica Monolith
Surface area	1.06 m^2/g	0.36 m^2/g
Composition:		
SiO_2	49.2 %	95 %
Al_2O_3	36.0 %	4.1 %
MgO	14.5 %	0.0
	Trace amounts of Fe, Ti, Li, Na, K, Ca oxides	Trace amounts of Mg, Ca, K, Hf oxides
Dimensions	2.5 cm OD 7.6 cm length (each core) 1x1 mm^2 channels 62 ch/cm^2 cross section	1.6 cm OD 0.6 cm ID 22.9 cm length
Configuration	3 cores aligned axially	1 monolith tube

F. EXPRESSION OF RESULTS

Feed ratio is defined as the number of C–Cl bonds in the feed divided by the total number of C–Cl bonds and hydrogen atoms. For example, CH_2Cl_2 alone has a feed ratio of 0.5 since it has two C–Cl bonds as well as two hydrogen atoms. Addition of water to the feed provides more hydrogen atoms, effectively reducing the feed ratio by an amount which depends on the fraction of water in the CH_2Cl_2 feed. Some graphs in the following sections will have a y-axis label such as "percent Cl to $CHCl_3$." This is interpreted as the number of chlorine atoms in $CHCl_3$ formed as a product divided by the total number of chlorine atoms reacted (expressed as a percent). Similarly, "percent C to CO_2" means the number of carbon atoms in CO_2 formed as a product divided by the number of carbon atoms reacted (expressed as a percent). The C–Cl formed/reacted ratio is a measure of total C–Cl bonds formed in products (other than $COCl_2$) divided by the number reacted (expressed as a percent).

The general trends in conversion and product selectivity for the three primary catalysts at different Cl/(Cl+H) atomic ratios in the feed (obtained by varying the moisture content of the air and/or the concentration of the chlorinated hydrocarbon in the feed) are reported and discussed in Sections III, IV and V. Along with the formation of deep oxidation products (CO_2 and HCl) during the reaction of the chlorinated hydrocarbon in dry air, other higher chlorinated products such as $CHCl_3$, CCl_4, and C_2Cl_4 are also produced, probably via oxychlorination reaction pathways.

The importance of catalyst thermal stability and its effect on activity and selectivity are demonstrated for the KCl/CuO primary catalyst system (Section III). The method of stabilization via formation of an SLP catalyst lays a foundation for subsequent development of a new SLP system (KCl/V_2O_5).

SECTION III

THERMAL STABILITY STUDIES

A. INTRODUCTION

Deep oxidation of halogenated hydrocarbons (e.g. C_2HCl_3, CH_2Cl_2) at moderate temperatures (450–500°C) generates considerable amounts of HCl. This highly active compound often reacts with metal oxide catalysts to form corresponding metal chlorides, causing significant changes in catalyst activity, selectivity and stability. Copper oxide was chosen here as a test catalyst in order to document and better understand these changes so that their effects might be minimized during selection of future catalyst candidates. Copper oxide is not a selective catalyst for deep oxidation because it reacts with HCl to produce cupric chloride, which is not stable at the reaction temperatures and sublimes.

$$CH_2Cl_2 + O_2 \longrightarrow CO_2 + 2\ HCl \qquad [R1]$$

$$2\ HCl + CuO \longrightarrow CuCl_2 + H_2O \qquad [R2]$$

$$CuCl_{2\,(s)} \xrightarrow{\Delta} CuCl_{2\,(g)} \qquad [R3]$$

A stabilizing agent such as KCl is required to minimize the loss of cupric chloride. This section will discuss the investigation of the thermal stability of the KCl modified copper oxide catalyst in the presence of gaseous HCl. Activity and selectivity of this catalyst for the deep oxidation of methylene chloride (to produce HCl and CO_2) are also studied because of the potential application to catalyst optimization in the environmental cleanup of chlorinated organic wastes.

B. BACKGROUND

The thermal stability of cupric chloride (Reference 27) improves with addition of chlorides of alkali, alkaline earth, or rare earth metals. By addition of a moderate amount of KCl to the catalyst, a low volatility mixed melt is formed. The addition of KCl up to 10 mole percent (Reference 28,29) improves the activity of the catalyst for the Deacon reaction. Elemental chlorine produced by this mechanism could damage the support or encourage formation of higher chlorinated hydrocarbons.

$$4\ HCl + O_2 \longrightarrow 2\ H_2O + 2\ Cl_2 \qquad [R4]$$

$$CH_2Cl_{2\,(g)} + Cl_{2\,(g)} \longrightarrow CHCl_{3\,(g)} + HCl_{(g)} \qquad [R5]$$

$$CHCl_3(g) + Cl_2(g) \longrightarrow CCl_4(g) + HCl(g) \quad [R6]$$

In the deep catalytic oxidation of chlorinated compounds (of interest in the current study), oxychlorination exists as an undesirable side reaction. According to Muganlinskii et al. (Reference 23), oxychlorination may be considered as a system of two concurrent modes of oxidation (by oxygen and by chlorine).

$$CH_2Cl_2(g) + HCl(g) + 0.5\ O_2(g) \longrightarrow CHCl_3(g) + H_2O(g) \quad [R7]$$

According to Golodets (Reference 27), for oxychlorination reactions involving organic compounds, the activity of the $KCl/CuCl_2$ catalyst increases as the KCl content is increased up to 1 mole of KCl per mole of $CuCl_2$. For ratios of $KCl/CuCl_2$ greater than 1, catalytic activity decreases.

Solomonik et al.(Reference 30,31), reported formation of CuCl as a stable intermediate in the conversion of $CuCl_2$ to CuO at temperatures above 300°C. Hence, it may also be present on the support surface.

The melting points and vapor pressures (Reference 32) of the pure compounds involved in the $KCl/CuCl_2$ system are shown below.

TABLE 2. PROPERTIES OF PURE COMPONENTS

Compound	Melting Point (°C)	Vapor Pressure at 500°C (mm Hg)
CuO	1326	$<1.3 \times 10^{-7}$
KCl	760	3.9×10^{-7}
CuCl	422	0.5
$CuCl_2$	622	294.0

The vapor pressure of $CuCl_2$ at 500°C is substantially higher than that of the other compounds listed in Table 2, suggesting a greater tendency to sublime. Fontana et al.(Reference 33) have reported phase diagrams of the ternary melt system $CuCl-CuCl_2-KCl$ and some kinetic data on the adsorption of oxygen into these melts. According to them, the $KCl/CuCl_2$ complex has a lower melting point than that of $CuCl_2$. This phenomenon, described as the freezing point depression of $CuCl_2$ by KCl, is normally accompanied by a boiling point elevation since both result from the same nonideality (Reference 34). Therefore, the vapor pressure of the complexes at a particular temperature is lower than that of the pure solvent ($CuCl_2$) at the same temperature.

An explanation of the $KCl/CuCl_2$ binary system has been published by Sachtler and Helle (Reference 35). According to them, the $KCl/CuCl_2$ catalyst will exist as a partial melt in equilibrium with one or more coexistent solids in the temperature range of 350 to 500°C. The composition of the melt depends on the temperature as well as the KCl content of the catalyst. Figure 9 shows that, at a temperature of 500°C (the temperature at which the current catalytic oxidation experiments were conducted) the composition and physical state of the catalyst will depend on the mole fraction of KCl in the catalyst. For KCl content in the range 0.25–0.72 mole fraction, the $KCl/CuCl_2$ catalyst exists as a total melt at 500°C. The 1:1 and 2:1 molar ratio (0.5 and 0.67 mole fraction, respectively) $KCl/CuCl_2$ catalysts used in the current study are therefore included in this complete melt region.

C. EXPERIMENTAL METHODS

1. Thermal Stability

The experimental setup, shown schematically in Figure 10, was designed to study the stability of catalyst samples exposed to HCl concentrations between 800 and 300,000 ppm. The experiments were usually run at 500°C on various supports and catalysts, and conducted in a relatively short period of time (100 hours). The catalyst sample to be exposed was placed in the vertical Pyrex® tube passing through the tube furnace. Dry grade air was bubbled into a gas washing bottle containing concentrated HCl solution. The effluent, containing HCl vapors at equilibrium with the HCl solution, was introduced into the HCl exposure apparatus. Therefore, the concentration of the HCl solution was varied as in the literature (Reference 36) to obtain different concentrations of HCl vapors (37 percent by weight HCl solution for a 284,200 ppm vapor, 30 percent for a 20,500 ppm vapor, and 22 percent for an 800 ppm HCl vapor). The method of introducing HCl vapor into the HCl exposure apparatus resulted in the introduction of some water vapor due to the partial pressure exerted by the water in the HCl solution (5,400 ppm H_2O with 284,200 ppm HCl, 10,200 ppm H_2O with 20,500 ppm HCl, and 17,100 ppm with 800 ppm HCl). For applications to deep oxidation processes where H_2O is an expected product, its introduction here was not of concern. HCl concentrations have been rounded off to 300,000; 20,000, and 800 ppm, respectively, in the rest of this text for simplicity.

The concentration of HCl vapors in the HCl exposure apparatus was verified for the intermediate (20,000 ppm HCl) as well as the high (300,000 ppm HCl) concentration vapors by trapping the effluent air–HCl vapor mixture from the gas washing bottle in a NaOH trap for a certain amount of time. The NaOH solution was back-titrated and the computed concentration of HCl

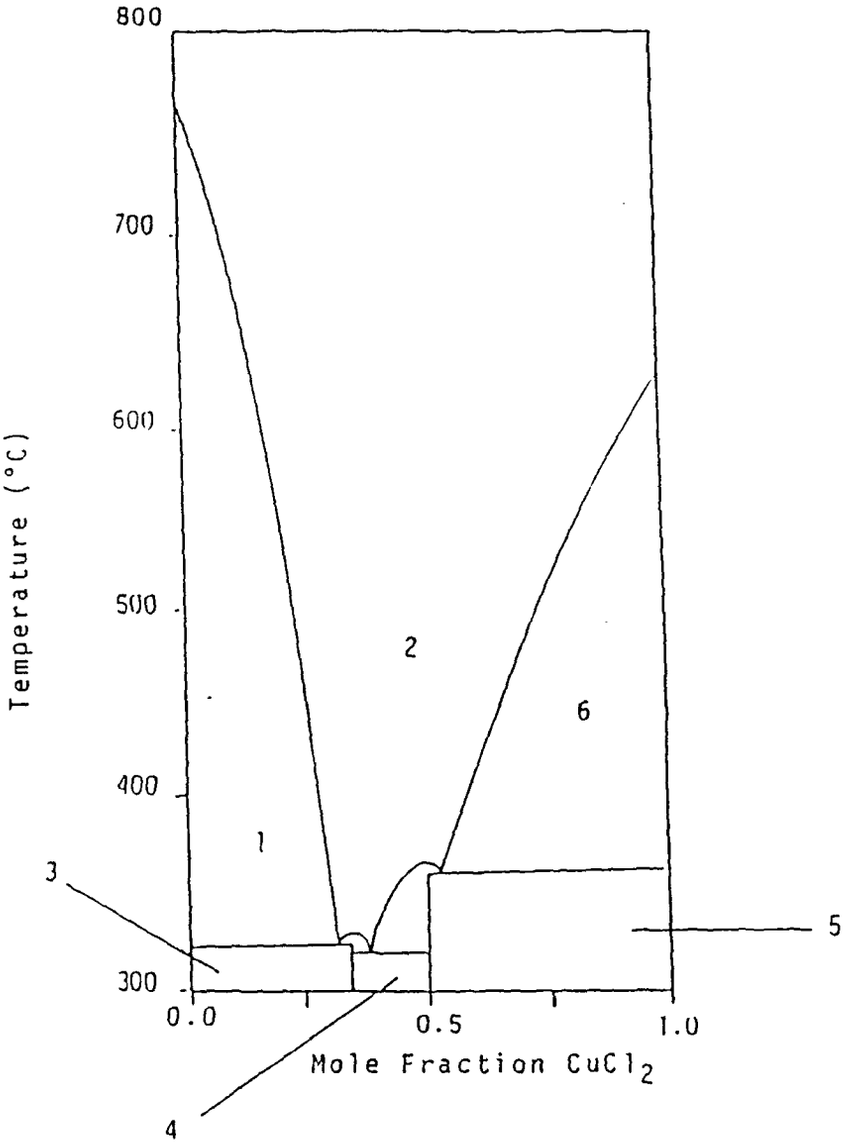

1. Melt + KCl
2. Melt
3. KCl + K_2CuCl_4
4. $KCuCl_3$ + K_2CuCl_4
5. $KCuCl_3$ + $CuCl_2$
6. Melt + $CuCl_2$

Figure 9. The KCl vs. $CuCl_2$ Binary Phase Doagram

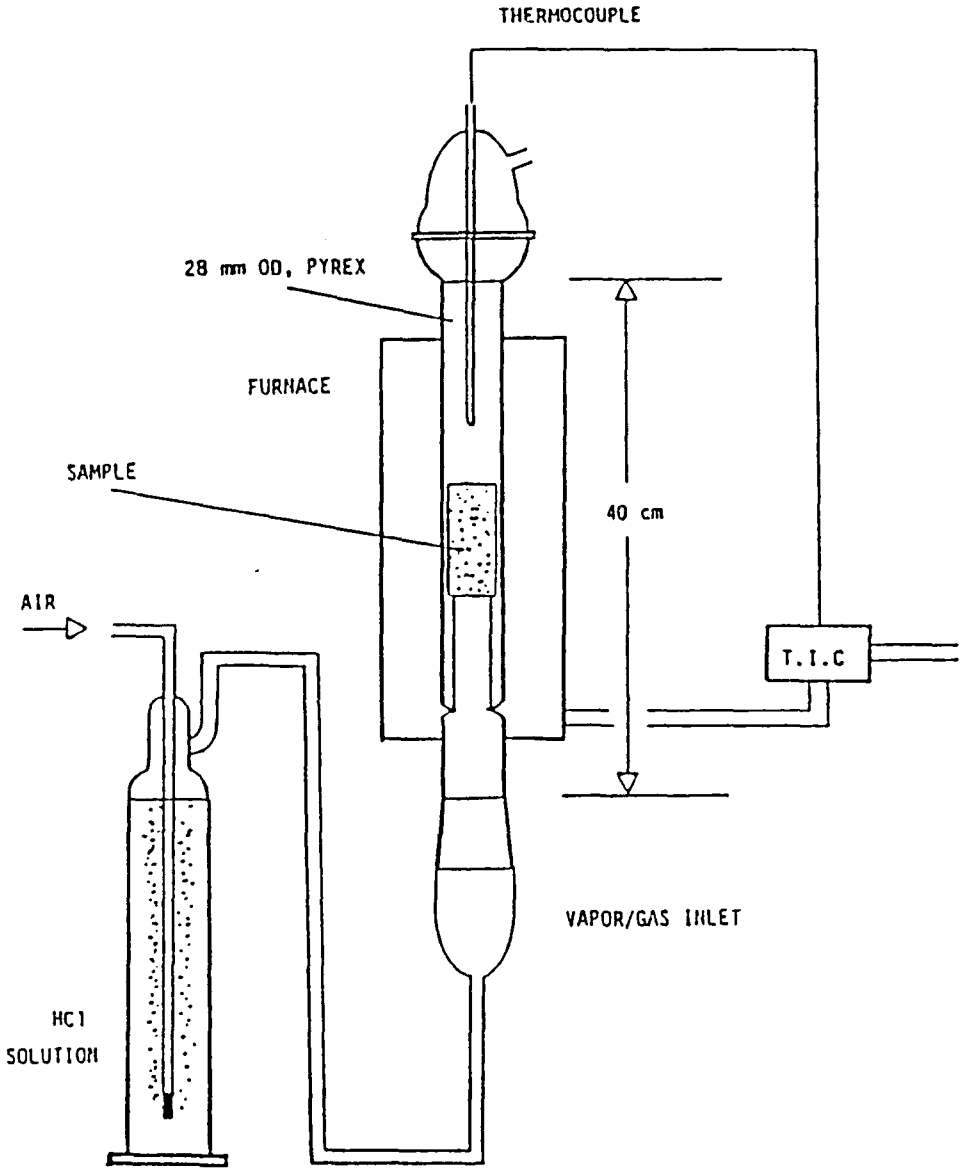

Figure 10. Schematic of the HCl Exposure Apparatus

vapor in the air–HCl mixture was within ±10 percent of the value predicted (Reference 14) by the vapor–liquid equilibrium data for 25°C.

The catalyst/support sample was oven–dried at 200°C for 1 hour and then weighed. After weighing, the sample was placed in the vertical Pyrex® tube of the HCl exposure apparatus. The furnace was turned on, and dry grade air (10–15cc/minute at room temperature and pressure (RTP): 23°C and 1 atm) was passed through the Pyrex® tube for 1 hour. This was done to allow the furnace to equilibrate at the set temperature (500°C). The gas washing bottle was then connected, and HCl vapors were introduced into the Pyrex® tube as previously discussed. The sample was exposed to these vapors for the desired time, and then the gas washing bottle was disconnected. The sample was removed from the HCl exposure apparatus and placed in an oven at 200°C for 1 hour and then weighed.

This procedure was repeated until sufficient data were obtained to generate a weight loss versus time curve, which normally required 80–100 hours of exposure.

2. X–Ray Diffraction

An Automated Powder X–ray Diffractometer (Phillips APD 3720) was used to identify and elucidate the structure of catalysts and other intermediate chemical species formed in the course of the thermal stability experiments.

3. Catalytic Oxidation Experiments

A series of catalytic oxidation experiments using CH_2Cl_2 (2,000–4,000 ppm) and dry air (500 cc/minute at RTP) was conducted at 500°C using a fresh 1:1 KCl/CuO catalyst (2.75 percent by weight) supported on a silica monolith tube (0.36 m^2/g surface area) in the reactor system described earlier (Section II). The objectives were to characterize the activity and selectivity of both the KCl/CuO and $KCl/CuCl_2$ catalysts at 500°C, as well as transient mixtures which occur at reaction conditions.

D. RESULTS AND DISCUSSION

1. Thermal Stability Experiments

The weight loss data obtained from the thermal stability experiments were normalized as a fraction of the initial amount of catalyst present in the sample to facilitate comparisons among the different catalyst loadings (typically 1.5 percent by weight) and stability experiments performed. These normalized values were plotted as a function of exposure time for each experiment and are presented graphically.

a. Cordierite Support

The influence of HCl vapors on the cordierite support was first checked by exposing a sample of it to 300,000 ppm HCl vapors with air at 500°C. The sample underwent a weight loss of 0.1 percent after 82 hours of exposure.

b. Cordierite Supported KCl and $CuCl_2$

The influence of HCl vapors on both cordierite-supported KCl and cordierite-supported $CuCl_2$ was determined. Figure 11 shows the normalized weight loss curve obtained for KCl supported on cordierite during exposure to 300,000 ppm HCl vapors with air at 500°C. The sample showed a steady weight loss with exposure time, owing to the low vapor pressure of KCl (3.9×10^{-4} mm Hg) at 500°C rather than any chemical interaction between KCl and HCl. Figure 11 seems to verify this by showing data for one test with a similar sample of supported KCl exposed to air only at 500°C in the HCl exposure apparatus; wherein the sample lost 28 percent less weight than did the sample exposed to HCl vapors after 70 hours of exposure. This difference is probably caused by the slight instability of the support itself. As described earlier, the cordierite support, when exposed to 300,000 ppm HCl vapors for 82 hours, lost 0.1 percent of its original weight. Although the weight loss was not significant in absolute terms (4.9 mg lost after 82 hours of exposure from a sample weighing 5.07 g initially), it was sufficiently high to account for the difference in weight loss observed for the supported KCl exposure experiments.

The influence of HCl vapors on supported $CuCl_2$ was far more severe. As shown in Figure 12, when a sample of $CuCl_2$ supported on cordierite was exposed to 300,000 ppm HCl vapors in air at 500°C, all of the $CuCl_2$ was lost from the cordierite support in less than 20 hours. This result was not surprising, considering that $CuCl_2$ has a vapor pressure of 294 mm Hg at 500°C and that the presence of HCl kept the copper salt in the chlorinated form. Therefore, the $CuCl_2$ most likely sublimed from the support surface. This was visually confirmed by the formation of a yellow deposit on the cooler parts of the HCl exposure apparatus.

Figure 12 also shows data from another sample of $CuCl_2$ on cordierite which was exposed only to dry grade air (no HCl) at 500°C in the HCl exposure apparatus. The sample weight dropped sharply within the first 5 hours of exposure before stabilizing at a value corresponding to 56 percent of the original weight of $CuCl_2$ sample. The initial loss in weight appears to be from two sources: the chemical conversion of $CuCl_2$ to CuO (which is a lower molecular weight entity), and to the simultaneous sublimation of some of the $CuCl_2$. Since CuO is

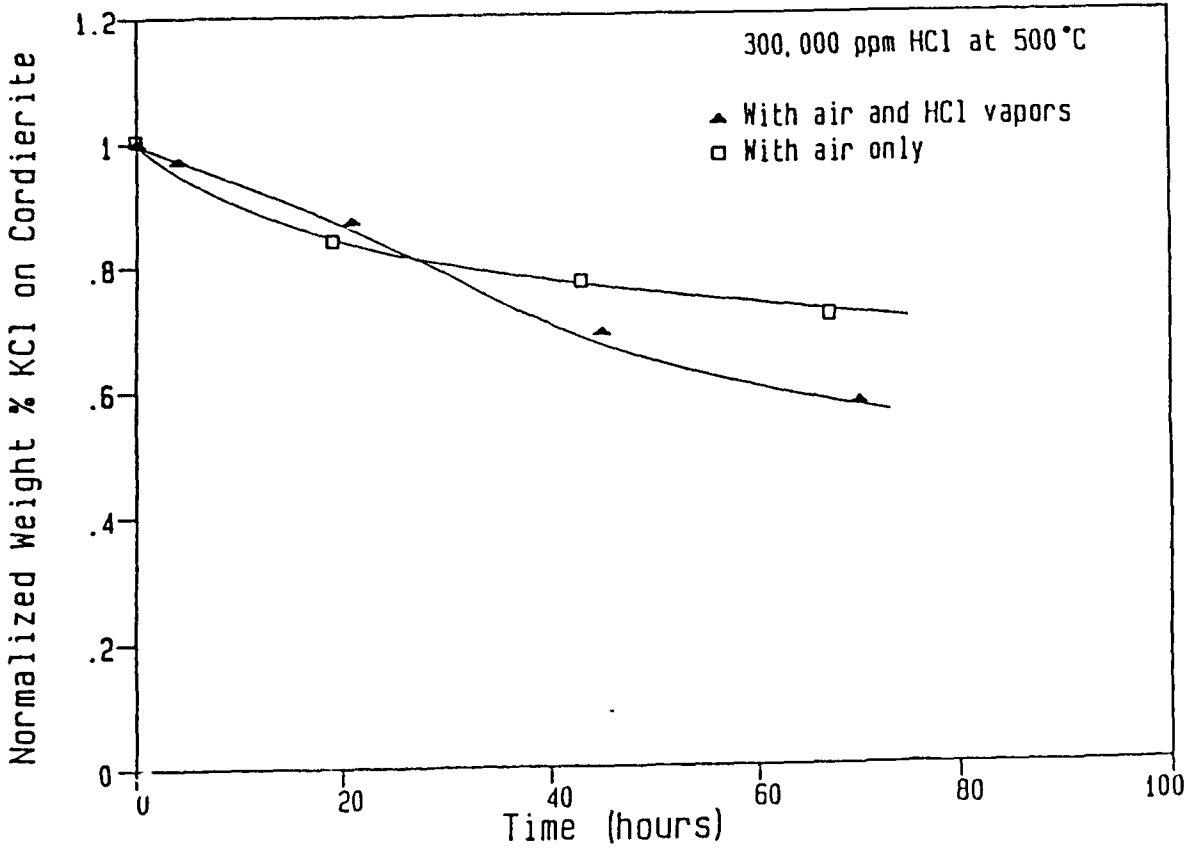

Figure 11. Effect of High Concentration HCl with Air on Supported KCl

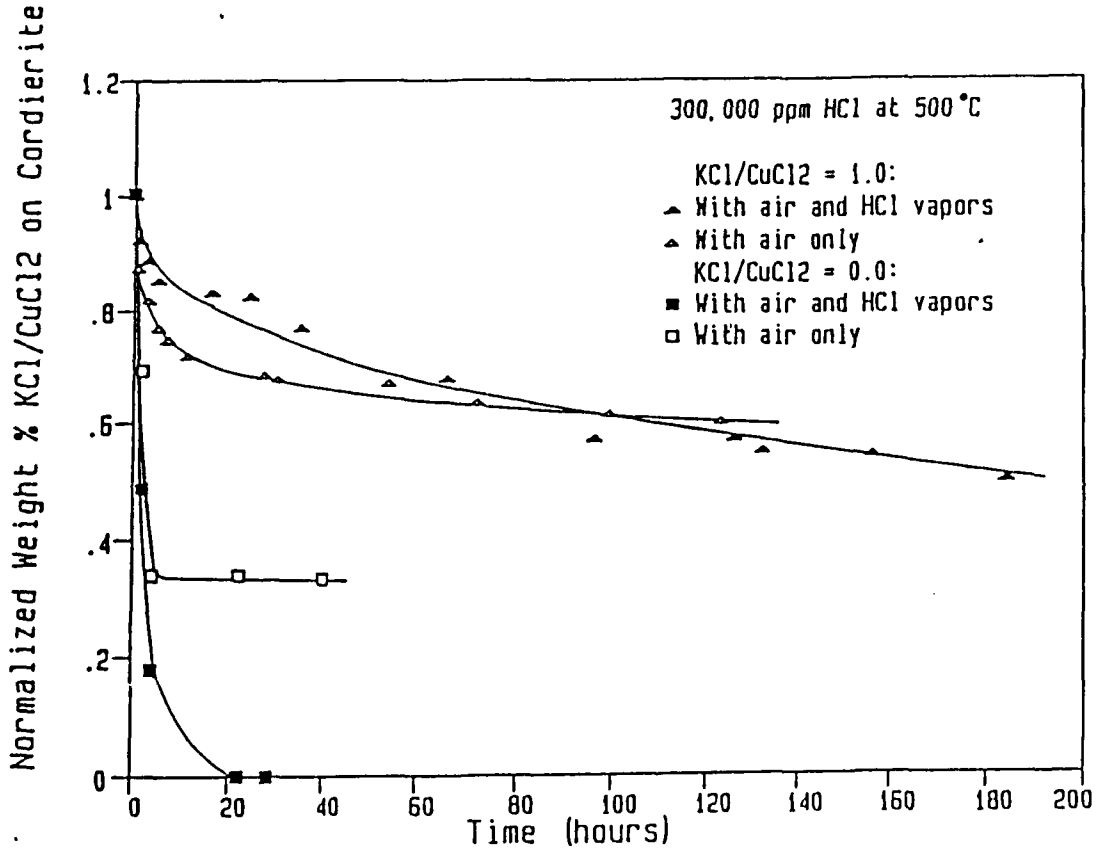

Figure 12. Effect of High Concentration HCl with Air on Supported $KCl/CuCl_2$ Catalysts

thermally stable in the presence of only dry air, the weight loss curve levels off after about 5 hours, as expected.

To confirm that the loss of $CuCl_2$ was due solely to its high vapor pressure at 500°C, a sample of $CuCl_2$ supported on cordierite was exposed to an environment of only nitrogen at 500°C in the HCl exposure apparatus. The presence of only nitrogen ruled out the possibility of any $CuCl_2$ being converted into CuO. This was followed by exposing a similar sample to nitrogen and 300,000 ppm HCl vapors at 500°C. The weight loss curves shown in Figure 13 indicate that the rate of loss of $CuCl_2$ in an oxygen free environment is independent of the presence of HCl vapors. This confirms that the role of HCl is to keep the copper in the volatile $CuCl_2$ form rather than as the stable oxide.

c. Cordierite Supported $KCl/CuCl_2$

A sample of 1:1 molar ratio mixture of $KCl/CuCl_2$ catalyst supported on cordierite was exposed to 300,000 ppm HCl vapors with air at 500°C. Even after 200 hours of exposure the sample lost only 48 percent of its original weight of catalyst, as shown in Figure 12. This is a significant improvement over the $CuCl_2$ catalyst which was completely stripped within 20 hours under identical conditions.

Figure 12 also shows weight loss for a sample of 1:1 $KCl/CuCl_2$ supported on cordierite which was exposed only to air at 500°C in the HCl exposure apparatus. The result is a rapid loss of weight as the $CuCl_2$ is converted into CuO, after which its weight nearly levels off. A slight decrease with time is probably due to the slow sublimation of KCl present in the catalyst system.

d. Cordierite Supported CuO and KCl/CuO

Next, the influence of KCl addition on the stability of the CuO catalyst was studied. Three supported catalyst samples, the first with only CuO, the second with KCl/CuO in the molar ratio 0.5:1, and the third with KCl/CuO in the ratio 1:1, were exposed to 300,000 ppm HCl vapors at 500°C. As shown in Figure 14, increasing the KCl/CuO ratio significantly increases the stability of the KCl/CuO catalyst. An interesting observation is the ≈10 percent initial increase in weight of the 1:1 molar ratio KCl/CuO catalyst in the first two hours of exposure. As explained earlier, the HCl chlorinates the CuO to $CuCl_2$ which is a higher molecular weight entity. Normally, the $CuCl_2$ is lost from the support surface at 500°C, but the presence of KCl in the catalyst greatly inhibits its loss causing a net initial increase in catalyst weight. However, after the initial weight gain, the sample gradually loses weight owing to the reduced but steady loss of $CuCl_2$ from the support

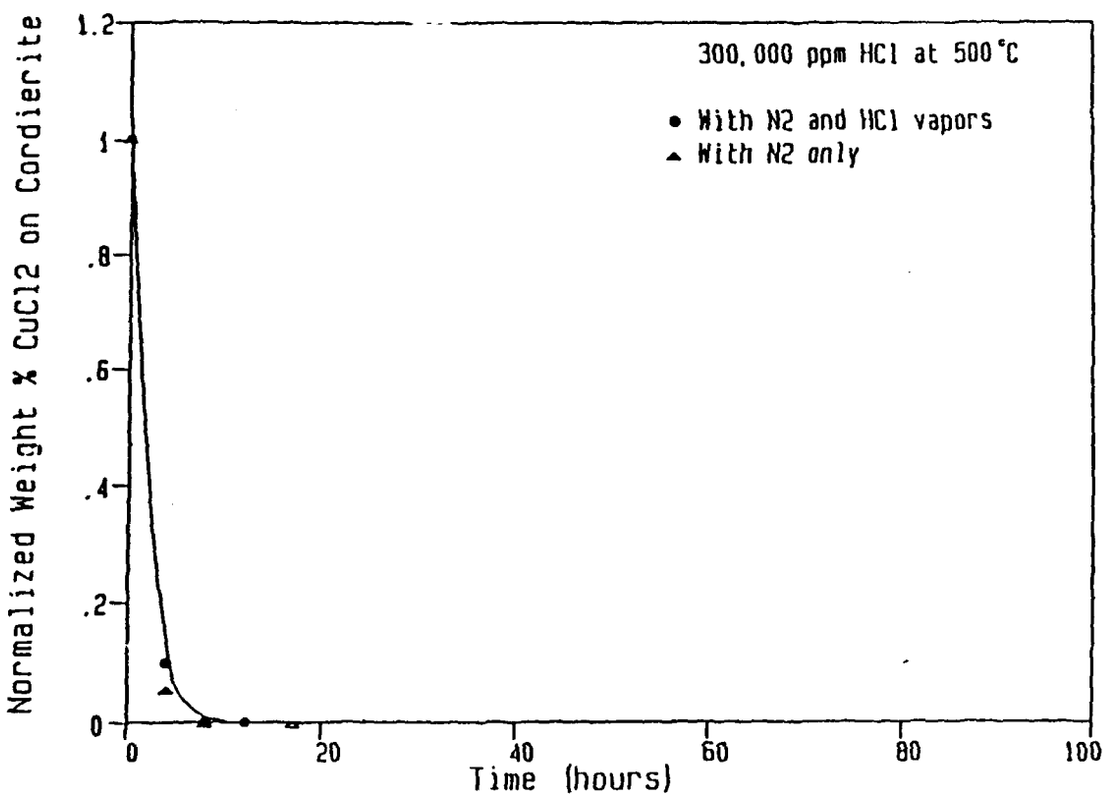

Figure 13. Effect of High Concentration HCl with Nitrogen on Supported $CuCl_2$ Catalyst

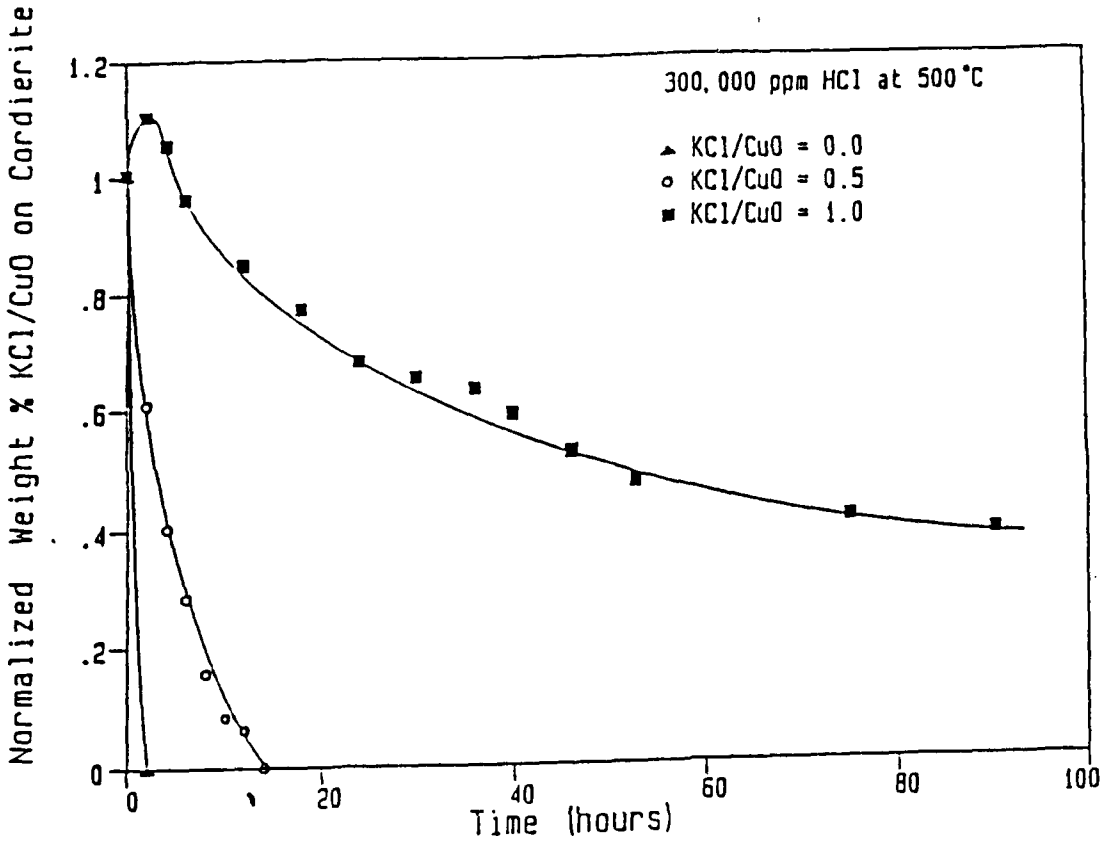

Figure 14. Effect of High Concentration HCl with Air on Supported KCl/CuO Catalyst

surface. The initial increase in weight was not observed for the supported 0.5:1 molar ratio KCl/CuO catalyst, probably because the lower content of KCl in the catalyst results in a relatively higher rate of loss of $CuCl_2$ from the support surface, overshadowing the effect of chlorination of the CuO.

e. Effects of HCl Concentration

The effect of varying HCl concentration on the dynamic conversion of CuO into $CuCl_2$ was also investigated. Supported samples of CuO and KCl/CuO catalysts were exposed to environments containing 20,000 or 800 ppm HCl at 500°C. As shown in Figure 15, all the CuO was lost in 30 hours of exposure to 20,000 ppm HCl vapors, whereas for the same exposure time the KCl/CuO suffered a loss of only ≈20 percent of its original KCl/CuO weight. The initial increase in weight of the KCl/CuO catalyst, which was observed in the earlier experiment with 300,000 ppm, was less sharp in this case with 20,000 ppm HCl vapors (increase of only 0.5 percent in 2 hours of exposure). This was due to the low concentration of HCl vapors which resulted in a low rate of chlorination of the CuO in the KCl/CuO catalyst.

Figure 15 also shows the weight change data for a set of stability experiments performed at the lower HCl vapor concentration of 800 ppm. This documents the behavior of the KCl/CuO and CuO catalysts under conditions similar to those observed in the catalytic oxidation reactor, where the concentrations of gaseous HCl produced were in the range of 400 to 800 ppm for the low surface area catalyst experiments. As observed in the earlier experiments at higher HCl concentrations, the KCl/CuO catalyst initially gained weight over several hours. However, the sample took 35 hours to reach the maximum weight, probably because of the low HCl concentration present.

Figure 16 compares the stability data previously obtained for the 1:1 KCl/CuO and CuO catalysts in the presence of 300,000, 20,000 and 800 ppm HCl vapors with air at 500°C. As expected, catalyst stability increases with a decrease in HCl concentration, although the result is highly nonlinear. The life of the 1:1 KCl/CuO catalyst does not change substantially with exposure to HCl concentrations in the range of 20,000 to 300,000 ppm. However, at 800 ppm HCl concentration the stability increases significantly. The life of the CuO catalyst (KCl/CuO = 0.0) also increases substantially between 20,000 and 800 ppm HCl exposure, suggesting a significant change in catalyst form in that concentration region.

Figure 16 indicates that the difference in stability between the 1:1 KCl/CuO and CuO formulations becomes more apparent when a sufficient amount of $CuCl_2$ is produced

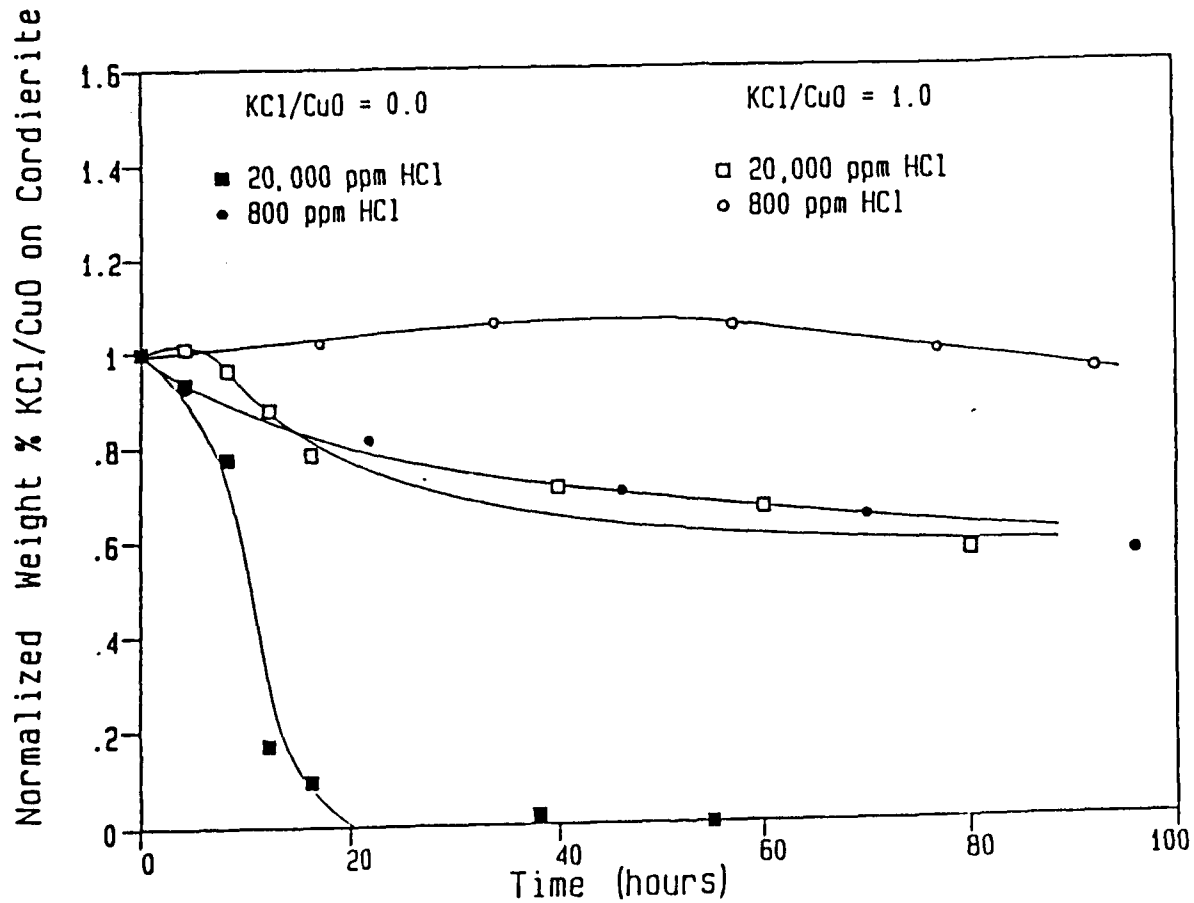

Figure 15. Effect of Low Concentration HCl with Air on Supported KCl/CuO Catalyst

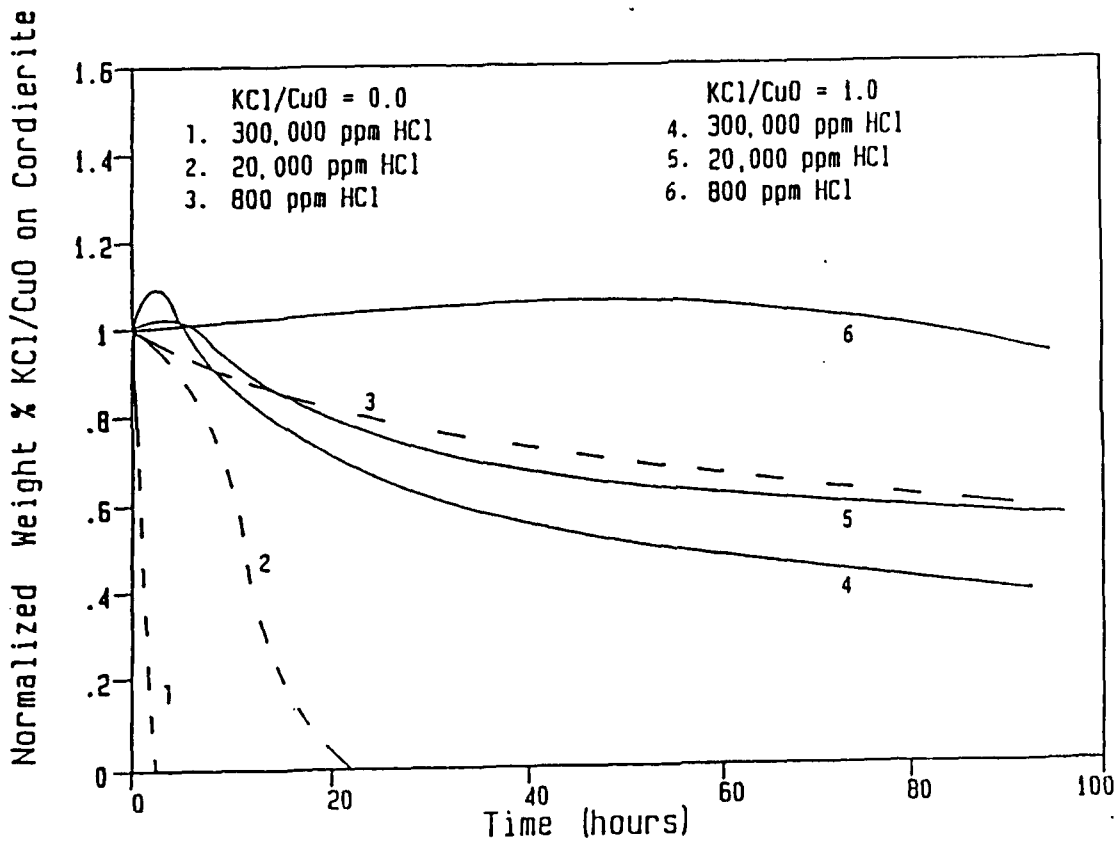

Figure 16. Effect of Change in HCl Concentration on the Stability of Supported KCl/CuO Catalyst in the Presence of Air

(from HCl exposure) to interact with the KCl in the KCl/CuO catalyst and enhance its stability. The process is shown by reaction (8).

$$\begin{matrix}\text{CuO} \\ \left[\begin{matrix}\text{thermally} \\ \text{stable}\end{matrix}\right]\end{matrix} \quad \begin{matrix}+\text{HCl} \\ \rightleftharpoons \\ 500^{0}\text{C}\end{matrix} \quad \begin{matrix}\text{CuCl}_2 \\ \left[\begin{matrix}\text{thermally} \\ \text{unstable}\end{matrix}\right]\end{matrix} \quad \begin{matrix}+\text{KCl} \\ \rightleftharpoons \\ 500^{0}\text{C}\end{matrix} \quad \begin{matrix}\text{KCl/CuCl}_2 \\ \left[\begin{matrix}\text{low vapor press.} \\ \text{melt, stable}\end{matrix}\right]\end{matrix} \quad [R8]$$

Thus, HCl vapors convert the CuO into $CuCl_2$, while the oxygen in the environment (146,000 ppm O_2 with 300,000 ppm HCl, and 204,000 ppm O_2 with 20,000 ppm HCl) converts the $CuCl_2$ back to CuO. When KCl is present in the system, it further interacts with the $CuCl_2$ to form a low vapor pressure thermally stable melt.

f. Supported KCl/CuO, Cr_2O_3 and KCl/V_2O_5

A comparison of catalyst thermal stability at 500°C and 300,000 ppm HCl is shown in Figure 17 for all three primary catalyst systems (KCl/CuO, Cr_2O_3 and KCl/V_2O_5) studied. Descriptions and other performance criteria for the Cr_2O_3 and KCl/V_2O_5 catalyst (not yet discussed) are found in Sections IV and V, respectively.

The stability results from Figure 17 show that KCl/V_2O_5 on LSA silica has the lowest rate of catalyst loss, with Cr_2O_3 next and KCl/CuO last. Although the same ordering of catalyst stability might not necessarily obtain on every potential support material, it is impressive that melt stabilization of the V_2O_5 by KCl addition can bring about such significant stability improvement.

2. X-Ray Diffraction Data

To elucidate the proposed thermal instability mechanism of the copper catalyst further, four X-ray diffraction (XRD) experiments were performed on the KCl/CuO and $KCl/CuCl_2$ catalysts to investigate any KCl-CuO or $KCl-CuCl_2$ interactions that might exist. Sample 1 was obtained as the yellow deposit collected at the top of the HCl exposure apparatus after running 1:1 KCl/CuO in the presence of HCl vapors. As expected, XRD confirmed the deposit to be $CuCl_2$, which had formed and then sublimed from the catalyst support surface onto the cooler region at the top.

Sample 2 was prepared by boiling a 1:1 molar ratio aqueous solution of $Cu(NO_3)_2 \cdot 3H_2O$ and KCl to dryness. This was followed by calcining the salt mixture at 500°C for 12 hours in a furnace to give the KCl/CuO catalyst. The catalyst sample was analyzed to determine whether any chemical interaction existed between the CuO and KCl. Both species were detected as separate compounds by XRD, indicating the absence of any KCl/CuO complex.

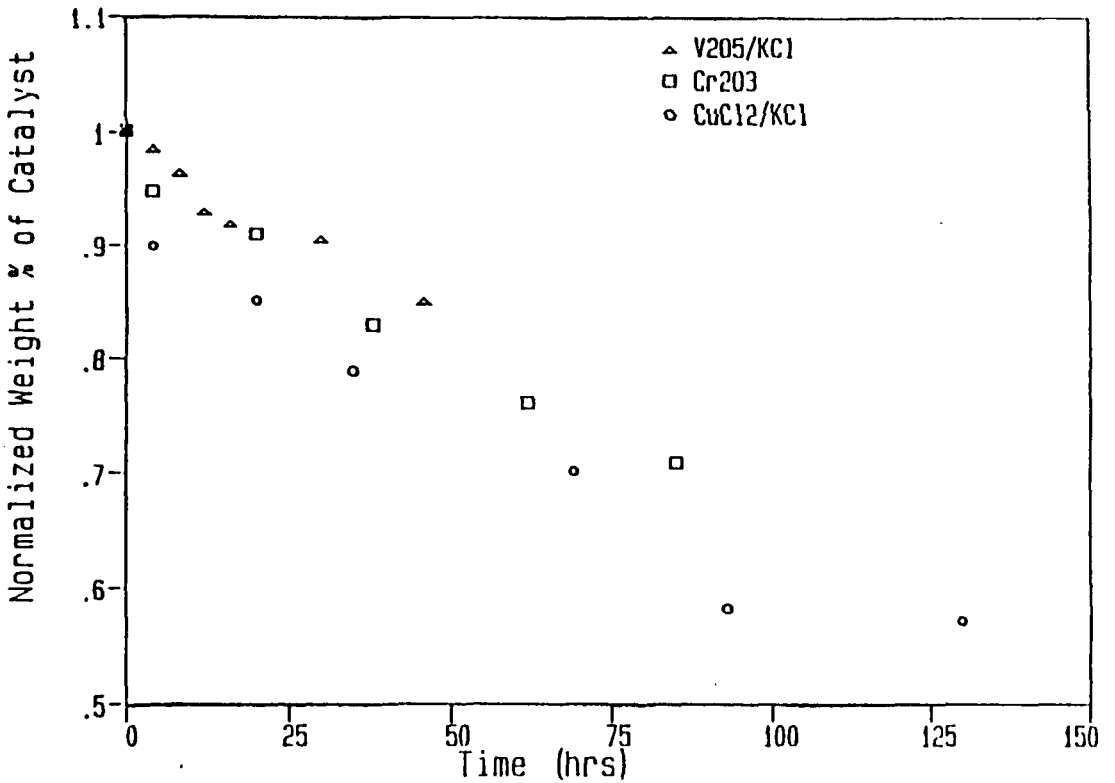

Figure 17. Effect of 300,000 ppm of HCl and Air on Catalysts

Sample 3 was prepared by dissolving an equimolar mixture of KCl and $CuCl_2$ salts in distilled water and then heating the solution to dryness at 200°C. The resulting solid was analyzed by XRD to identify the product formed. Two complexes ($KCuCl_3$, K_2CuCl_4) were identified. These complexes have low melting points, in the range of 320 to 360°C. Therefore at 500°C, the normal reactor operating temperature, the complexes mentioned above exist as a melt on the support surface and are substantially less volatile than $CuCl_2$.

Sample 4 was prepared by exposing a portion of Sample 2 to HCl vapor (300,000 ppm in air) at 500°C for 18 hours. The XRD analysis of the resulting solid revealed the presence of the K_2CuCl_4 complex. The detection of K_2CuCl_4, and not $KCuCl_3$ in the exposed 1:1 KCl/CuO mixture, confirms the slowness of the CuO to $CuCl_2$ transition, during which a portion of the $CuCl_2$ formed undoubtably sublimes. These simultaneous processes probably resulted in the local ratio of KCl to $CuCl_2$ being greater than 2, causing the formation and detection of only K_2CuCl_4 upon cooling.

3. Comparisons of KCl/CuO Versus KCl/$CuCl_2$

The importance of electrophilic surfaces (TMO) versus nucleophilic surfaces (TMCl) can be demonstrated by observing activity and selectivity of the KCl/CuO and KCl/$CuCl_2$ catalysts. Deep oxidation products can be expected by the former; oxychlorination products by the latter. Transient test results are documented herein which show this to be the case.

A series of catalytic oxidation experiments using a methylene chloride feed was conducted in the monolithic reactor system described earlier. The objectives were to characterize the activity and selectivity of both the KCl/CuO and KCl/$CuCl_2$ catalysts at 500°C. Possible reactions that could occur in catalytic oxidation experiments with a methylene chloride feed are shown in Table 3. The free energy changes for all these reactions were found to be negative, hence, plausible.

TABLE 3. REACTIONS INVOLVING METHYLENE CHLORIDE

1.	$CH_2Cl_2 + O_2 \longrightarrow CO_2 + 2\ HCl$
2.	$4\ HCl + O_2 \longrightarrow 2\ Cl_2 + 2\ H_2O$
3.	$2\ CH_2Cl_2 + 2\ HCl + O_2 \longrightarrow 2\ CHCl_3 + 2\ H_2O$
4.	$2\ CHCl_3 + 2\ HCl + O_2 \longrightarrow 2\ CCl_4 + 2\ H_2O$
5.	$4\ CH_2Cl_2 + Cl_2 + O_2 \longrightarrow 4\ CHCl_3 + 2\ H_2O$
6.	$4\ CHCl_3 + 2\ Cl_2 \longrightarrow 4\ CCl_4 + 2\ H_2O$
7.	$CH_2Cl_2 + Cl_2 \longrightarrow CHCl_3 + HCl$
8.	$CHCl_3 + Cl_2 \longrightarrow CCl_4 + HCl$

The first set of experiments was conducted in the reactor using a fresh 1:1 KCl/CuO catalyst (2.75% by weight) supported on

a silica monolith tube (0.36 m^2/g surface area). Starting with this catalyst, experimental runs with a feed of methylene chloride (2,000–4,000 ppm) and dry air (500 cc/minute at RTP) were conducted at 500°C. The activity of the catalyst, measured in terms of percentage conversion of methylene chloride versus total run time, is shown in Figure 18. Initial conversion of almost 30 percent is seen to increase over the course of 15 hours cumulative run time, leveling out at about 44 percent thereafter. The observed increase in catalyst activity is most likely due to the chlorination of the CuO catalyst by the HCl produced during the oxidation reaction. Thus the $CuCl_2$ form of the catalyst appears more active. As further verification, a fresh 1:1 molar ratio $KCl/CuCl_2$ catalyst (2.6 percent by weight) supported on a silica monolith tube (0.42 m^2/g surface area) was also run in the reactor setup. Initial conversion of methylene chloride over the fresh $KCl/CuCl_2$ catalyst was 78 percent, but dropped sharply to 44 percent over a period of 10–12 hours as shown in Figure 18. The initial high conversions over the $KCl/CuCl_2$ catalyst again indicate that the $CuCl_2$ form of the catalyst may have a higher activity than the CuO form for conversion of methylene chloride.

For the methylene chloride feed concentrations (2,000–4,000 ppm) used in these runs, corresponding levels of vapor phase HCl were determined to be in the 400–800 ppm range, similar to the low concentration levels used in the previous HCl exposure apparatus. Thus the slow changes in catalyst form (oxide-to-chloride) observed in those experiments probably occur over similar time scales in the reactor, and are manifested here as changes in catalyst activity. Visual examination of the catalyst monoliths before and after reactor service also confirm these changes. The initially gray KCl/CuO catalyst appears after exposure as reddish-brown ($KCuCl_3$) with small gray "islands" of CuO remaining, similarly, the initially reddish-brown $KCuCl_3$ (from the 1:1 $KCl/CuCl_2$ catalyst) shows numerous small gray regions after reactor exposure. Chemical reactions involving the KCl/CuO catalyst itself under the conditions existing in the reactor (i.e., 400–800 ppm HCl with air at 500°C) are listed in Table 4.

TABLE 4. REACTIONS INVOLVING THE KCl/CuO CATALYST

1.	$CuO + 2\ HCl \longrightarrow CuCl_2 + H_2O$
2.	$2\ CuCl_2 \longrightarrow 2\ CuCl + Cl_2$
3.	$2\ CuCl + O_2 \longrightarrow 2\ CuOCl$
4.	$2\ CuOCl \longrightarrow 2\ CuO + Cl_2$
5.	$CuCl_2 + KCl \longrightarrow KCuCl_3$
6.	$CuCl_2 + 2\ KCl \longrightarrow K_2CuCl_4$

These results add credibility to the idea that stabilization of activity after sufficient run time is brought

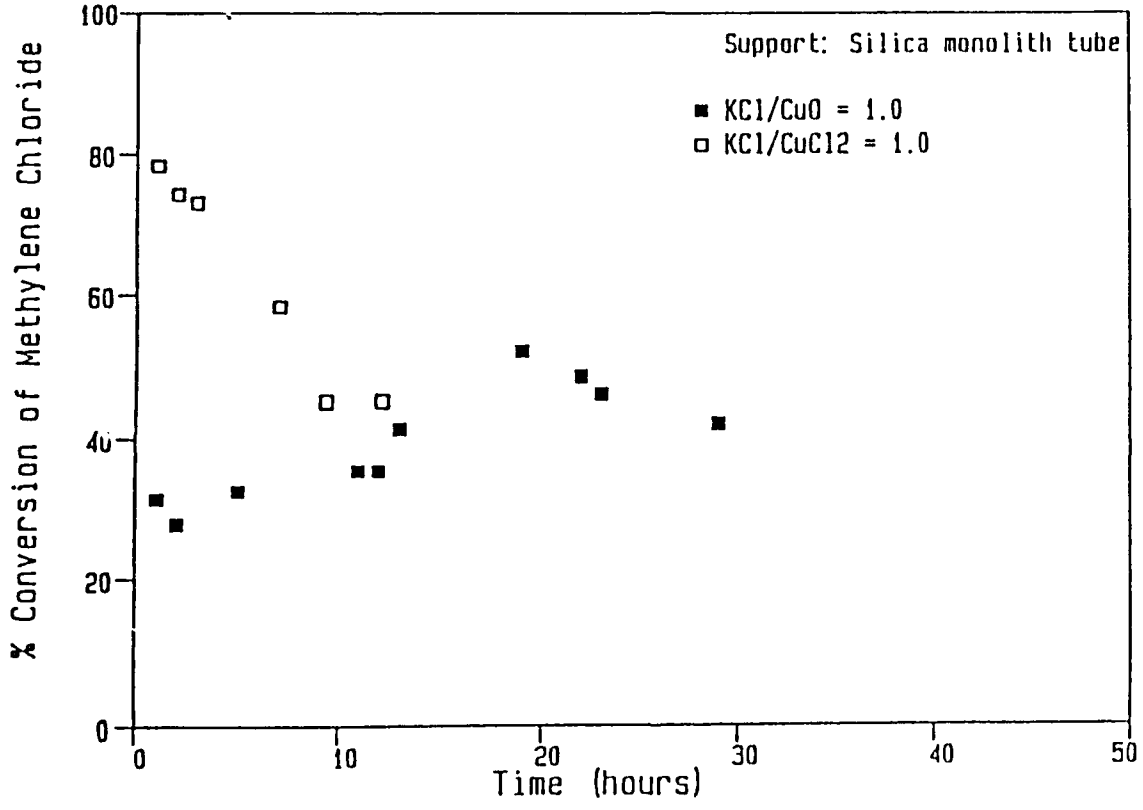

Figure 18. Activity of the Supported KCl/CuO and KCl/$CuCl_2$ Catalysts with Run Time

about by an equilibrium oxide–chloride intermediate catalyst state which exists for a particular reactor concentration of HCl and oxygen.

Along with methylene chloride conversions versus time, a limited amount of catalyst selectivitiy data was also obtained as shown in Table 5, but only for the 1:1 KCl/CuO catalyst system. The results show that selectivity for the oxychlorination product ($CHCl_3$) increased significantly from about 0.2 to 0.5 as the KCl/CuO catalyst "aged" over 22 hours.

TABLE 5. SELECTIVITY FOR AGING KCl/CuO CATALYST

Run Time Hours	Methylene Chloride Conversion, %	Selectivity $CHCl_3$	Selectivity CCl_4
1	31.0	0.200	0.094
2	27.9	0.283	0.143
5	32.1	0.290	0.174
11	35.3	0.229	0.082
12	35.4	0.410	0.156
13	41.4	0.357	0.116
19	51.7	0.466	0.197
22	48.0	0.549	0.148

Identification of selectivity trends for CCl_4 formation (which would be expected to increase with $CHCl_3$ to form CCl_4) was hampered by excessive scatter in the data (Table 5). However, the tendency for increased oxychlorination product with time on stream coincides with the known conversion of the catalyst from the oxide to chloride form during HCl exposure.

E. CONCLUSIONS

Based on the foregoing discussion, the following conclusions can be drawn:

1. The addition of KCl to the CuO catalyst greatly increases its stability in the presence of HCl vapors at moderately elevated temperatures.

2. High HCl concentrations keep the catalyst in the chlorinated form and encourage loss of catalyst through sublimation of $CuCl_2$.

3. High oxygen concentrations keep the catalyst partly in the CuO form and increase catalyst stability.

4. Increasing the $CuCl_2$ content in the catalyst increases its activity and changes its selectivity towards higher chlorination products.

5. The activity and selectivity of the fresh 1:1 KCl/CuO and 1:1 KCl/$CuCl_2$ catalysts are initially quite different, but after sufficient run time (25+ hours) the two catalysts appear to approach a common intermediate oxide–chloride state as verified by similar activity levels.

SECTION IV

STUDY OF KCl/CuO AND Cr_2O_3 CATALYSTS

A. INTRODUCTION

Catalytic oxidation of methylene chloride (CH_2Cl_2) and trichloroethylene (C_2HCl_3) in dry and humidified air, using two catalyst systems, will be discussed in this section. The first catalyst is comprised of a 1:1 molar ratio KCl/CuO supported on low surface area (LSA) silica. At reaction temperatures (500°C in this study), and under conditions where HCl and/or Cl_2 are present along with oxygen, the CuO in this catalyst is partially converted to the more volatile $CuCl_2$. The ratio of CuO to $CuCl_2$ on the catalyst surface is believed to be dynamic, varying with local HCl/O_2 ratios (Reference 37). Cr_2O_3 is the second catalyst system used in this study, again on LSA silica. This catalyst is a solid at reaction temperatures (500°C) and remains primarily in an oxide rather than chloride form under reactor conditions (Reference 38). It has been used commercially for deep oxidation processes (Reference 39,40).

Comparison of the reaction products for the two catalysts suggests that the KCl/CuO system is generally more selective toward oxychlorination pathways (via nucleophilic substitution), while Cr_2O_3 favors deep oxidation (with electrophilic adsorption of oxygen as the probable first step).

The experimental procedure followed in this section for catalytic oxidation of chlorinated hydrocarbon is described in Section II.

B. RESULTS AND DISCUSSION

Neither catalyst showed significant deactivation during the course of the experiments, although the fresh KCl/CuO catalyst did initially require time to reach its steady state ratio of CuO to $CuCl_2/CuCl$.

Two chlorinated hydrocarbons, methylene chloride (CH_2Cl_2) and trichloroethylene (C_2HCl_3) have been used as feeds, both separately and as mixtures, to evaluate activity and selectivity of the above catalysts during air oxidation at 500°C.

1. Oxidation of CH_2Cl_2

Catalyst activity results for both catalyst systems are shown in Figure 19. The average conversion of CH_2Cl_2 is about 60 percent for the Cr_2O_3 catalyst and about 40 percent for the KCl/CuO catalyst. The lower activity of the latter catalyst is mainly an outcome of this catalyst's high affinity for HCl

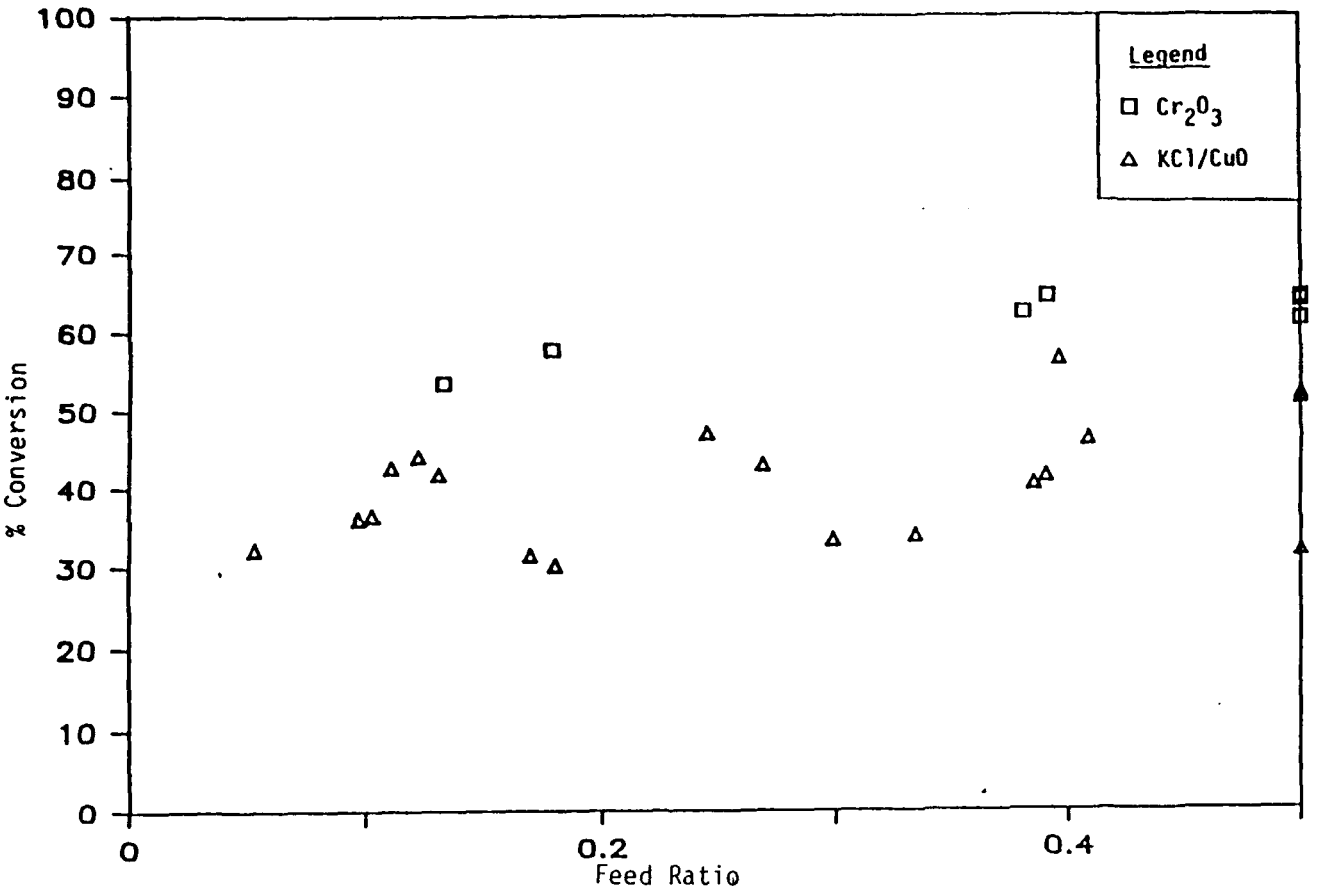

Figure 19. Conversion of Methylene Chloride over Chromia and Copper Based Catalysts

(a reaction product), as discussed in section III. For each catalyst there is a slight trend towards lower conversions as the feed ratio is decreased by addition of water vapor to the feed. The competition by H_2O for surface sites may be responsible for this result.

Formation of chloroform ($CHCl_3$), shown in Figure 20, is substantial (20–60 percent) for the KCl/CuO catalyst but much less (4–12 percent) for the Cr_2O_3. This difference is consistent with the high affinity of the $CuCl_2/CuCl$ components of the catalyst for HCl (Reference 27), which encourages the oxychlorination of CH_2Cl_2 according to Reaction (9).

$$2\ CH_2Cl_2 + 2\ HCl + O_2 \rightleftharpoons 2\ CHCl_3 + 2\ H_2O \qquad [R9]$$

In comparison, the Cr_2O_3 surface is known (Reference 27) to chemisorb O_2 preferentially over HCl.

With water addition (decreasing feed ratios), $CHCl_3$ production decreases significantly for the KCl/CuO catalyst. This trend can most likely be explained from Reaction (9) where increases in H_2O concentration would be expected to limit progress of the forward reaction.

Formation of carbon tetrachloride (CCl_4) over each catalyst, as shown in Figure 21, follows a pattern similar to $CHCl_3$ production, probably as the result of further oxychlorination of the $CHCl_3$ previously formed:

$$2\ CHCl_3 + O_2 + 2\ HCl \rightleftharpoons 2\ CCl_4 + 2\ H_2O \qquad [R10]$$

The HCl required for Reactions (9) and (10) is obtained from the parallel deep oxidation reaction:

$$CH_2Cl_2 + O_2 \longrightarrow 2\ HCl + CO_2 \qquad [R11]$$

The reverse Deacon reaction may also supply HCl under appropriate conditions:

$$2\ Cl_2 + 2\ H_2O \rightleftharpoons 4\ HCl + O_2 \qquad [R12]$$

An alternate approach (Reference 21,23) suggests that HCl formed in the deep oxidation process is continually converted into Cl_2 by the Deacon reaction and that the oxychlorination is more correctly a direct chlorination. In reality both mechanisms may occur simultaneously.

The production of HCl over each catalyst is shown in Figure 22. Although data are somewhat scattered, significantly higher net production of HCl over the Cr_2O_3 catalyst is clearly

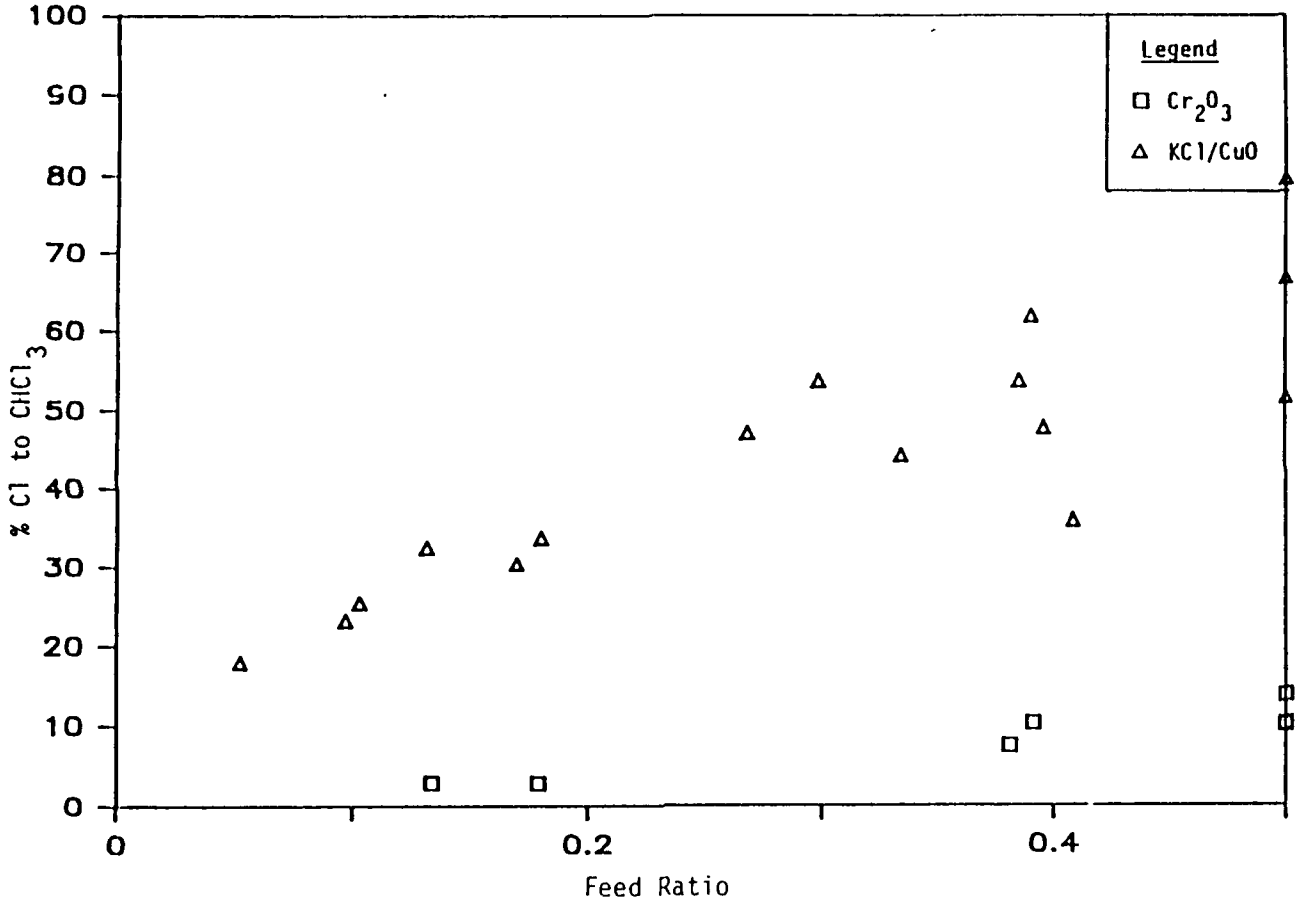

Figure 20. Selectivity of Methylene Chloride to $CHCl_3$ over Chromia and Copper Based Catalysts

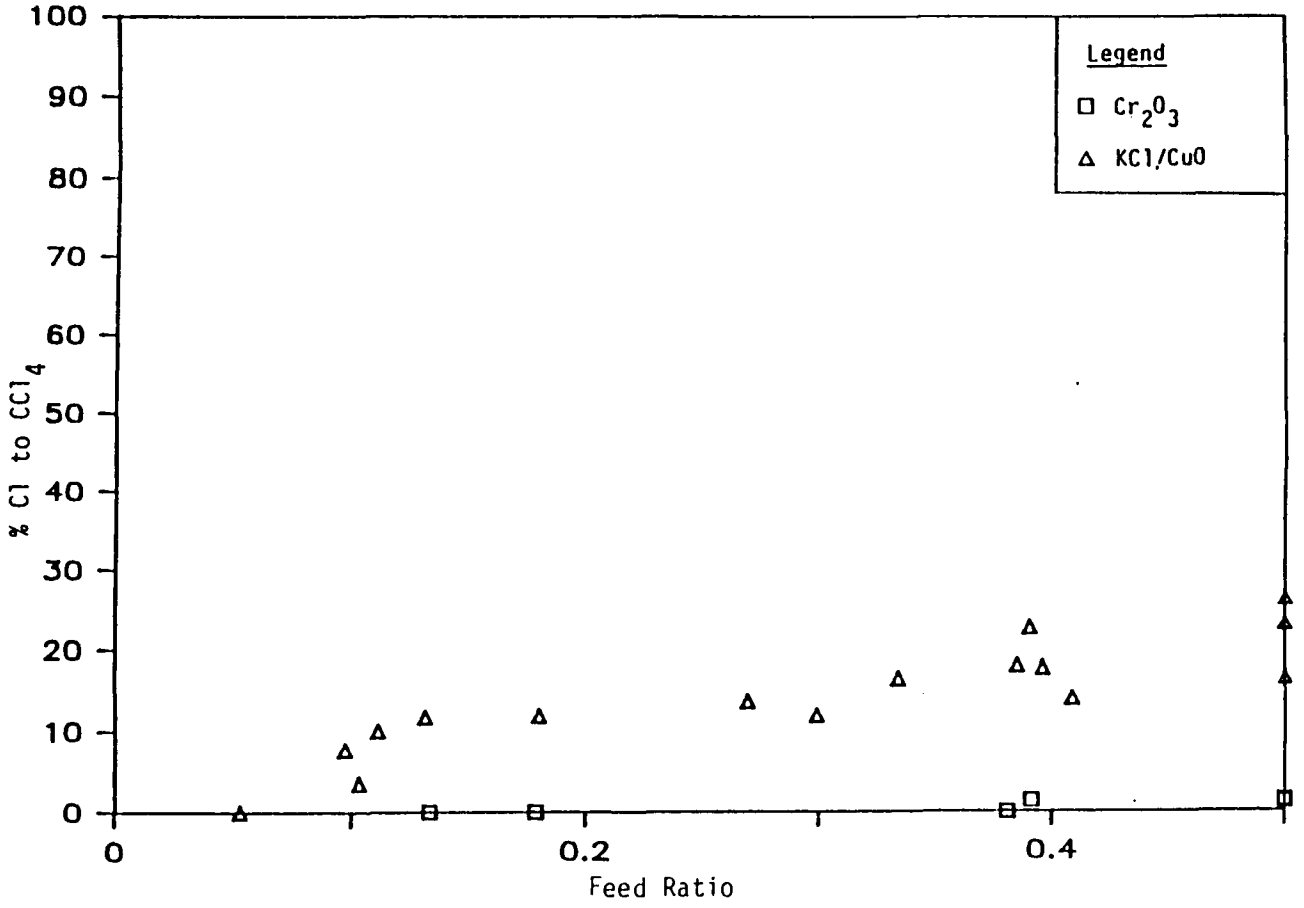

Figure 21. Selectivity of Methylene Chloride to CCl_4 over Chromia and Copper Based Catalysts

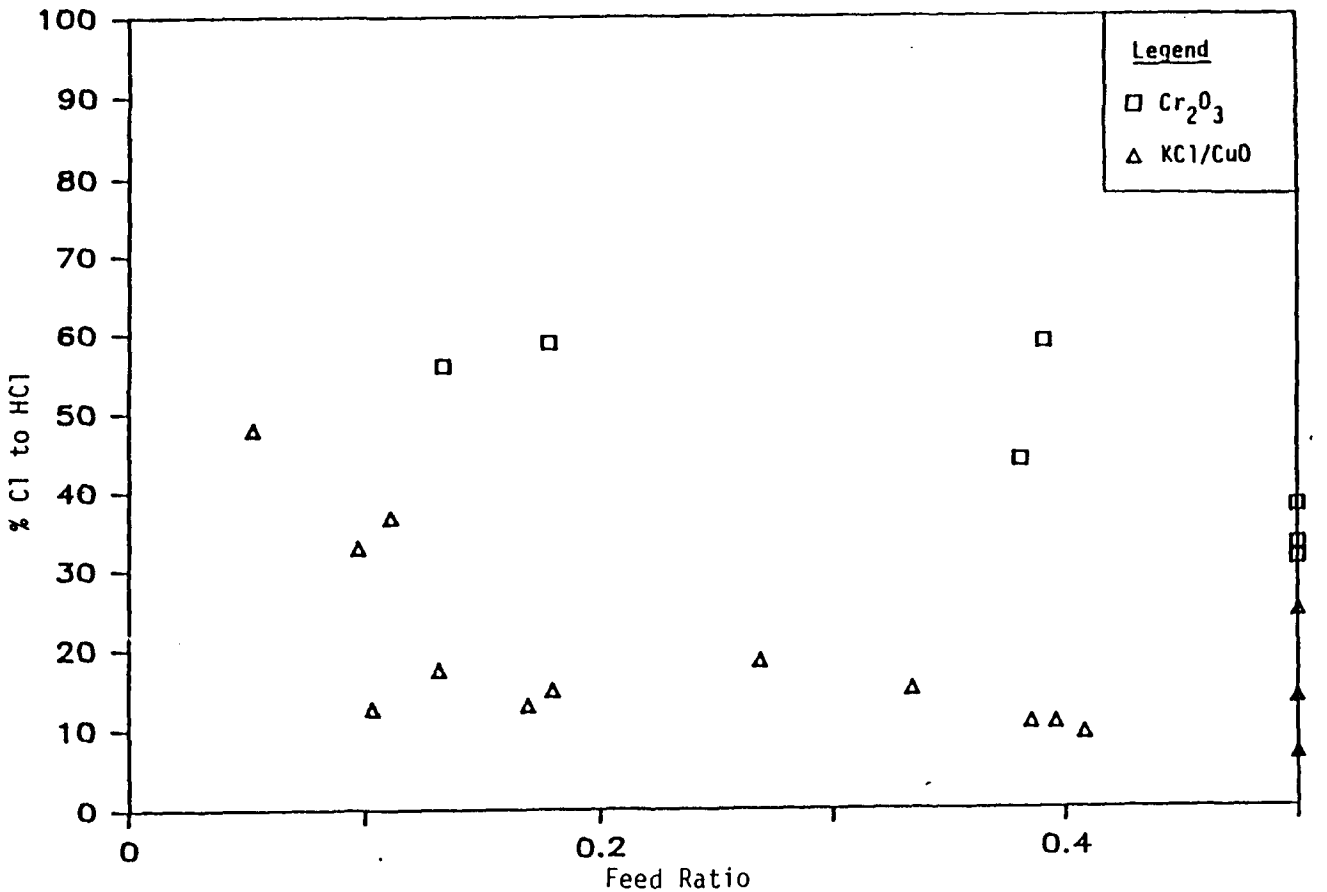

Figure 22. Selectivity of Methylene Chloride to HCl over Chromia and Copper Based Catalysts

seen. This is reasonable because the Cr_2O_3 catalyst surface, which exhibits higher affinity for O_2 than for HCl, more readily desorbs the latter rather than chemisorbing it for use in subsequent oxychlorination reactions, as is the case with $CuCl_2/CuCl$. The trend toward increases in HCl formation for both catalysts, as water vapor is added to the feed, agrees with Reactions (9) and (10), which show that H_2O addition to discourage parallel reactions consumes HCl. As expected, this trend is less noticeable for the Cr_2O_3 catalyst since the oxychlorination reactions are not highly favored anyway, in agreement with the expected paucity of HCl remaining on the Cr_2O_3 surface.

Based on the limited data shown in Figure 23, it appears that Cl_2 production decreases for both catalysts with increasing water vapor concentration as expected from the reverse Deacon Reaction (12). The generally higher Cl_2 production for the Cr_2O_3 catalyst will result in higher HCl production.

Figure 24 gives the percentage carbon–chlorine bonds remaining in products for a given level of CH_2Cl_2 conversion, reflecting the overall efficiency of each catalyst toward oxychlorination versus deep oxidation pathways. The relatively poor performance of the KCl/CuO catalyst for deep oxidation, especially at high feed ratios (low water vapor addition), underscores the selectivity of this catalyst toward oxychlorination as compared to the basic deep oxidation tendencies for Cr_2O_3.

2. Oxidation of C_2HCl_3

C_2HCl_3 is a significantly different molecule from CH_2Cl_2. It has two carbon atoms, a carbon–carbon double bond, and a Cl–to–H ratio of three. These differences suggest the potential for a wider spectrum of oxidation products as well as differences in individual selectivities.

Conversion levels for C_2HCl_3 over Cr_2O_3 and KCl/CuO are shown in Figure 25 as a function of feed ratio. With Cr_2O_3, conversion of C_2HCl_3 averages about 60 percent, independent of H_2O addition, and is almost identical to CH_2Cl_2 conversions over the same catalyst. Since deep oxidation is the primary process for Cr_2O_3 catalysis, this result suggests the same rate limiting step (e.g. diffusion or chemisorption of C_2HCl_3 or O_2). In contrast, C_2HCl_3 conversion over the KCl/CuO catalyst averages significantly less than CH_2Cl_2 conversions (25 percent versus 40 percent), and is now independent of H_2O addition. The loss in activity of the KCl/CuO catalyst for C_2HCl_3 destruction could be predicted based on its primary function as an oxychlorination catalyst. With only one hydrogen atom, yield of HCl (a necessary reactant for oxychlorination) is limited to only one molecule per molecule of C_2HCl_3 reacted. The activity of the

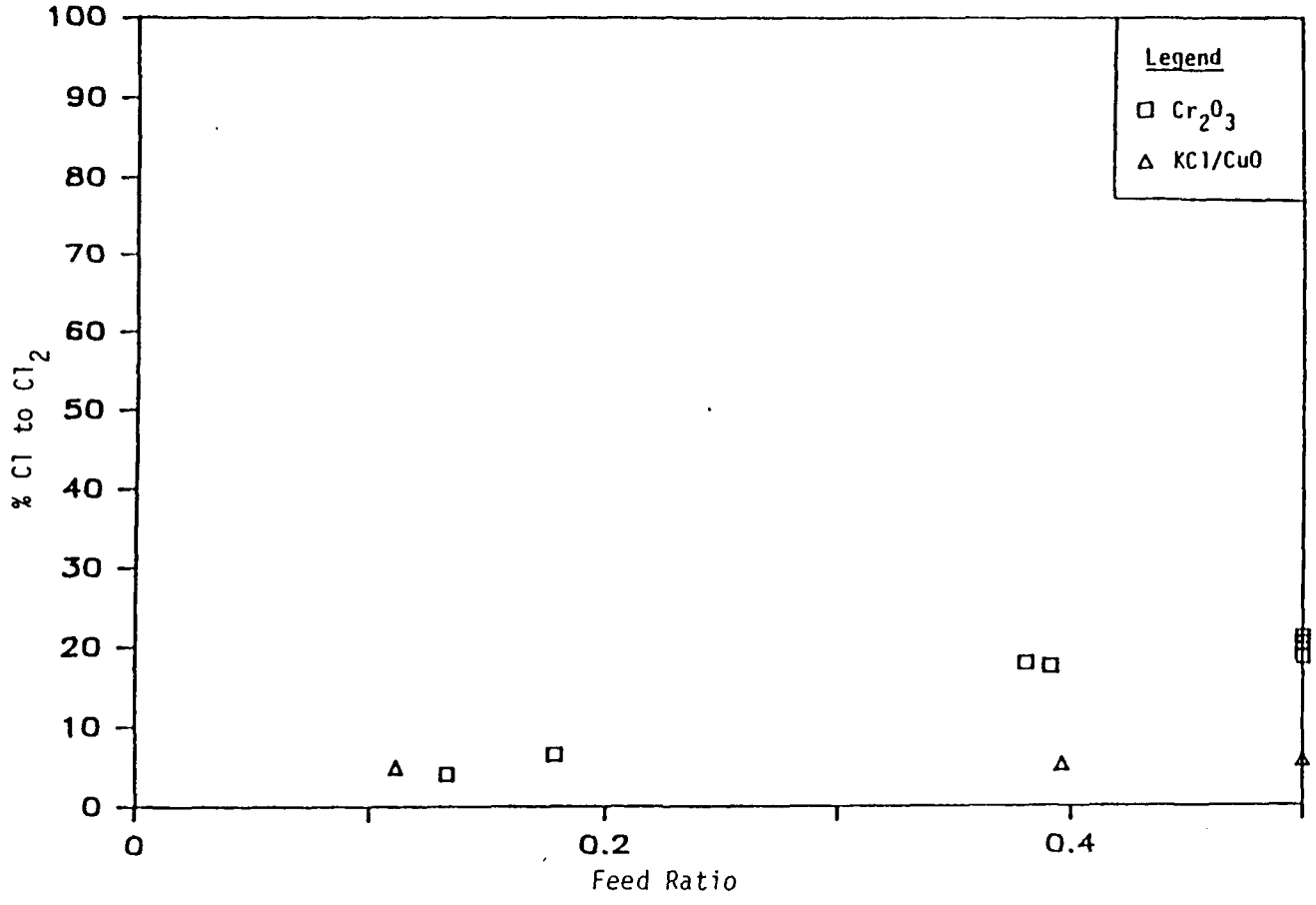

Figure 23. Selectivity of Methylene Chloride to Cl_2 over Chromia and Copper Based Catalysts

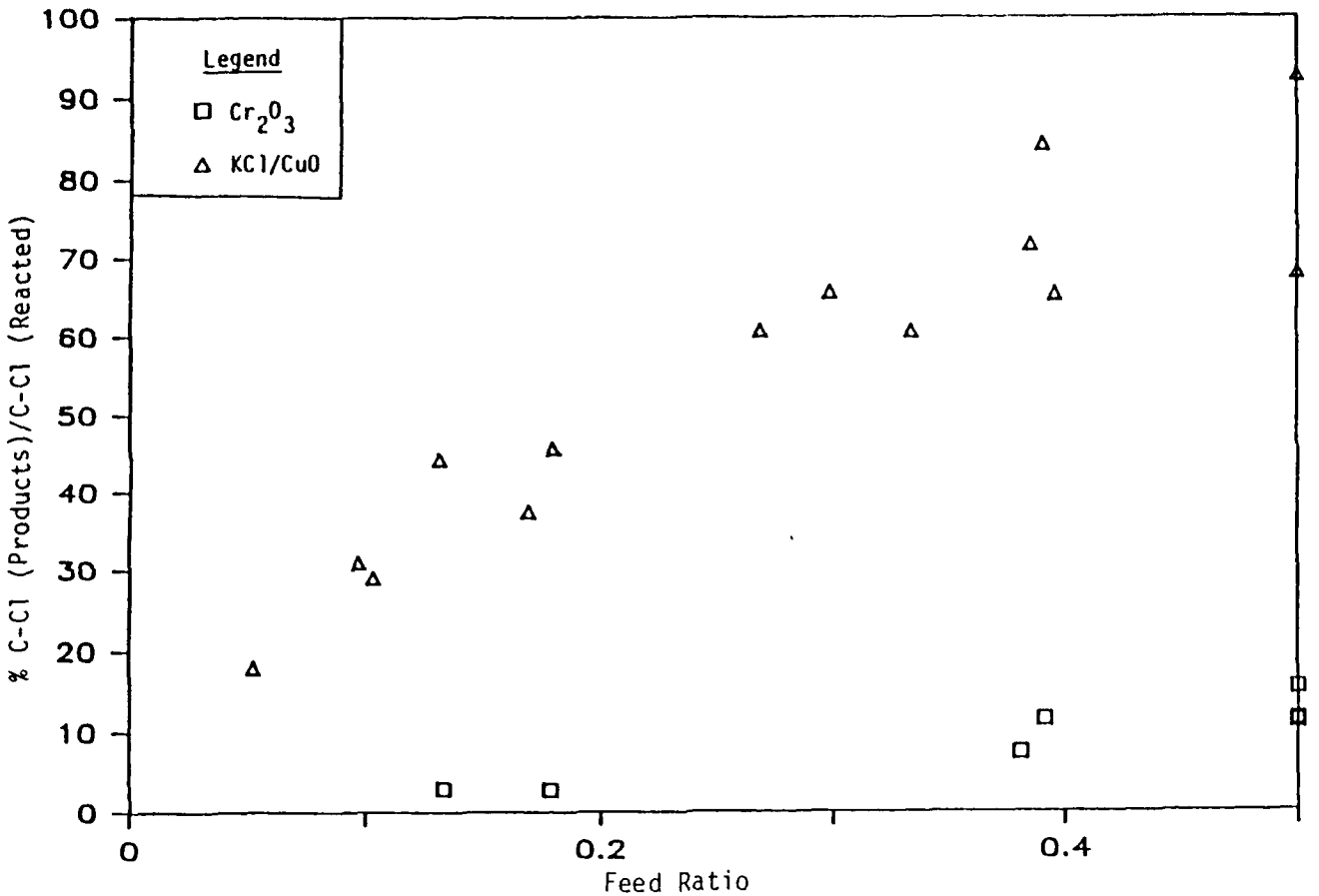

Figure 24. Percentage C-Cl Bonds Remaining in Products after Methylene Chloride Oxidation versus Feed Ratio

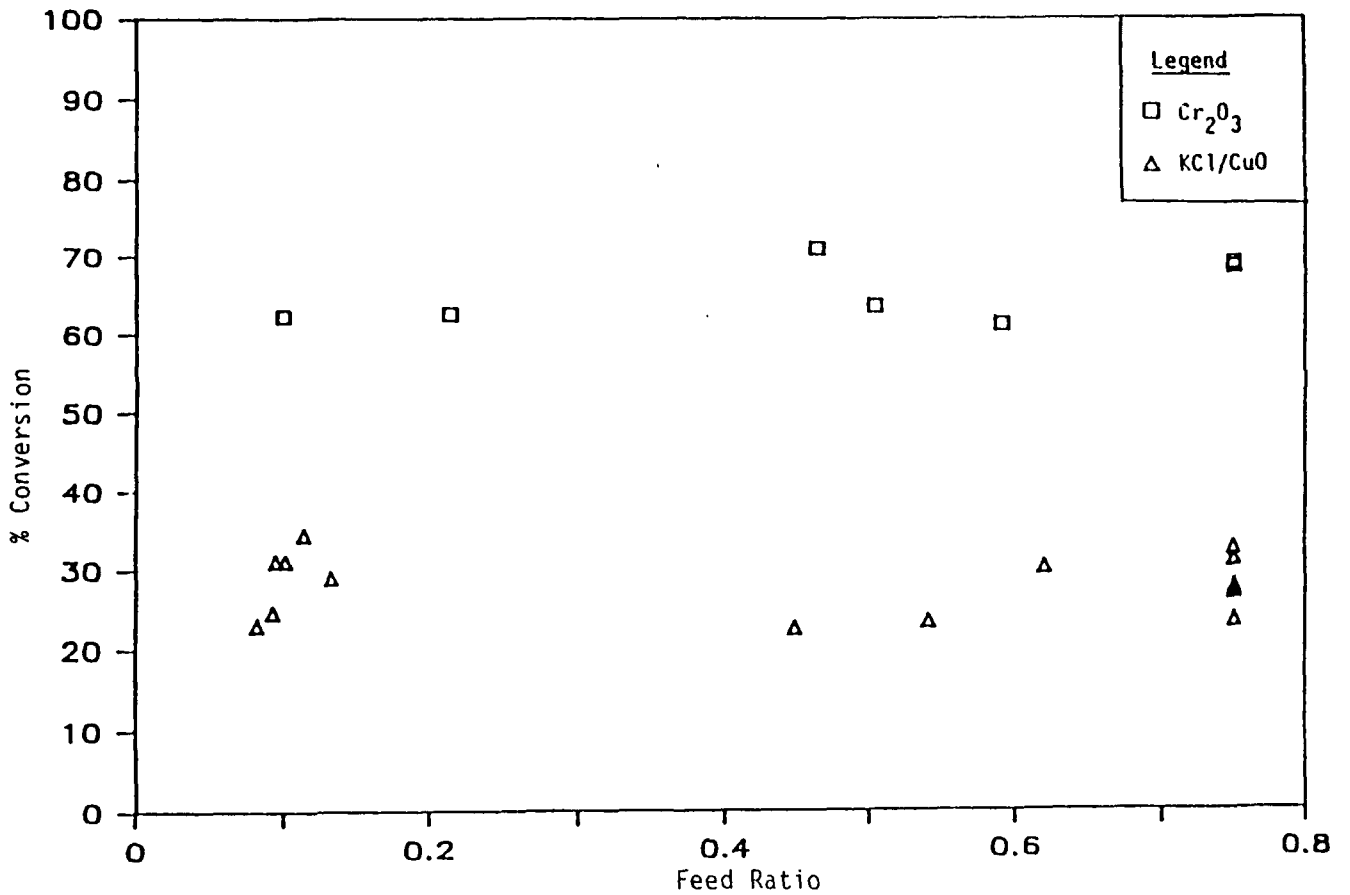

Figure 25. Conversion of Trichloroethylene over Chromia and Copper Based Catalysts

KCl/CuO may therefore be limited by its deep oxidation capability which requires two moles O_2 per mole C_2HCl_3 according to Reaction (13), and as previously mentioned, KCl/CuO is known to have a lower O_2 affinity than Cr_2O_3.

$$C_2HCl_3 + 2\ O_2 \longrightarrow 2\ CO_2 + HCl + Cl_2 \qquad [R13]$$

No $CHCl_3$ was formed by either catalyst when using the C_2HCl_3 feed. This is logical since neither oxychlorination of C_2HCl_3 (by KCl/CuO) nor deep oxidation of C_2HCL_3 (by Cr_2O_3) is likely to produce $CHCl_3$.

Selectivity for CCl_4, shown in Figure 26, is minor for both catalysts and in the range of 0–4 percent. For either catalyst the small quantities observed could have been obtained from oxidation of another product (C_2Cl_4), as shown and discussed below.

$$C_2Cl_4 + O_2 \longrightarrow CO_2 + CCl_4 \qquad [R14]$$

Figure 27 shows selectivity with both catalysts for formation of perchloroethylene (C_2Cl_4), a product not detected during CH_2Cl_2 oxidation. With Cr_2O_3 catalyst, almost no C_2Cl_4 (1–2 percent) was found, whereas with KCl/CuO, selectivity to C_2Cl_4 ranged from about 40 percent down to 20 percent with higher water addition. This significant difference again emphasizes the basic contrasting behavior of these two catalysts, with oxychlorination, a highly favored route for the KCl/CuO catalyst, but not for Cr_2O_3.

$$2\ C_2HCl_3 + 2\ HCl + O_2 \longrightarrow 2\ C_2Cl_4 + 2\ H_2O \qquad [R15]$$

Formation of HCl during C_2HCl_3 oxidation is shown in Figure 28. Trends for HCl production with both catalysts are similar to the CH_2Cl_2 results discussed previously, indicating increased HCl as the feed ratio is reduced. However, values for HCl produced over either catalyst with C_2HCl_3 feed are 10–20 percent lower than with CH_2Cl_2 feed on a normalized basis. This probably reflects the fact that C_2HCl_3 is hydrogen deficient as compared to CH_2Cl_2.

Unfortunately, production of Cl_2 from C_2HCl_3 oxidation was documented only for the Cr_2O_3 catalyst. These results (in the range of 5–10 percent) are slightly lower than corresponding values for CH_2Cl_2 oxidation over Cr_2O_3, but show the same decreasing trend with H_2O addition presumably because of the reverse Deacon reaction to produce HCl.

Small amounts of phosgene ($COCl_2$), from 0–5 percent, were detected after C_2HCl_3 oxidation with both catalysts (at the high end with KCl/CuO and at the low end with Cr_2O_3), independent of H_2O addition. Since $COCl_2$ was not detected

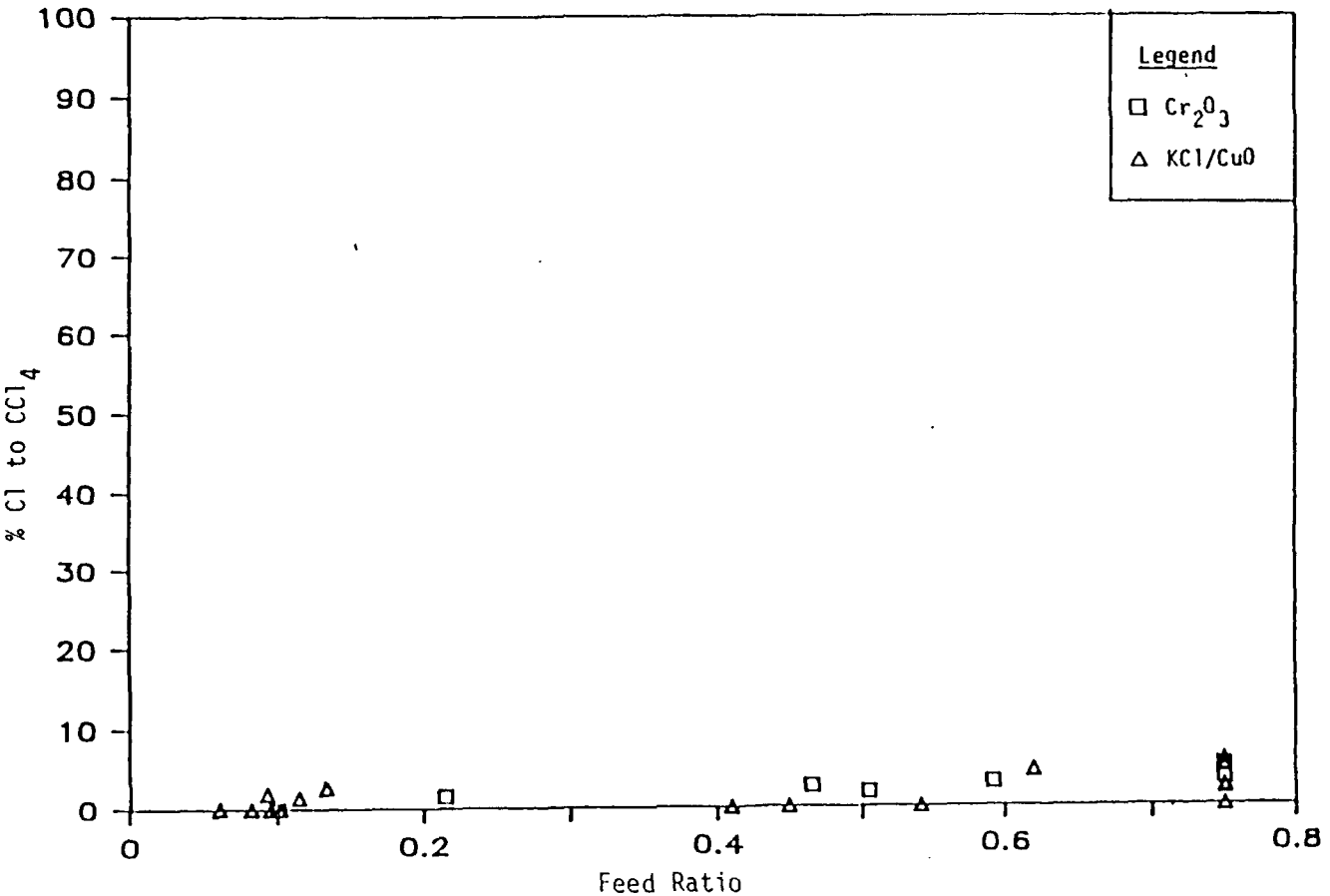

Figure 26. Selectivity of Trichloroethylene to CCl_4 over Chromia and Copper Based Catalysts

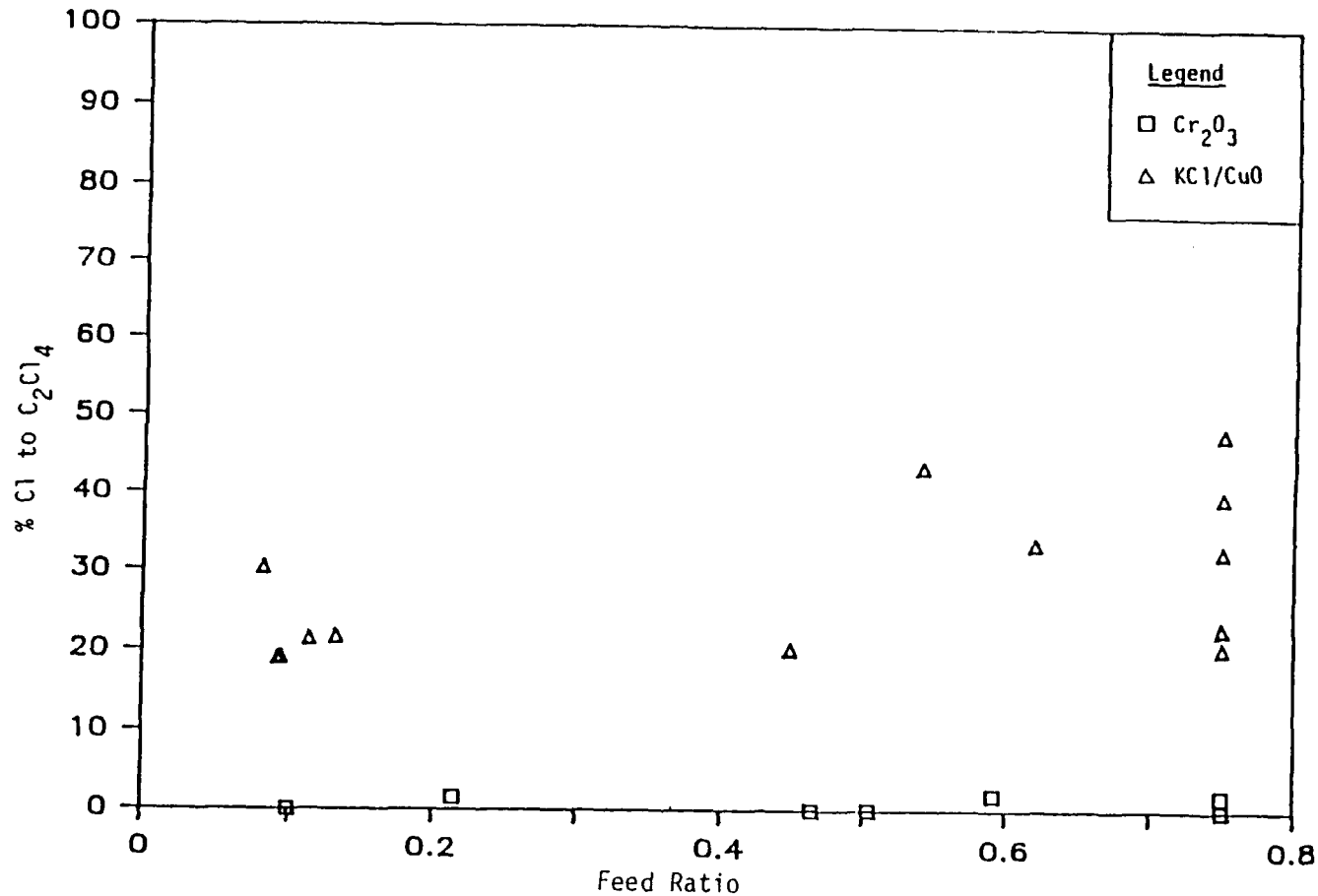

Figure 27. Selectivity of Trichloroethylene to C_2Cl_4 over Chromia and Copper Based Catalysts

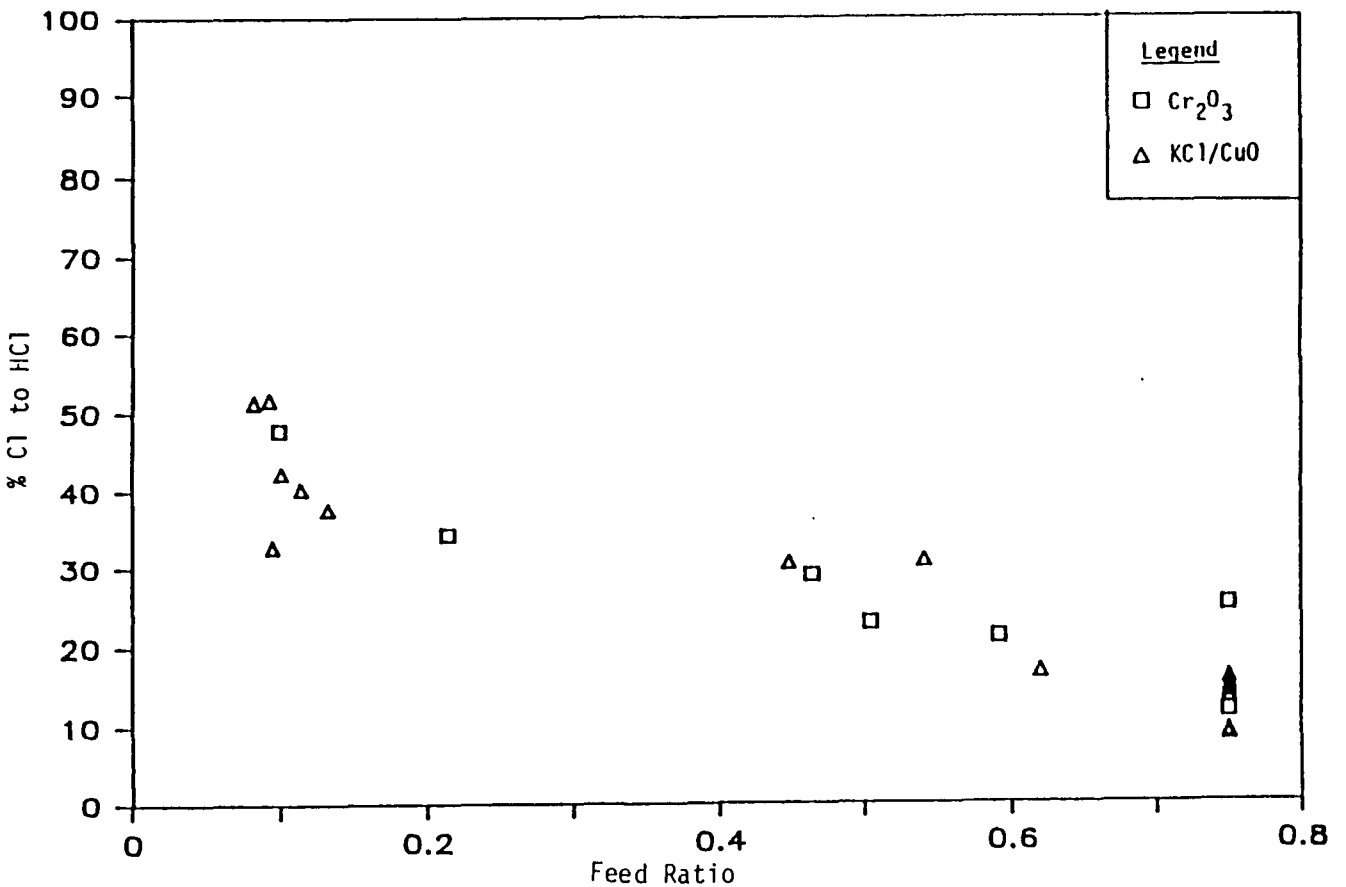

Figure 28. Selectivity of Trichloroethylene to HCl over Chromia and Copper Based Catalysts

during CH_2Cl_2 oxidation, it probably arises from the further oxidation of the intermediate product C_2Cl_4,

$$C_2Cl_4 + O_2 \longrightarrow 2\ COCl_2 \qquad [R16]$$

although an additional direct oxidation route over the Cr_2O_3, may also be possible.

$$C_2HCl_3 + O_2 \longrightarrow COCl_2 + HCl + CO \qquad [R17]$$

No chlorinated ethanes were detected in any C_2HCl_3 oxidation runs, suggesting that addition across the C–C double bond reported (Reference 41) to occur at lower temperatures (300–350°C), does not proceed to any appreciable extent with either catalyst at 500°C.

Figure 29 summarizes the C–Cl bond breaking efficiency of both catalysts for a C_2HCl_3 feed. As expected, the Cr_2O_3 is again superior to the KCl/CuO catalyst because of its selectivity toward deep oxidation rather than oxychlorination.

3. Oxidation of C_2HCl_3/CH_2Cl_2 Mixture

For the Cr_2O_3 catalyst only, a series of oxidation runs using a 1:1 mole ratio C_2HCl_3/CH_2Cl_2 mixed feed, with and without water addition, was carried out to determine the existence and magnitude of any competitive effects. Since variations compared to results from single component oxidation runs are small, data are summarized below without use of graphical presentation.

Results with the Cr_2O_3 catalyst show that conversion of C_2HCl_3 in C_2HCl_3/CH_2Cl_2 mixtures is enhanced from about 65 percent (as a single component feed) to about 75 percent (C_2HCl_3/CH_2Cl_2 mixed feed). Conversely, CH_2Cl_2 conversion drops from about 60 percent (as a single component) to 50 percent when present in the C_2HCl_3/CH_2Cl_2 mixture. The reason for these modest changes in activity could be because of competitive chemisorption effects, with surface affinity for C_2HCl_3 somewhat greater than for CH_2Cl_2. Product selectivity showed no unpredictable changes using mixed C_2HCl_3/CH_2Cl_2 feeds, being an approximate average of the results obtained from separate C_2HCl_3 and CH_2Cl_2 oxidations over the Cr_2O_3 catalyst.

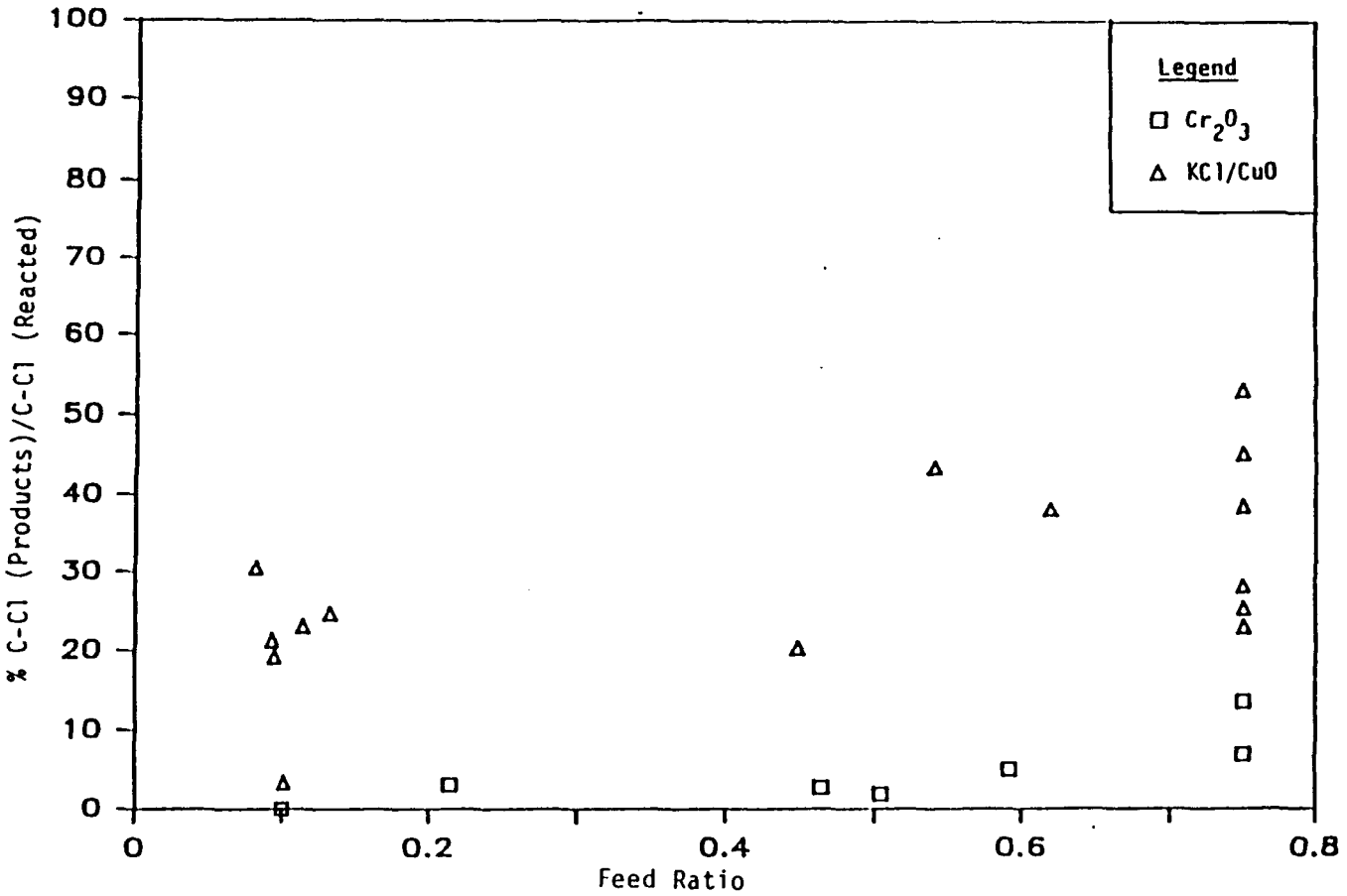

Figure 29. Percentage C-Cl Bonds Remaining in Products after Trichloroethylene Oxidation versus Feed Ratio

SECTION V

STUDY OF KCl/V_2O_5 CATALYST

A. INTRODUCTION

The emphasis of this section is to understand reaction pathways for the new SLP catalyst, KCl/V_2O_5, by variation of experimental conditions, including feed composition, residence time, catalyst preconditioning, etc. The experimental setup i.e., the reactor and analytical techniques, is discussed in Section II.

CH_2Cl_2, $CHCl_3$ and CCl_4 were used as reactants to evaluate this catalyst system. Varying amounts of water vapor were also added to some of the feed streams to determine its effects on conversion and product distribution for each chlorinated methane.

The competition for reaction sites as well as any effects related to interaction of the reactants or products were also studied by using mixtures of these chlorinated methanes as feed. CH_2Cl_2 alone was used as a benchmark feed to study long term usage of this catalyst and effects of residence time on the spectrum of products. Also, studies were conducted to show the effects of adsorbed and lattice oxygen on catalyst performance. Finally, the relative merits of HCl and Cl_2 as chlorinating agents were investigated.

B. RESULTS AND DISCUSSION

1. Chlorinated Feed Trials

In this part, presentation and discussion of results of trials using CH_2Cl_2, $CHCl_3$ or CCl_4 feeds with and without water are made. The amount of water added can approach 100 percent relative humidity at room temperature (about 20,000 ppm), allowing the concentration of water to be an order of magnitude greater than for the chlorinated feed.

Figure 30 shows the conversion of the various feeds versus the feed ratio. CH_2Cl_2 feed shows a conversion of nearly 50 percent without water vapor present, decreasing to slightly over 20 percent at the lowest attained feed ratio, which corresponds to the addition of 20,000 ppm water vapor. This result could perhaps be explained by the competition for catalyst sites between CH_2Cl_2 and H_2O. In addition, water inhibits the Deacon reaction, and therefore, direct chlorination, as well as oxychlorination reactions. Inhibition of these reactions may also explain, in part, why conversion is decreasing.

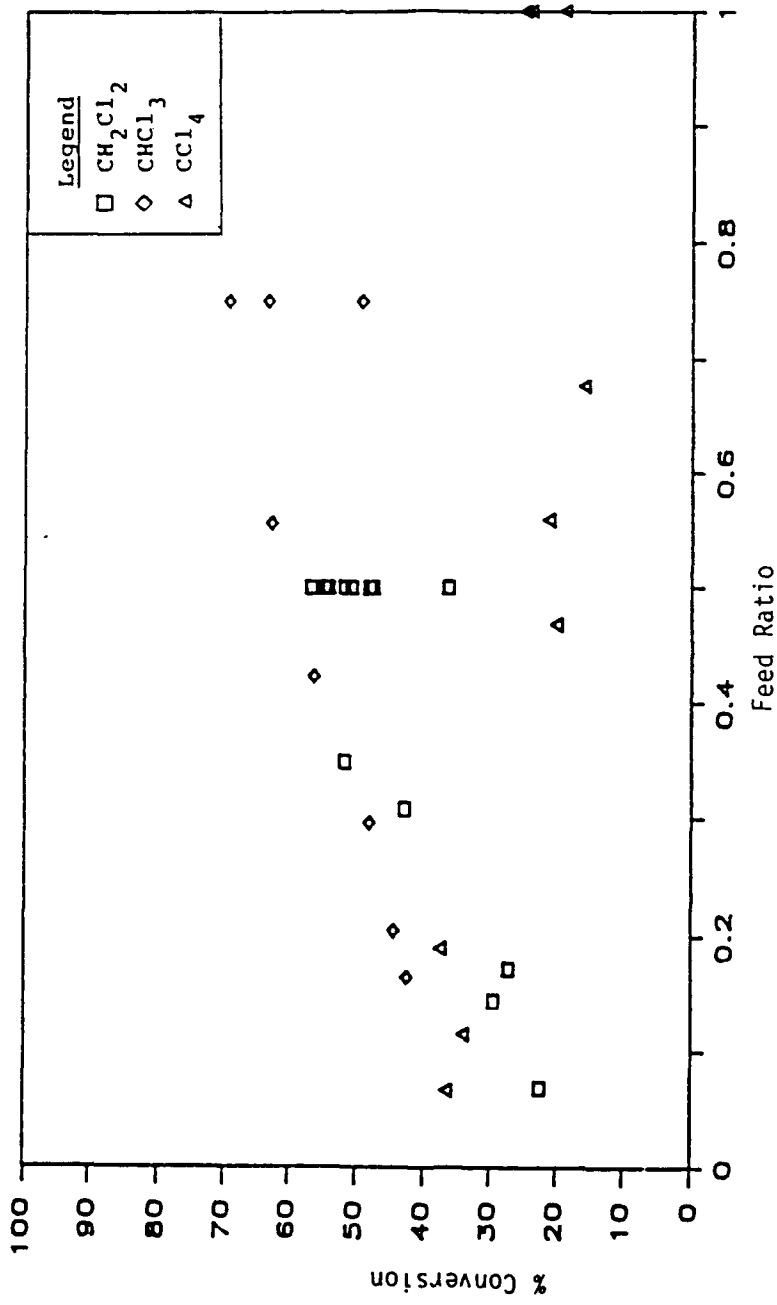

Figure 30. Conversion of Chlorinated Methanes versus Feed Ratio

Interestingly, $CHCl_3$ feeds were found to yield the highest conversions over the range of feed ratios studied. It was initially felt that $CHCl_3$ would be more stable and more resistant to catalytic oxidation because of its less favorable free energy change for complete oxidation. Conversions without water were over 60 percent, decreasing to just over 40 percent as more water was added. The low conversion at a feed ratio of 0.75 is explained later in this section. $CHCl_3$ was also unique in that formation of C_2 molecules (C_2Cl_4 and C_2Cl_6 in particular) was noted when $CHCl_3$ was reacted. No C_2-hydrocarbons were detected for runs made with CCl_4 or CH_2Cl_2. Perhaps because $CHCl_3$ has more pathways for reaction, it tends to have a higher conversion.

Overall, inhibition of $CHCl_3$ conversion by H_2O seemed to be less than for CH_2Cl_2. This may be because CH_2Cl_2 forms more products of higher chlorination than does $CHCl_3$. These reactions are strongly inhibited by water, and since water is a product, this may be partly responsible for the decrease in conversion. Another reason for the decrease in $CHCl_3$ conversion is that $CHCl_3$ is also in competition with water for reaction sites.

As expected, CCl_4 generally showed the poorest conversion of the three chlorinated methanes. CCl_4 was unique in that its conversion increased with increased water addition. CCl_4 was also unique in that it formed no chlorinated organics as did $CHCl_3$ and CH_2Cl_2. Therefore, there are no reactions involving CCl_4 which are inhibited by water. Chlorine formed by oxidation of CCl_4 can be consumed by water via the reverse Deacon reaction, thus encouraging further oxidation of CCl_4.

Several runs were made with each chlorinated methane without addition of water. As shown in Figure 30, these data fall into a range of percentages rather than a single point. These differences can be related to a number of factors including errors in precision and changes in the catalyst surface. Other deviations in the data can occur because of the human error involved in the collection and injection of samples as well as fluctuations in the flow in the reactor, and daily changes in the performance of GC/MS.

Any changes in catalyst surface appeared to occur over long periods of time (20–40 hours of operation) and therefore it was difficult to assign any error to this factor. However, in some runs, the change in conversion (sometimes as much as 10 percent as in Figure 30) from one run to the next was greater than any changes in material balance (which were as minute as 1-2 percent). Several of the runs with low conversions were the first runs for that day, indicating the catalyst may not have been properly oxidized before the experiments had started.

In addition, all of these errors are cumulative, which helps to explain the deviations seen in some of the following figures. Figures using selectivity criteria usually suffer most since two errors are being divided creating yet another, possibly greater error.

Figure 31 shows the C–Cl formed/reacted ratio versus feed ratio. Both CH_2Cl_2 and $CHCl_3$ show reduced amounts of chlorinated organics for higher amounts of water addition. This results from inhibition of the Deacon reaction, thus inhibiting direct chlorination. Water also inhibits oxychlorination, and probably also inhibits formation of C_2–organics from $CHCl_3$.

The scatter of the data for CH_2Cl_2 runs without water was high because some runs included had low conversions. As mentioned earlier, these runs were the first runs of the day, indicating that an insufficient time was allowed for the catalyst surface to oxidize. Also, these data were created by the division of two numbers with error, thus exacerbating the error.

Although the C–Cl formed/reacted data for $CHCl_3$ do not include C_2Cl_6, it is suspected that C–Cl formed/reacted ratios for $CHCl_3$ feed will still remain lower than those of CH_2Cl_2 for any given feed ratio. Even if it is assumed that C_2Cl_6 formation is equal to that of C_2Cl_4 (approximately 10–15 percent of converted chlorine at a *feed ratio of* 0.75), the C–Cl formed/reacted ratio would overall still be lower for $CHCl_3$ at any feed ratio. If this is assumed, along with the fact that CH_2Cl_2 forms two chlorinated methanes ($CHCl_3$ and CCl_4) and $CHCl_3$ forms only one (CCl_4) along with C_2Cl_4 and C_2Cl_6, it appears that chlorination of chlorinated methanes occurs more readily than formation of C_2–chlorinated hydrocarbons.

As mentioned previously, CCl_4 does not form any chlorinated hydrocarbons. Therefore, its C–Cl formed/reacted ratio is zero throughout the feed ratio range.

Figure 32 shows $CHCl_3$ production from CH_2Cl_2 as a function of feed ratio. As expected, the trend generally shows that $CHCl_3$ production decreases as more water vapor is added. This results from inhibition by H_2O of oxychlorination of CH_2Cl_2 and by the reverse Deacon reaction (thus inhibiting direct chlorination).

Figure 33 shows CCl_4 production as a function of feed ratio. For either reactant, the trends show CCl_4 production decreasing as more water vapor is added. Also, as expected, CCl_4 production is much greater for $CHCl_3$ than for CH_2Cl_2. CCl_4 production from CH_2Cl_2 requires twice as much chlorinating agent (either Cl_2 or HCl) as does $CHCl_3$ and is the result of two reactions in series. As seen in Figure 34, the proportion of

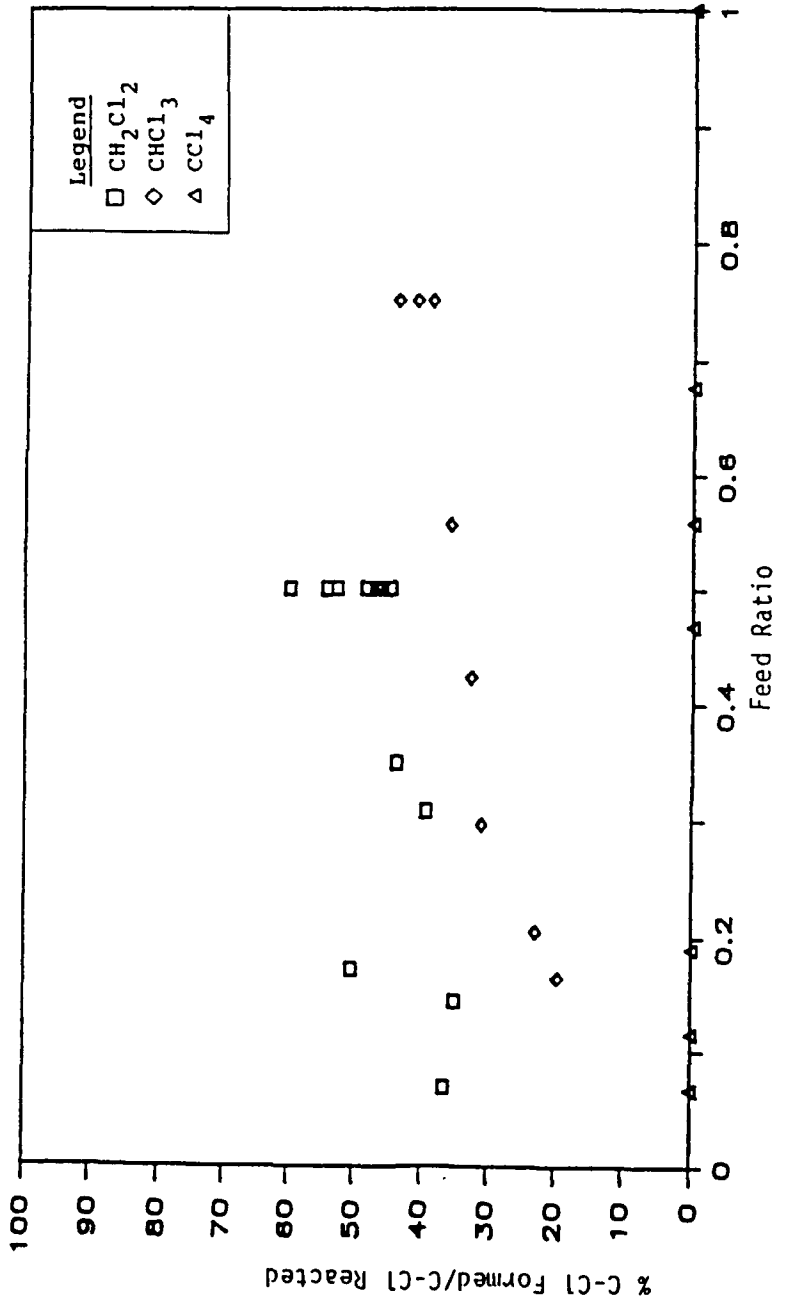

Figure 31. Chlorination Efficiency of Chlorinated Methanes versus Feed Ratio

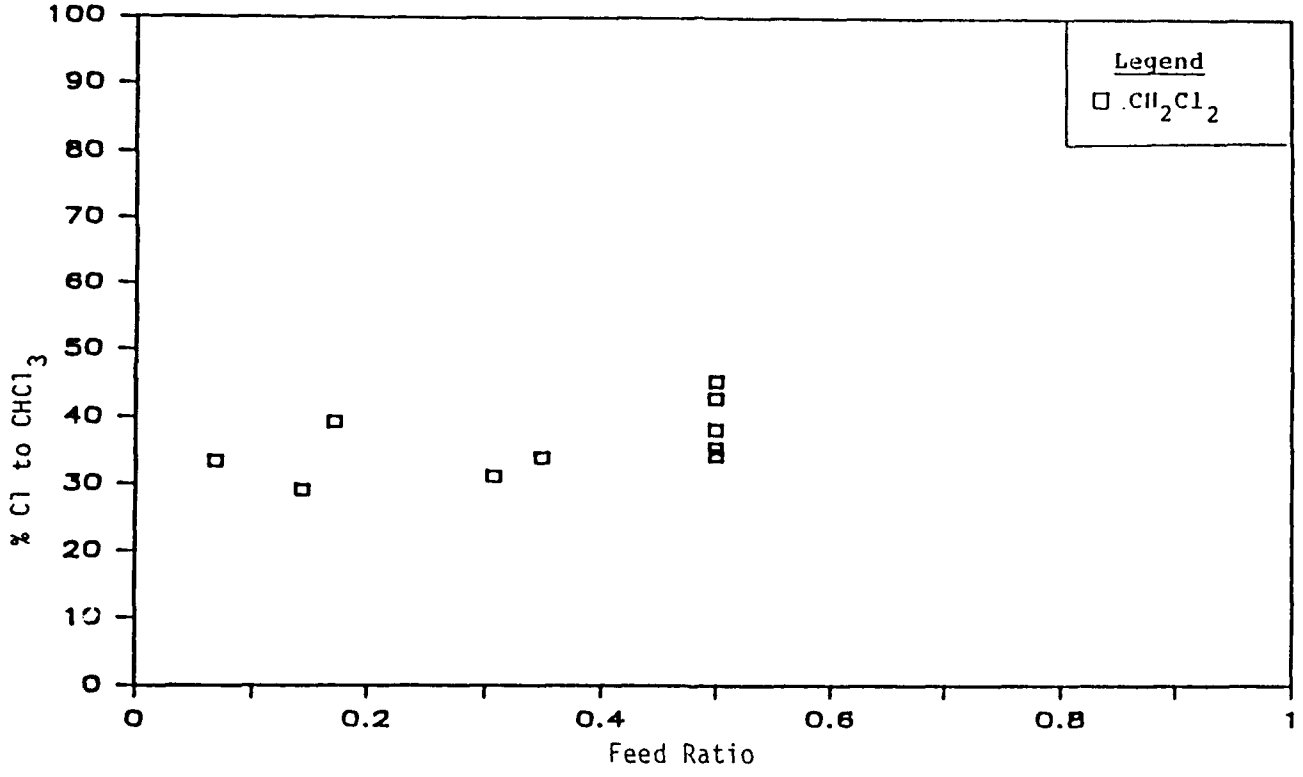

Figure 32. Selectivity to $CHCl_3$ versus Feed Ratio for Chlorinated Methane Reactant

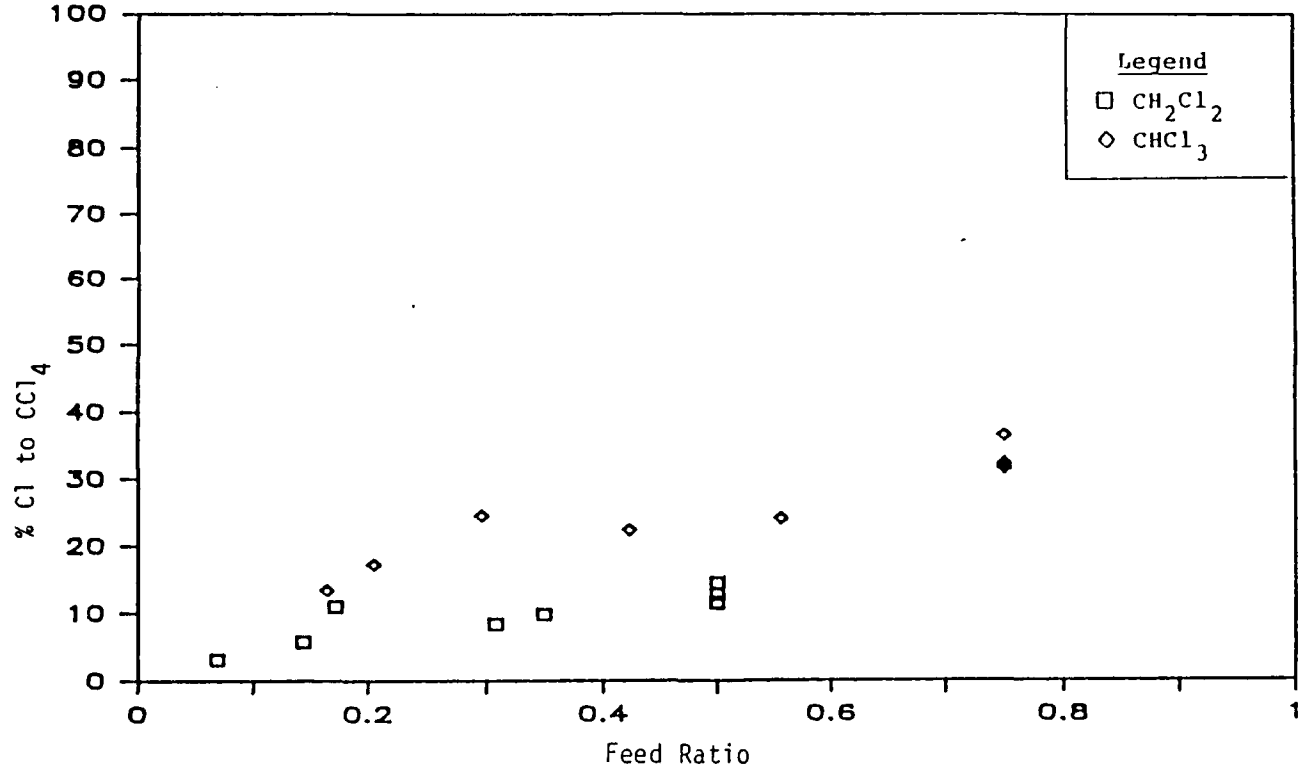

Figure 33. Selectivity to CCl_4 versus Feed Ratio for Chlorinated Methane Reactant

CCl_4 to $CHCl_3$ in the reactor effluent is fairly similar for either CH_2Cl_2 or $CHCl_3$ feeds. This suggests that formation of CCl_4 occurs primarily by chlorination of $CHCl_3$, making chlorination of CH_2Cl_2 to form CCl_4 directly an unlikely alternative.

Figure 35 shows C_2Cl_4 production as a function of feed ratio for each reactant. As previously mentioned, formation of C_2-chlorinated organics was noted only for $CHCl_3$ feed. Both C_2Cl_4 and C_2Cl_6 were formed when $CHCl_3$ was reacted. Formation of these products can be described by the following reactions:

$$4\ CHCl_3 + O_2 \rightarrow 2\ C_2Cl_6 + 2\ H_2O \qquad [R18]$$

$$C_2Cl_6 \rightarrow C_2Cl_4 + Cl_2 \qquad [R19]$$

$$4\ CHCl_3 + O_2 \rightarrow 2\ C_2Cl_4 + 2\ Cl_2 + 2\ H_2O \qquad [R20]$$

Reaction (18) should be considered both as an intermediate step in the production of C_2Cl_4, and as a final reaction in the production of C_2Cl_6 which was actually found in the product spectrum. The Gibbs free energies of reaction for the above reactions are -44,724, -1,128, and -46,980 cal/mole, respectively. These reactions appear to account for the trend noted in Figure 35 in that H_2O tends to inhibit formation of C_2Cl_4. Although it was not quantified, C_2Cl_6 peak areas were similar to those for C_2Cl_4, probably indicating that it was being formed in amounts similar to those of C_2Cl_4. Formation of C_2Cl_6 also appeared to be inhibited by water as predicted in Reaction (18).

Another potential route for formation of C_2Cl_4 would be as shown in Reaction (21).

$$2\ CHCl_3 \rightarrow C_2Cl_4 + 2\ HCl \qquad [R21]$$

This reaction path does not seem as viable mainly because C_2Cl_6 would have to be formed by the reverse of Reaction (19), giving it a positive Gibbs free energy of reaction.

Of great curiosity is the fact that only $CHCl_3$ produces C_2Cl_4 or C_2Cl_6. Reaction (22) proposes a pathway by which C_2Cl_4 could be formed from CH_2Cl_2.

$$2\ CH_2Cl_2 + O_2 \rightarrow C_2Cl_4 + 2\ H_2O \qquad [R22]$$

The Gibbs free energy for this reaction is -70,024 cal/mole which is far less than that of a more favorable pathway as shown in Reaction (23). This reaction has a Gibbs free energy of reaction of -170,520 cal/mole.

$$2\ CH_2Cl_2 + O_2 \rightarrow 2\ CO + 4\ HCl \qquad [R23]$$

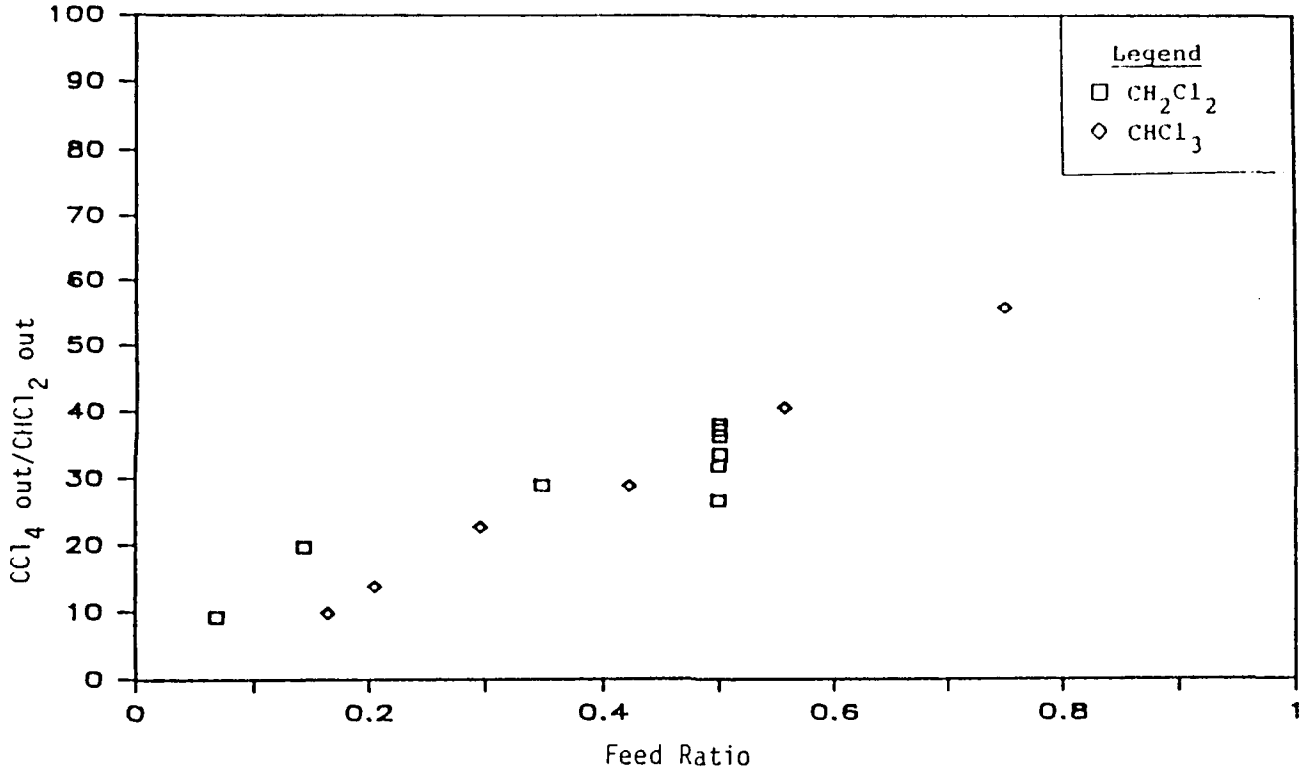

Figure 34. Relative Product Distribution of CCl_4 to $CHCl_3$ versus Feed Ratio for Chlorinated Methane Reactant

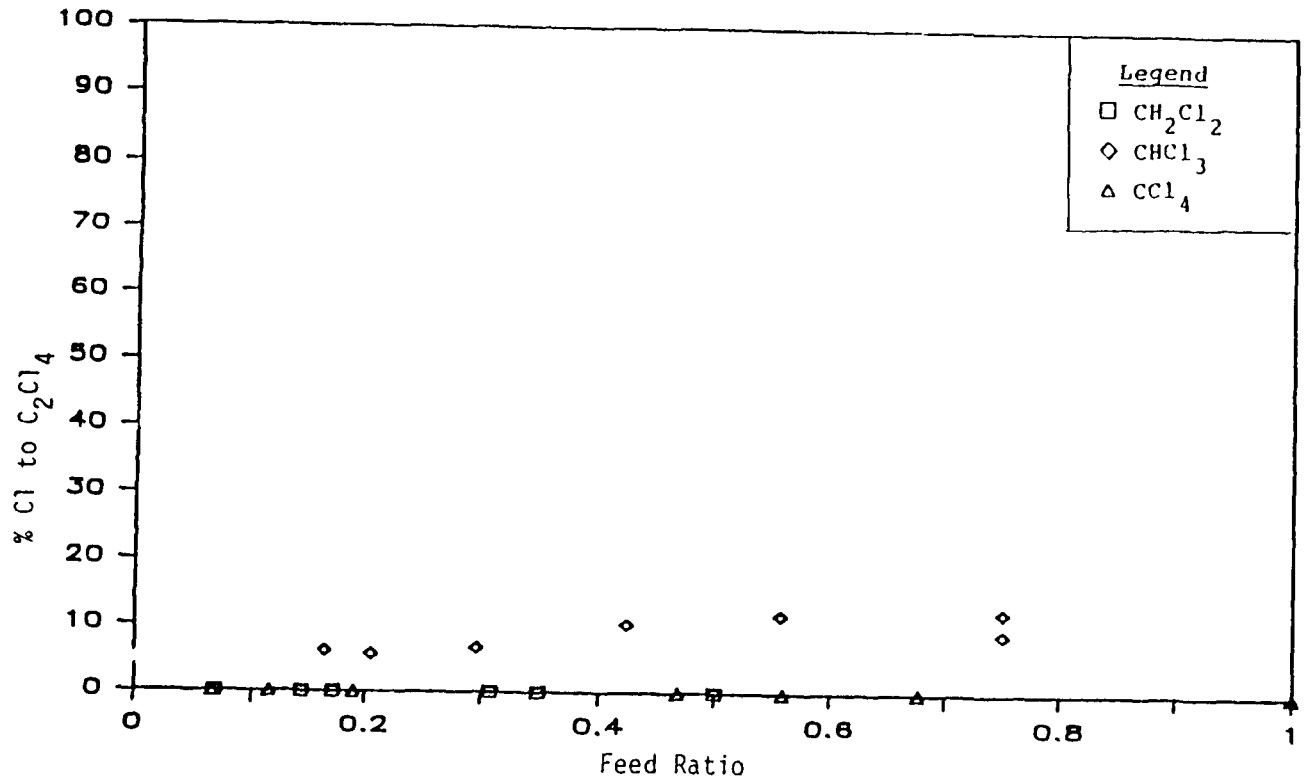

Figure 35. Selectivity to C_2Cl_4 versus Feed Ratio for Chlorinated Methane Reactant

Werner (Reference 42) states that C_2Cl_6 is a product of the thermal decomposition of $CHCl_3$ or CCl_4 as shown below.

$$2\ CCl_4 \rightarrow C_2Cl_6 + Cl_2 \qquad [R24]$$

This Reaction (24) has a Gibbs free energy of formation of +12,131 cal/mole at 500°C making it highly improbable that this reaction will occur. It is possible for $CHCl_3$ and CCl_4 to interact as shown in Reaction (25) to form C_2Cl_6 (allowing C_2Cl_4 to be formed via Reaction (19)).

$$CHCl_3 + CCl_4 \rightarrow C_2Cl_6 + HCl \qquad [R25]$$

This reaction has a low negative Gibbs free energy of formation of -3,759 cal/mole. In a stoichiometric feed of $CHCl_3$ and CCl_4, this reaction would have an equilibrium conversion of 22.7 percent at 500°C but this also assumes that products present in a run were inert. Since this reaction could also occur with CH_2Cl_2 feed (since both $CHCl_3$ and CCl_4 chlorinated hydrocarbons were noted as products), it does not appear likely that Reaction (25) is a viable pathway for formation of C_2Cl_4, especially when the presence of oxygen is considered.

Although $CHCl_3$ was present in CH_2Cl_2 runs, C_2-chlorinated hydrocarbons were not noted as products, possibly due to greater surface coverage by CH_2Cl_2 and lower concentrations of $CHCl_3$, leading to undetectable quantities of these products. A more likely reason may be that the surface bonding or oxidation state of the catalyst is different for $CHCl_3$ as a reactant and $CHCl_3$ as a product. When $CHCl_3$ is formed as a product, either by oxychlorination or direct chlorination of CH_2Cl_2, it creates a reduced surface site lacking in O_2. If this is true, then reactions (18) and (20) cannot occur. However, $CHCl_3$ as a reactant can adsorb on an oxidized site and react as shown in reactions (18) and (20).

Both C_2Cl_4 and C_2Cl_6 are very stable chemicals that are difficult to destroy. A set of two runs was performed using C_2Cl_4 as the reactant. One run included a high amount of water vapor and the second run contained none. Neither run showed any detectable products nor any conversion of the C_2Cl_4 feed.

Figure 36 shows HCl production for each of the chlorinated methanes. As expected, when no water is present, HCl production follows the trend CH_2Cl_2 > $CHCl_3$ > CCl_4. However, CCl_4 appears to be the greatest producer of HCl when large amounts of water are present. This can be explained by the fact that CCl_4 oxidation does not provide products of chlorination, but rather Cl_2, allowing formation of more HCl by the reverse Deacon reaction. As more water is added, more HCl can be formed.

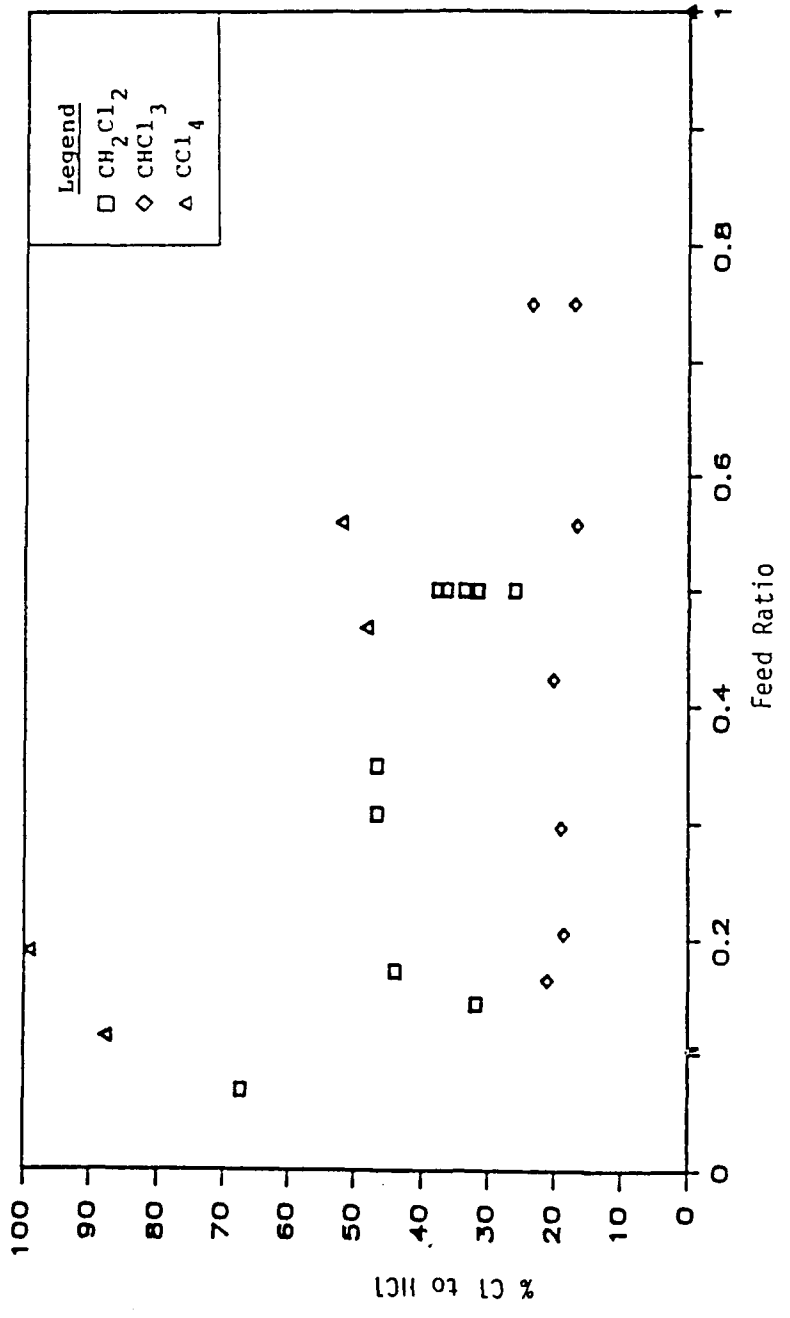

Figure 36. Selectivity to HCl versus Feed Ratio for Chlorinated Methane Reactant

CH_2Cl_2 also shows increased HCl as more water is added. The increase in HCl can be attributed to inhibition of the Deacon reaction as well as greater formation of HCl due to a relatively higher incidence of deep oxidation which also produces HCl.

$CHCl_3$ shows very little difference in selectivity to HCl as more water is added. It would be expected to increase, but only slightly since other chlorine-containing products are not decreasing as much as they are for CH_2Cl_2 feed.

HCl data tend to show more scatter than for other measured products. This can be explained by the fact that HCl data arise from only one point per run. Errors in HCl data can be caused by errors in titration of samples (inaccuracies in buret readings or in aliquots of NaOH added to each HCl sample) and time variations in reactor flow rate.

Figure 37 shows Cl_2 production for each of the chlorinated methanes. It appears that Cl_2 production for $CHCl_3$ and CH_2Cl_2 is fairly similar whereas CCl_4 runs (which did not produce any other organics) show significantly higher amounts of Cl_2. Increasing the water vapor level decreased the Cl_2 production for all the chlorinated organics. Reduction of Cl_2 levels for increased levels of water vapor was expected to occur by forcing the Deacon reaction to go in the reverse direction.

Figure 38 shows CO selectivity based on total converted carbon atoms. It is interesting to note that for feed ratio ranges less than 0.75, CO formation seems to be fairly independent of reactant. As will be seen later in this section, CO is used for $COCl_2$ formation, which can react further with H_2O to form CO_2 and HCl. However, since $COCl_2$ is even less prevalent than CO, it appears that CO formation is controlled primarily by its oxidation to form CO_2, as shown below.

$$2\ CO + O_2 \rightarrow 2\ CO_2 \qquad [R26]$$

In this case, the amount of CO present will limit the forward reaction, leaving the same relative amount of CO independent of reactant (i.e., the same extent of reaction is reached independent of reactant). This agrees with the two-step mechanism of Chang, et al. (Reference 43) which proposes that chlorinated hydrocarbons are first converted to CO, H_2O, Cl_2, and HCl. The second step involves Cl_2 and HCl inhibited oxidation of CO to CO_2. However, it is felt that the predominant route to CO_2 formation is by direct oxidation of the chlorinated hydrocarbon. First, excess oxygen is available to fully oxidize the chlorinated hydrocarbon. Second, complete oxidation to CO_2 and other inorganics is more favored thermodynamically than incomplete oxidation to CO and other

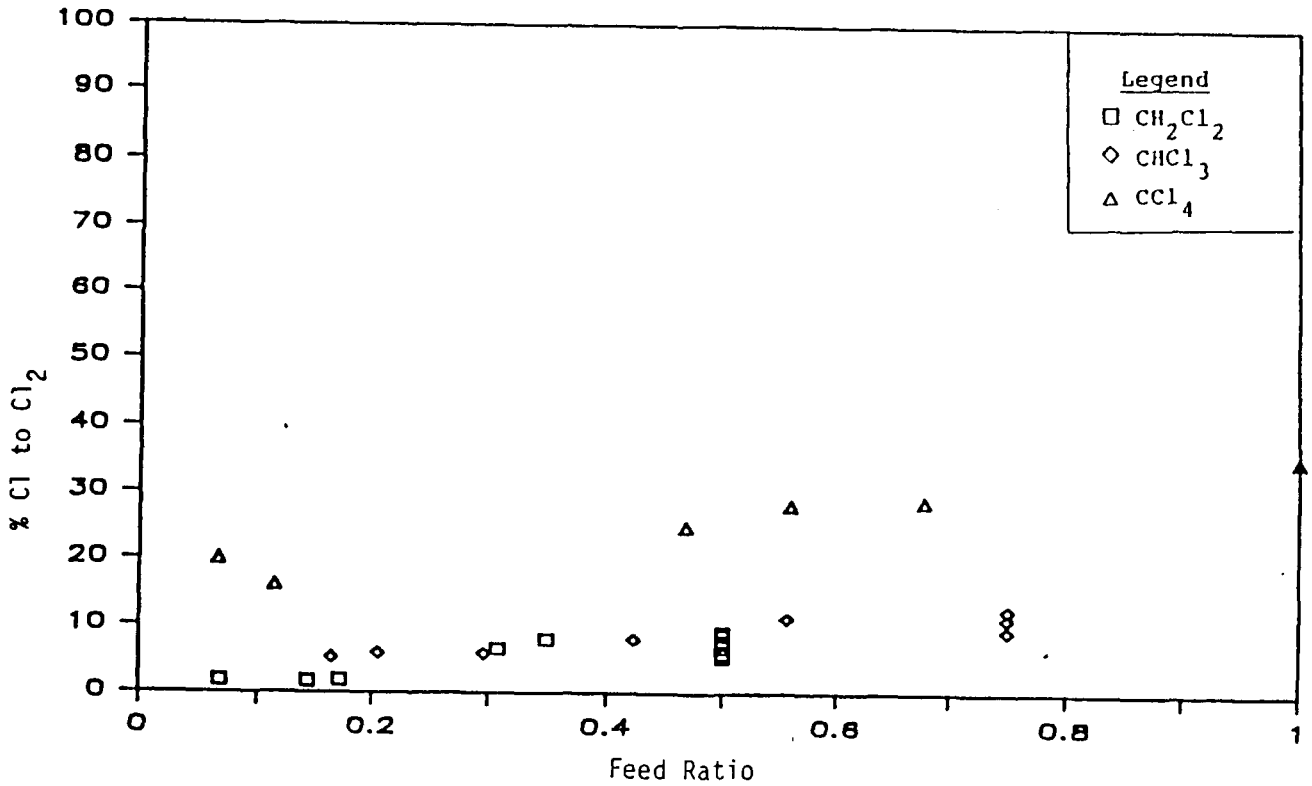

Figure 37. Selectivity to Cl_2 versus Feed Ratio for Chlorinated Methane Reactant

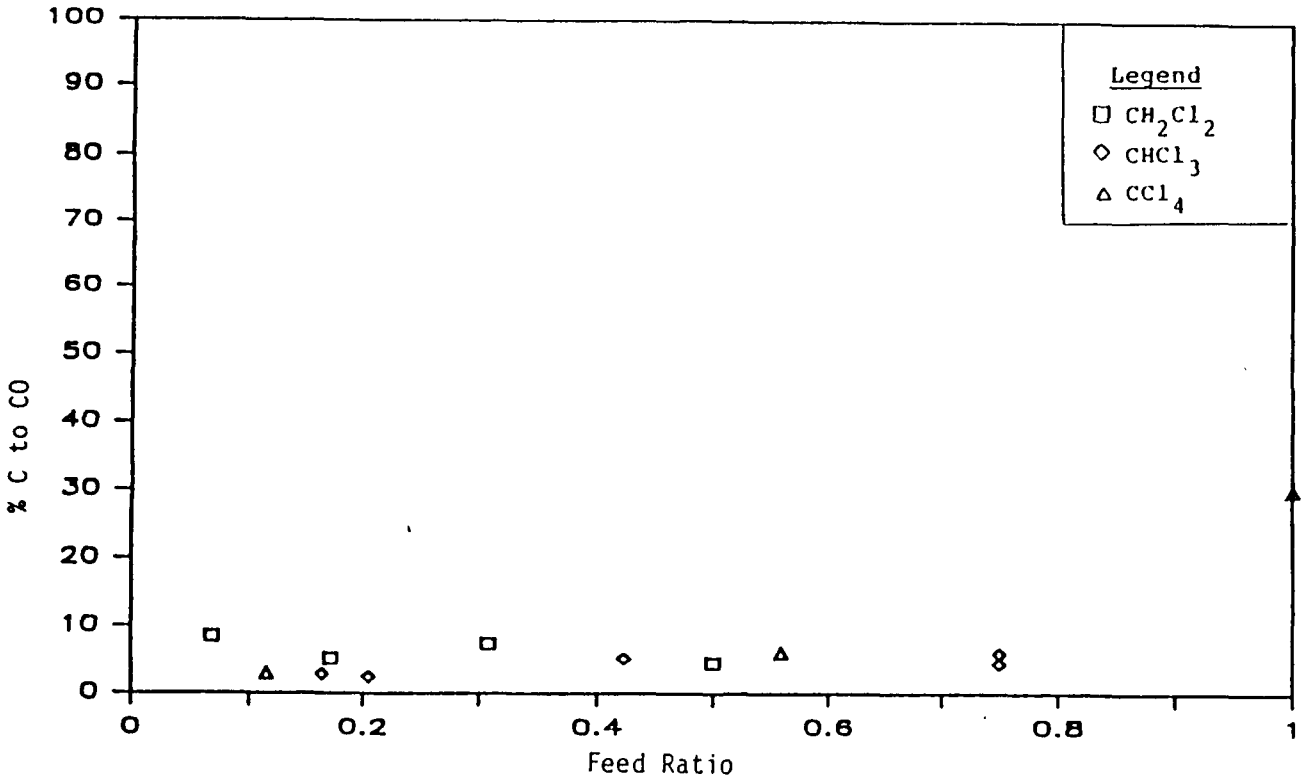

Figure 38. Selectivity to CO versus Feed Ratio for Chlorinated Methane Reactant

inorganics. The oxidation of CO to form CO_2 is merely the reaction that controls the final amount of CO in the effluent.

The very high amount of CO formed from oxidation of CCl_4 is not easily explained. This point was taken only once with a detector tube. The color change was not the same as for other experiments. It may simply represent an anomalous point.

Figure 39 shows $COCl_2$ production for CH_2Cl_2, $CHCl_3$, and CCl_4 feeds. It can be noted that $COCl_2$ formation is uniformly low for each chlorinated feed. Formation of $COCl_2$ from CO does not have favorable equilibrium thermodynamics. In addition, CO formation was also very low, thus further limiting possible formation of $COCl_2$ to the very small amounts.

Since $COCl_2$ production appears to be independent of the chlorinated methane reactant, it appears that $COCl_2$ is not formed directly from the reactant, but rather from oxychlorination, or to a lesser extent from direct chlorination of CO (formed by the incomplete oxidation of chlorinated methanes). Ashton and Ryan (Reference 44) have shown the following reactions to be the probable routes of formation for $COCl_2$.

$$COCl_2 + H_2O \rightarrow CO_2 + 2\ HCl \qquad [R27]$$

$$2\ CO + 4\ HCl + O_2 \rightarrow 2\ COCl_2 + 2\ H_2O \qquad [R28]$$

$$CO + Cl_2 \rightarrow COCl_2 \qquad [R29]$$

These reactions have Gibbs free energies of reaction of -49,170, -5,140, and -980 cal/mole at 500°C, respectively. When it is taken into account that Reaction (27) is far more favorable in a thermodynamic sense than either Reaction (28) or Reaction (29), it appears that $COCl_2$ formation will be negligible.

It also appears that $COCl_2$ formation does not depend on water vapor content since no increase or decrease in production was noted when the water vapor content was changed. This observation does not agree with Reactions (27) and (28) because they show that H_2O would inhibit $COCl_2$ formation. However, since addition of H_2O creates more HCl via the reverse Deacon reaction, the equilibrium in Reaction (28) is simultaneously pushed toward $COCl_2$ formation by HCl and pushed away by H_2O. This may help explain why $COCl_2$ is constant over the range of feed ratios. However, $COCl_2$ is noted as a product when HCl is absent (as in CCl_4 oxidation without water) leading to the conclusion that $COCl_2$ formation can occur by Reaction (29) as well. Therefore, it seems probable that the formation of $COCl_2$ occurs simultaneously by oxychlorination and direct chlorination of CO. Oxychlorination seems more favorable overall, especially in the low feed ratio ranges in which HCl is a more prominent

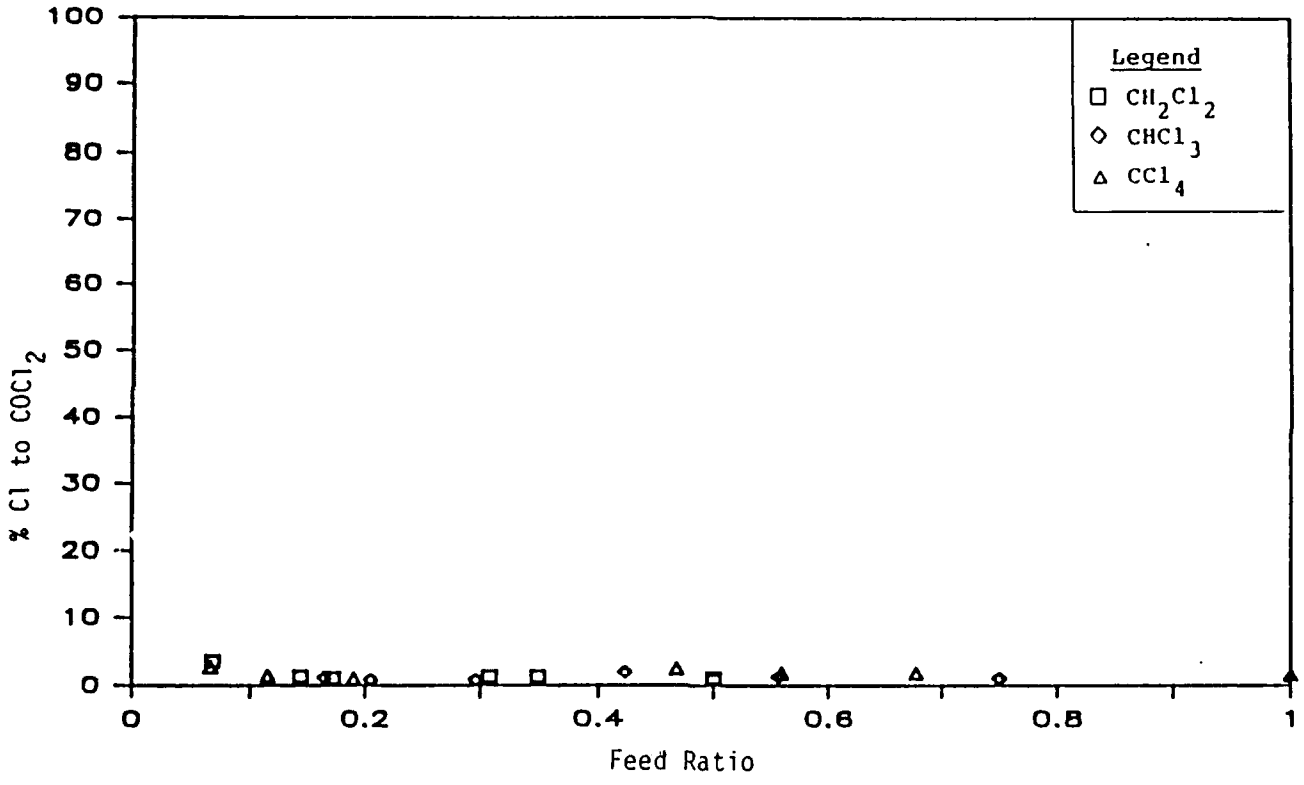

Figure 39. Selectivity to $COCl_2$ versus Feed Ratio for Chlorinated Methane Reactant

product. Formation of $COCl_2$ by direct chlorination of CO is probably significant only where Cl_2 is a more prominent product.

Figure 40 shows CO_2 formation for all three chlorinated methanes. The trend shows that selectivity to CO_2 is in the order CCl_4 > $CHCl_3$ > CH_2Cl_2. This is not surprising because other carbon-containing species are either independent of reactant and water (CO and $COCl_2$), or they are other chlorinated hydrocarbons. Since formation of chlorinated hydrocarbons is in the order CH_2Cl_2 > $CHCl_3$ > CCl_4, it appears that formation of CO_2 would be in the reverse order. It can also be seen that CO_2 increases with decreased feed ratio. This occurs because water tends to decrease further chlorination of chlorinated hydrocarbons, thereby enhancing deep oxidation and CO_2 formation. Increase in CO_2 formation with decreasing feed ratio occurs in the order CH_2Cl_2 > $CHCl_3$ > CCl_4.

Figure 41 shows the selectivity over the range of feed ratios of CO_2 to CO and CO_2. Although the selectivities for each chlorinated methane are similar, they appear to show that relative selectivity to CO_2 occurs in the order CCl_4 > $CHCl_3$ > CH_2Cl_2. This could have been easily predicted since CO formation is essentially independent of chemical reactant, whereas CO_2 formation is in the same order as above. It can be noted that all of these selectivities are generally 90 percent or better, indicating the predominance of CO_2 over CO. The fact that the selectivities are reactant-dependent and CO formation is reactant-independent tends to confirm that formation of CO is controlled by its oxidation to CO_2.

Figure 42 shows the selectivity of HCl to HCl and Cl_2. The figure shows a definite trend of higher HCl to Cl_2 as the amount of water is increased. These amounts are affected and controlled by the Deacon reaction. For any feed with a feed ratio greater than 0.5, the amount of HCl formed is further limited by the amount of hydrogen atoms in the feed. Therefore, when the Cl:H ratio is greater than 1, formation of Cl_2 will be an inevitable result for complete combustion. Overall, CH_2Cl_2 has the best HCl selectivity relative to Cl_2, while $CHCl_3$ and CCl_4 show very similar selectivities throughout most of the feed ratio range.

2. CH_2Cl_2 and $CHCl_3$ Mixtures

Presentation and discussion of results of trials using various mixtures of CH_2Cl_2 and $CHCl_3$ (without water addition) are given here. Figures 43 through 52 use the feed ratio range of 0.5 to 0.75. As the feed ratio increases, this indicates that the relative amount of $CHCl_3$ to CH_2Cl_2 is increasing.

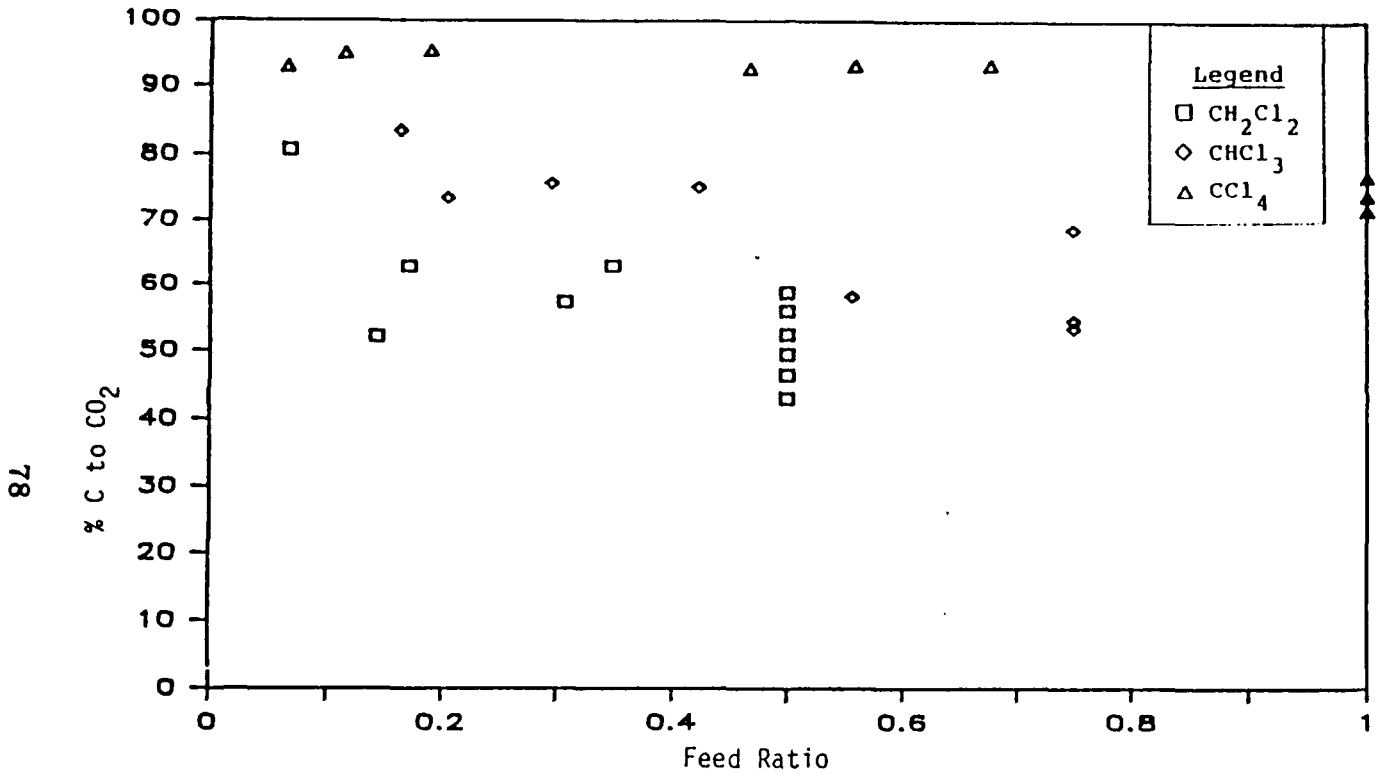

Figure 40. Selectivity to CO_2 versus Feed Ratio for Chlorinated Methane Reactant

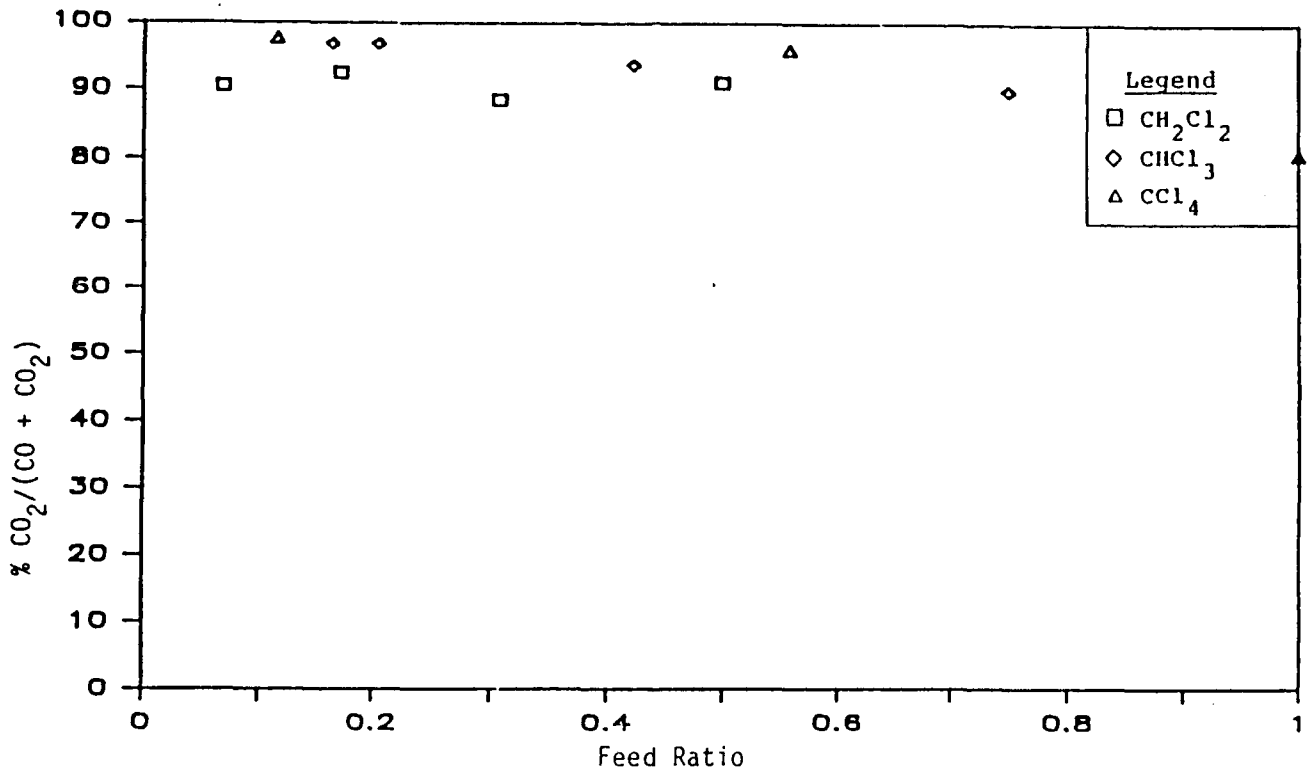

Figure 41. Relative Selectivity of CO_2 to CO and CO_2 versus Feed Ratio for Chlorinated Methane Reactant

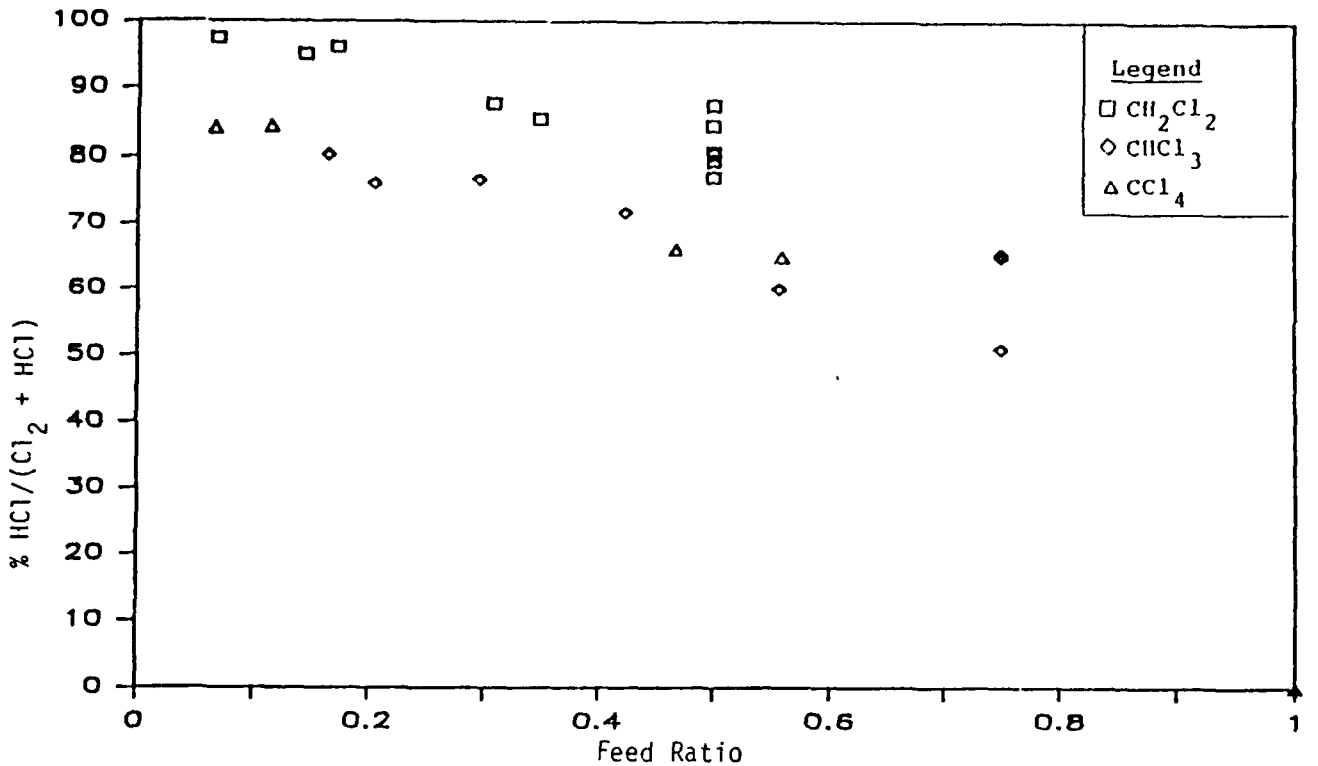

Figure 42. Relative Selectivity of HCl to HCl and Cl_2 versus Feed Ratio for Chlorinated Methane Reactant

Figure 43 shows the conversion of each reactant at different feed ratios. Interestingly, CH_2Cl_2 conversion actually increased as more $CHCl_3$ was added. A possible reason for the increase in CH_2Cl_2 conversion as more $CHCl_3$ was added may be preferential adsorption of CH_2Cl_2 over $CHCl_3$. In fact, a feed ratio of 0.55 showed a negative conversion for $CHCl_3$ indicating that more $CHCl_3$ was being formed than converted. In addition, $CHCl_3$ conversion increased as relative CH_2Cl_2 content decreased and was highest when no CH_2Cl_2 was present in the feed. These facts tend to confirm that KCl/V_2O_5 preferentially adsorbs CH_2Cl_2 over $CHCl_3$.

Figure 44 shows the overall conversion of $CHCl_3$–CH_2Cl_2 in mixtures. The overall conversion was determined by summing the inlet molar concentration times conversion for each reactant and dividing by the total molar concentration to yield the molar conversion of each of the two reactants. The decrease in efficiency as the feed ratio increased from 0.5 to 0.55 seems to be caused by the inability of $CHCl_3$ to adsorb when large amounts of CH_2Cl_2 are present. The increase in efficiency above a feed ratio of 0.55 may be due to improved adsorption of $CHCl_3$ as well as the tendency toward formation of C_2–chlorinated hydrocarbons.

Figure 45 shows C_2HCl_3 formation for the CH_2Cl_2–$CHCl_3$ mixture. C_2HCl_3 was not detected for pure feeds of either component and C_2HCl_3 formation was highest (about 3 percent) for a feed with nearly 1:1 CH_2Cl_2 to $CHCl_3$. Therefore, it is very probable that C_2HCl_3 is formed by the cooperation of $CHCl_3$ and CH_2Cl_2 on oxidized sites. The following reactions are proposed to describe the formation of C_2HCl_3.

$$2\ CH_2Cl_2 + 2\ CHCl_3 + O_2 \rightarrow 2\ C_2HCl_3 + 2\ Cl_2 + 2\ H_2O \quad [R30]$$

$$CH_2Cl_2 + CHCl_3 \rightarrow C_2HCl_3 + 2\ HCl \quad [R31]$$

$$2\ CH_2Cl_2 + 2\ CHCl_3 + O_2 \rightarrow 2\ C_2HCl_5 + 2\ H_2O \quad [R32]$$

$$2\ CHCl_3 \rightarrow C_2HCl_5 + HCl \quad [R33]$$

$$C_2HCl_5 \rightarrow C_2HCl_3 + Cl_2 \quad [R34]$$

$$CHCl_3 + CH_2Cl_2 \rightarrow C_2H_2Cl_4 + HCl \quad [R35]$$

$$C_2H_2Cl_4 \rightarrow C_2HCl_3 + HCl \quad [R36]$$

Of the foregoing, Reaction (31) does not seem as favorable as Reaction (30) or as the combination of Reactions (32) and (34) because Reaction (31) states that C_2HCl_3 formation could occur in pure CH_2Cl_2 feed since $CHCl_3$ is present as a product. Reaction (30) requires $CHCl_3$ to be on an oxidized site but $CHCl_3$ product is on a reduced site, and therefore it is not as likely

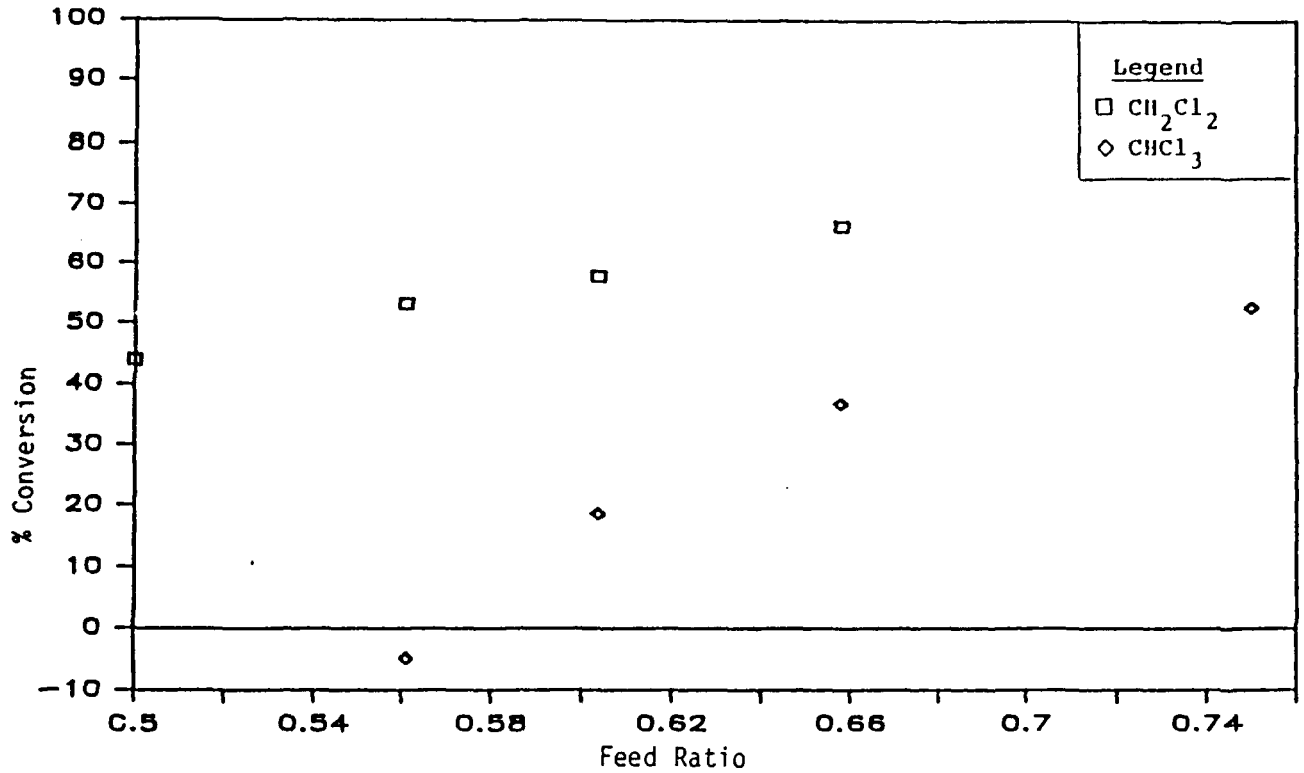

Figure 43. Conversion versus Feed Ratio for Mixtures of CH_2Cl_2 and $CHCl_3$

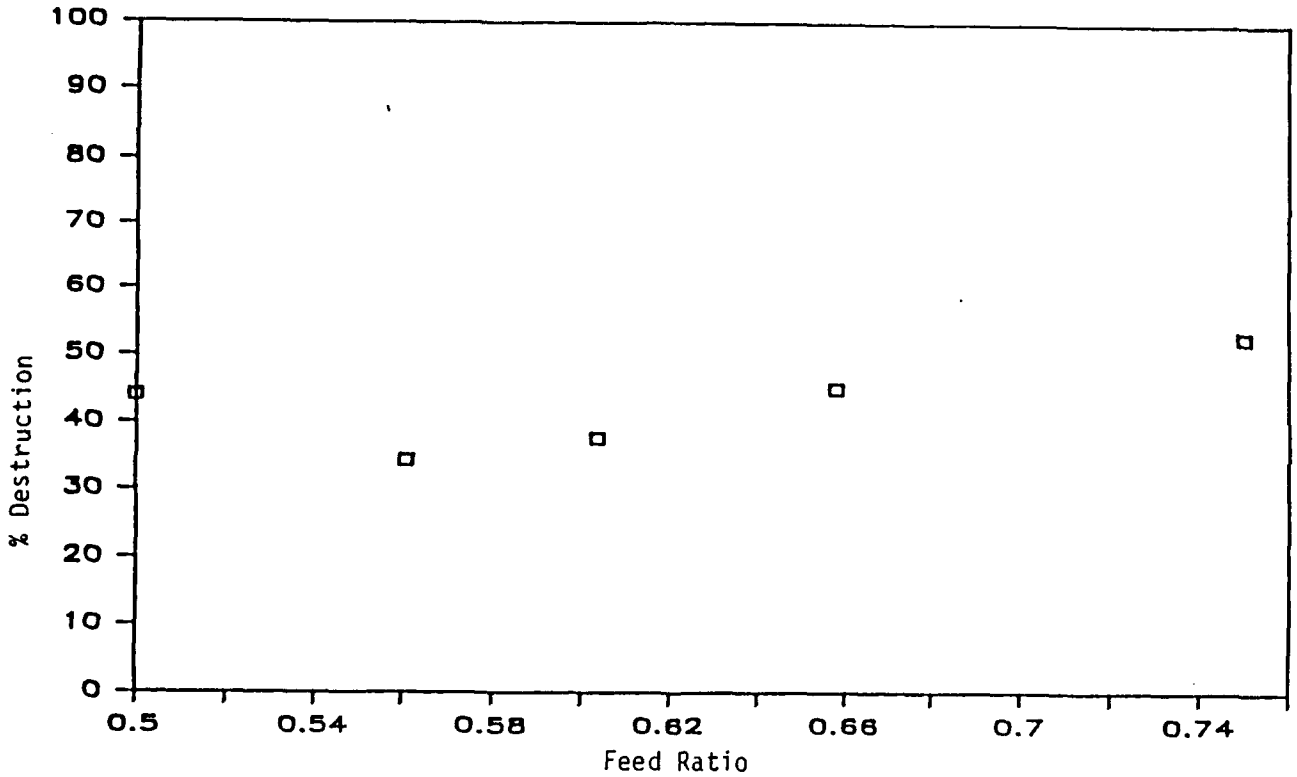

Figure 44. Destruction Efficiency versus Feed Ratio for Mixtures of CH_2Cl_2 and $CHCl_3$

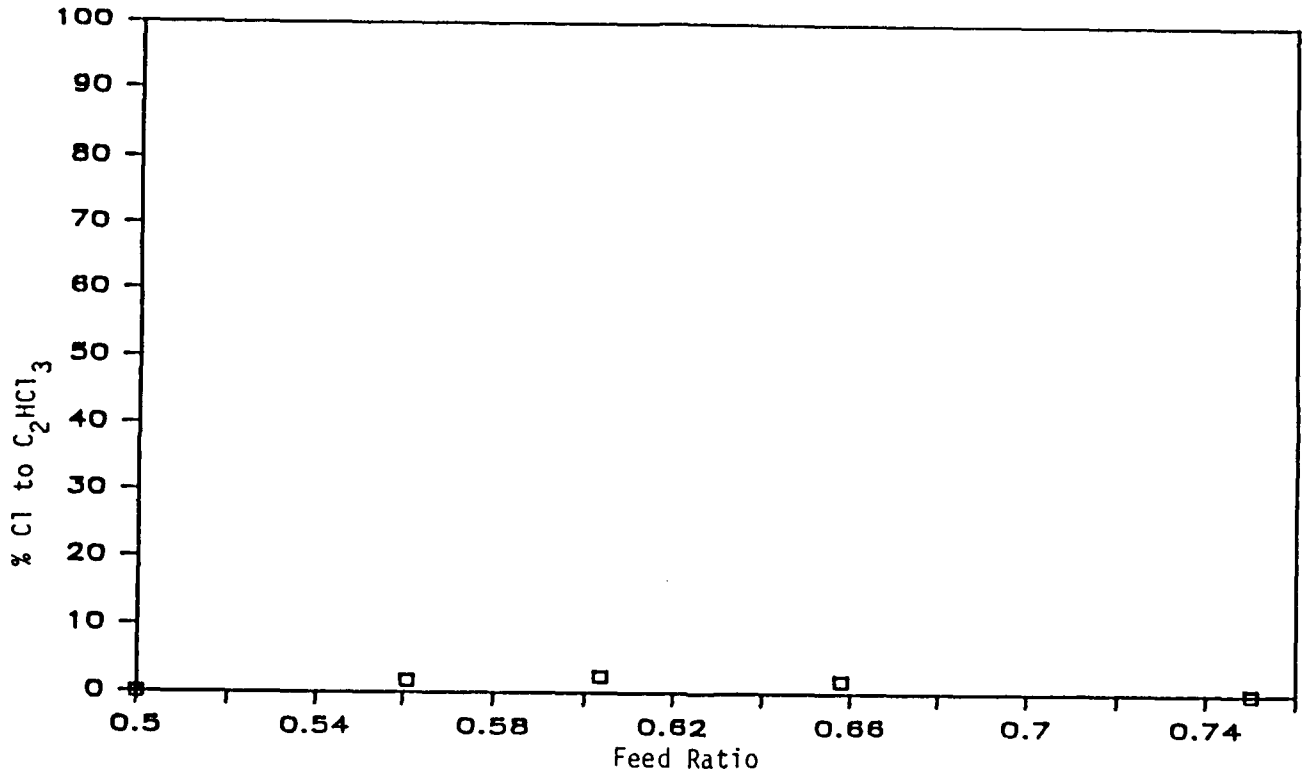

Figure 45. Selectivity to C_2HCl_3 versus Feed Ratio for Mixtures of CH_2Cl_2 and $CHCl_3$

that C_2HCl_3 will form when feeding CH_2Cl_2 alone. The fact that it does not form indicates that Reaction (31) is not as probable as Reaction (30).

Reaction (33) does not seem likely since formation of C_2HCl_5 is negligible for pure $CHCl_3$ feed. This appears to be confirmed by the fact that C_2HCl_3 (the decomposition product of C_2HCl_5) is also negligible as a product for pure $CHCl_3$ feed.

Reactions (35) and (36) collectively add up to Reaction (31). They do not seem as favorable as Reactions (30), (32), and (34) for the same reasons given for Reaction (31). However, Reaction (35) is the only reaction that can adequately explain formation of $C_2H_2Cl_4$, thus making it a probable pathway of formation.

Figure 46 shows the relative amounts of the chlorinated ethanes obtained in the $CHCl_3$–CH_2Cl_2 mixture runs. The relative amounts are based on the total integrated area on the GC/MS chromatogram for all the chlorinated ethanes. Even though the chlorinated ethanes were not quantified or calibrated, relative amounts in Figure 46 should be fairly representative since compounds of similar structure generally have similar response factors when based on the base peak of the mass spectrum.

Reaction (18) is thought to be the primary route of formation for C_2Cl_6. The reactants involved were $CHCl_3$ and O_2, therefore it is expected that the $CHCl_3$ feed alone would be the greatest producer of C_2Cl_6. This is confirmed by Figure 46, in which relatively negligible amounts of other chlorinated ethanes were formed.

If CH_2Cl_2 and $CHCl_3$ are fed in a 1:1 molar ratio (a feed ratio of 0.625), formation of $C_2H_2Cl_4$ and C_2HCl_5 should stoichiometrically be nearly equal as shown in reactions (32) and (35), if reaction rates are similar. This does appear to be the case, as seen by interpolation in Figure 46. At low feed ratios, $C_2H_2Cl_4$ production dominates C_2HCl_5 production. This would indicate that $C_2H_2Cl_4$ is being formed as shown in Reaction (37).

$$4\ CH_2Cl_2 + O_2 \rightarrow 2\ C_2H_2Cl_4 + 2\ H_2O \qquad [R37]$$

However, $C_2H_2Cl_4$ is not noted as a product when CH_2Cl_2 is reacted alone. A comparison of Figures 45 and 46 shows that production of C_2HCl_3 follows the relative formation of C_2HCl_5 suggesting that C_2HCl_3 may be formed from C_2HCl_5. C_2HCl_3 formation is probably using up relatively more C_2HCl_5 at the lower feed ratios since the formation of chlorinated ethanes increases from zero for CH_2Cl_2 feed to a maximum amount for $CHCl_3$ feed.

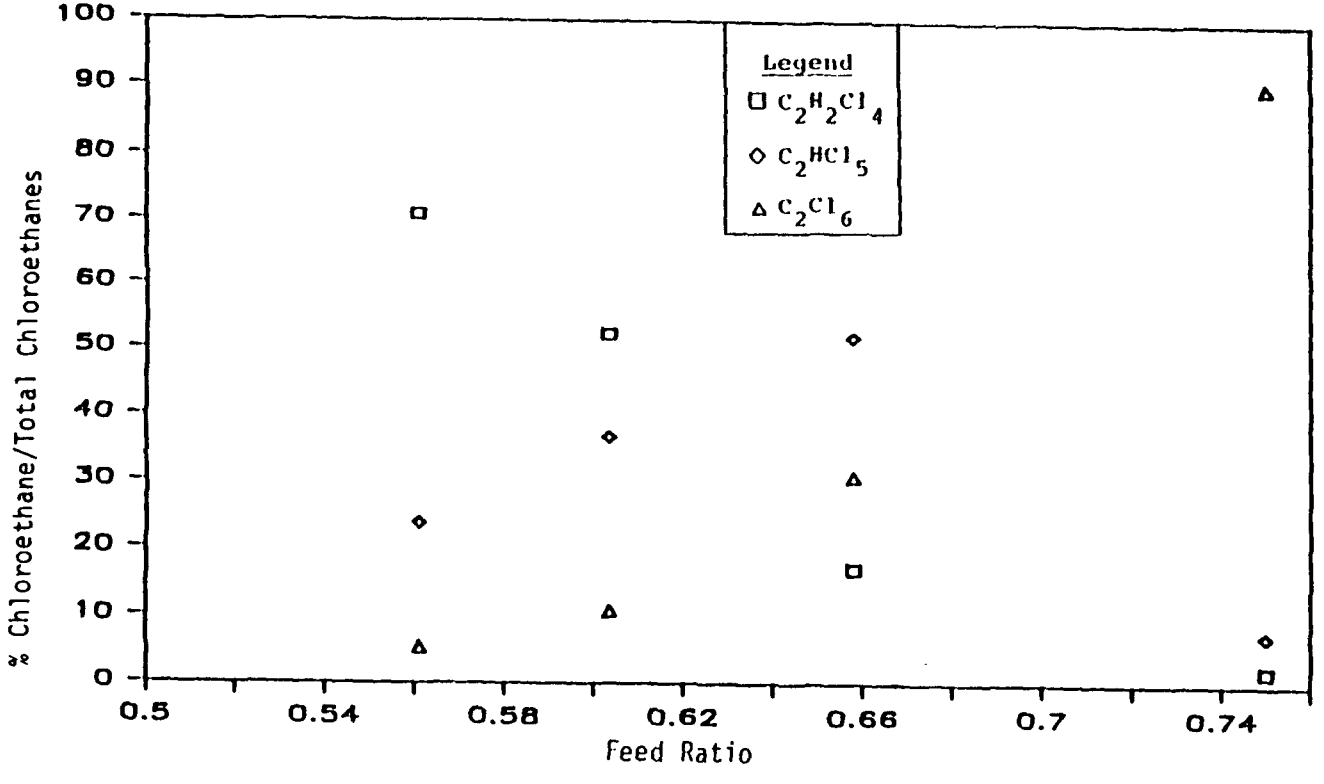

Figure 46. Relative Formation of Chlorinated Ethanes versus Feed Ratio for Mixtures of CH_2Cl_2 and $CHCl_3$

Figure 47 shows C_2Cl_4 production based on converted chlorine. As expected, C_2Cl_4 production increases as the relative amount of $CHCl_3$ is increased in the mixture, tending to confirm its method of formation from $CHCl_3$ via reactions (19) and (20).

Figure 48 shows CCl_4 production for these trials. The graph shows that CCl_4 production is greatest in the mixture runs. This may reflect the fact that formation of C_2-chlorinated hydrocarbons increases significantly as the feed ratio increases. This leaves less available $CHCl_3$ to form CCl_4. It may also indicate that some of the CH_2Cl_2 is being chlorinated directly to CCl_4 in the regions where CH_2Cl_2 is present, helping to increase CCl_4 formation in the mixture ranges of the feed ratio, although it does not seem likely that CH_2Cl_2 will directly chlorinate to CCl_4 as shown previously in Part 1.

Figure 49 shows Cl_2 production for the different feed ratios. Cl_2 production is greatest in the runs of pure $CHCl_3$ and pure CH_2Cl_2 with less formed in the mixture runs. This graph is a mirror image of the results shown in Figure 48. Cl_2 production is highest when CCl_4 production is lowest (for pure CH_2Cl_2 feed), decreasing to a low point when CCl_4 production has peaked for the mixture runs, and increasing again for the $CHCl_3$ run in which CCl_4 production has again decreased. This suggests an interaction between Cl_2 and CCl_4, but no mechanism can be suggested at this time to describe this relationship.

Figure 50 shows $COCl_2$ production versus feed ratio. $COCl_2$ production seems to be fairly independent of the mixture, agreeing with data presented previously in Part 1. The mechanism presented earlier, whereby $COCl_2$ was formed by a parallel route of either oxychlorination or direct chlorination of CO, still seems viable.

Figure 51 shows CO production versus feed ratio. Formation of CO shows very little dependence on reactant, although it does appear to be highest for CH_2Cl_2 and gradually decreasing as the feed ratio increases to 0.75. Generally, CO formation does not appear to be reactant-dependent but controlled by its oxidation to CO_2 as shown in Part 1.

Figure 52, which shows selectivity to HCl versus Cl_2 for the mixture trials, indicates that HCl formation is highest where CCl_4 formation is highest, again indicating that Cl_2 may be the primary chlorination agent, although it is difficult to draw concrete conclusions at this time.

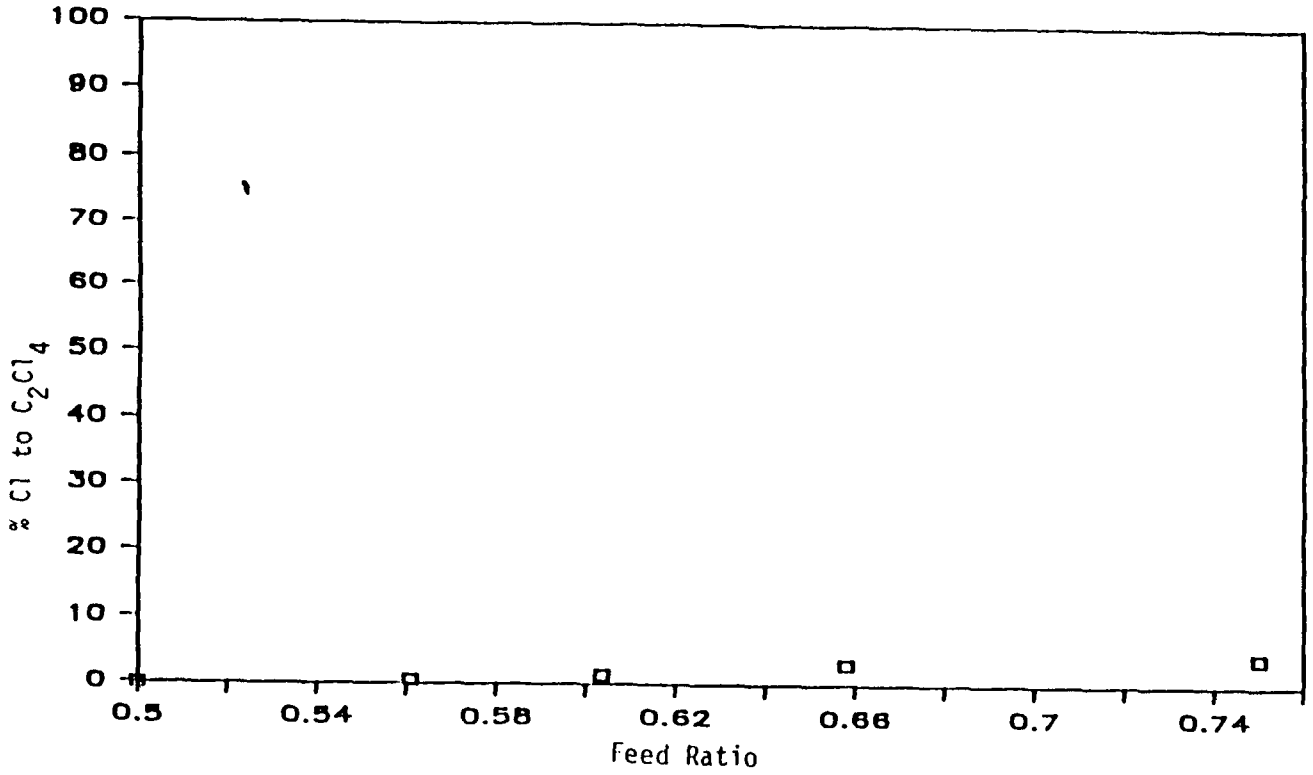

Figure 47. Selectivity to C_2Cl_4 versus Feed Ratio for Mixtures of CH_2Cl_2 and $CHCl_3$

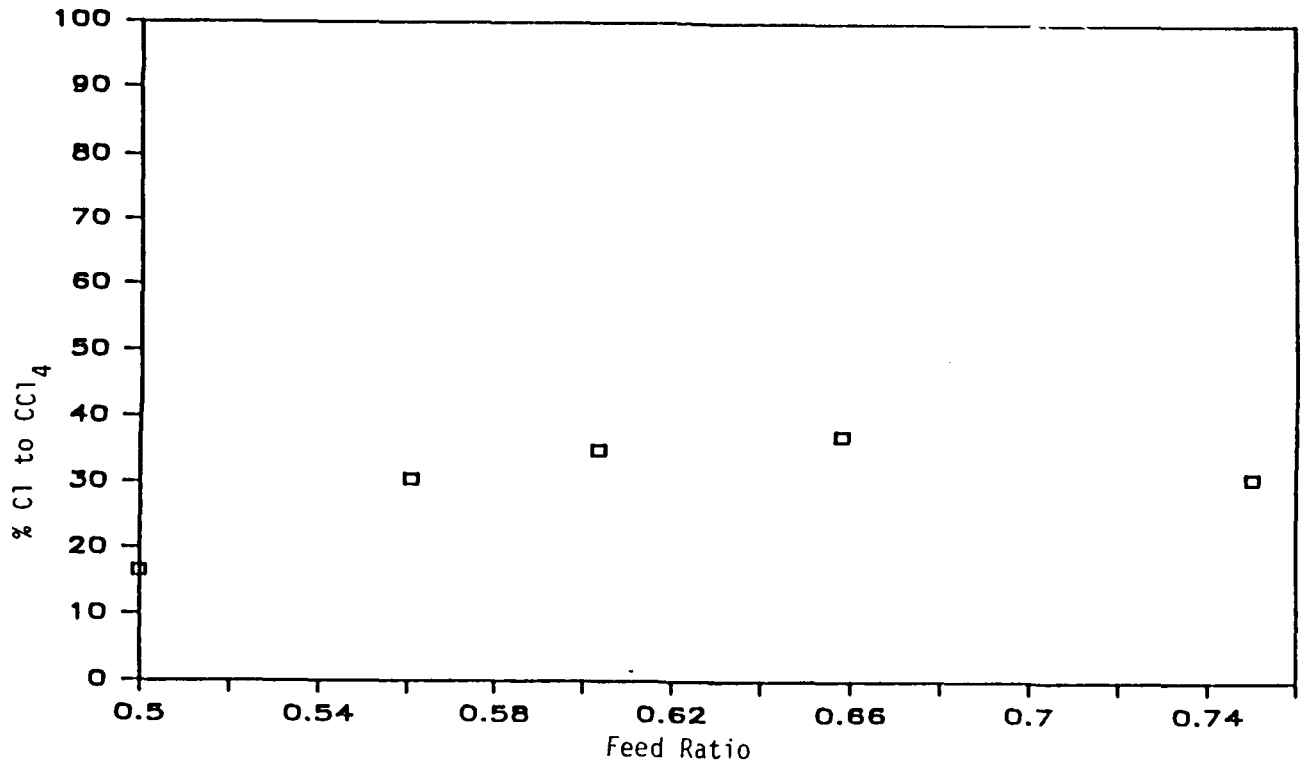

Figure 48. Selectivity to CCl_4 versus Feed Ratio for Mixtures of CH_2Cl_2 and $CHCl_3$

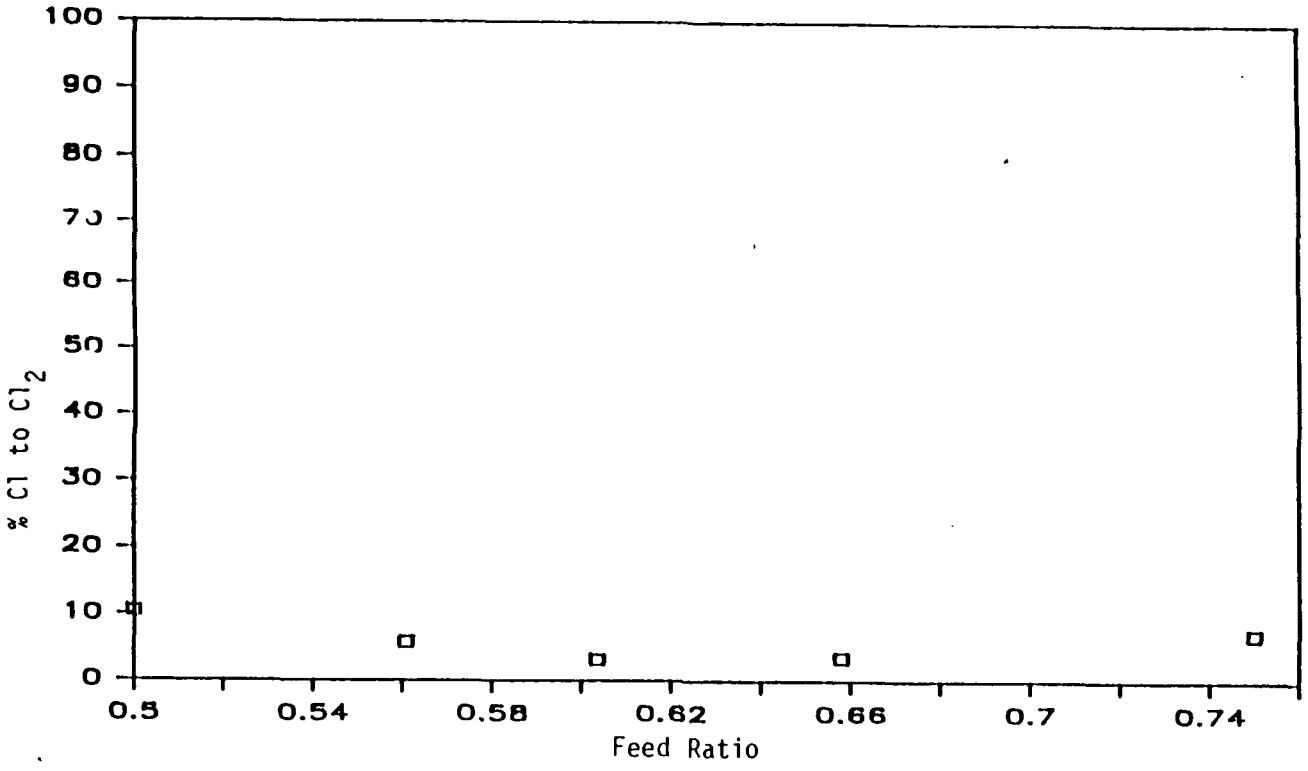

Figure 49. Selectivity to Cl_2 versus Feed Ratio for Mixtures of CH_2cl_2 and $CHCl_3$

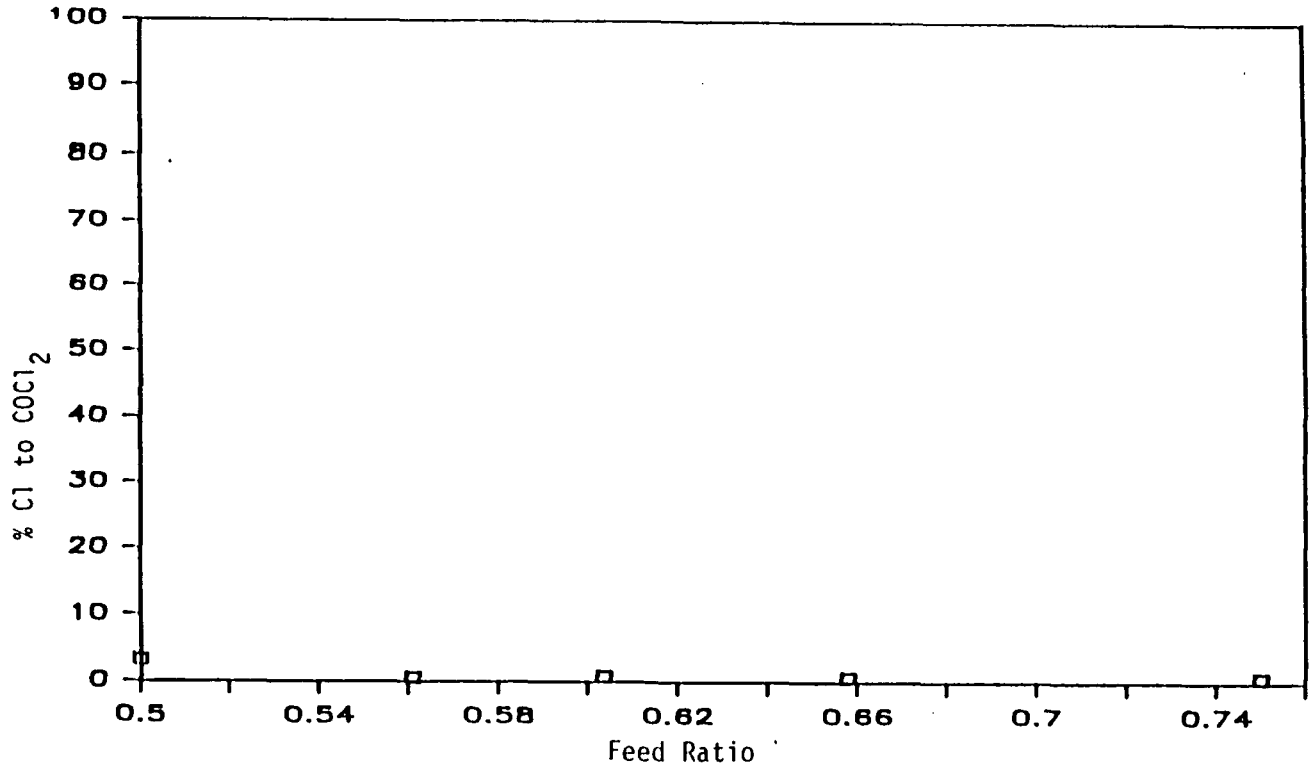

Figure 50. Selectivity to $COCl_2$ versus Feed Ratio for Mixtures of CH_2Cl_2 and $CHCl_3$

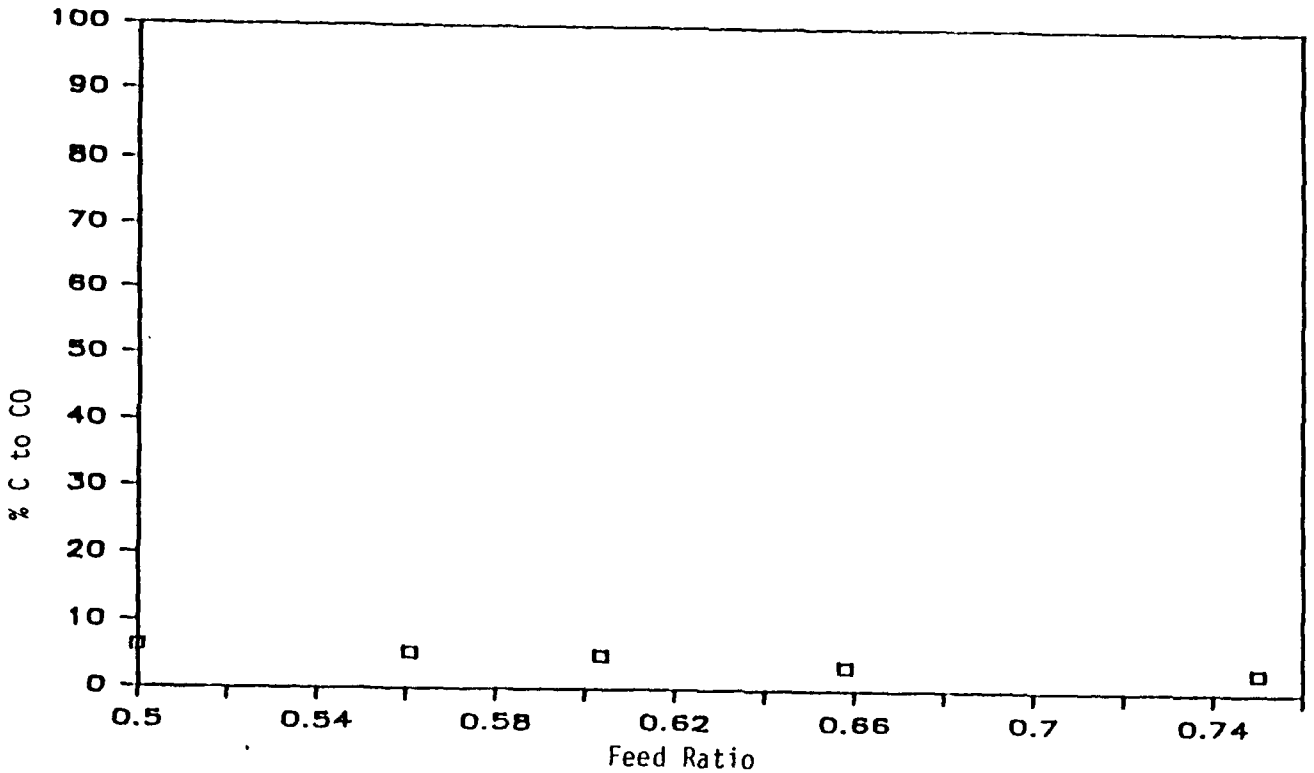

Figure 51. Selectivity to CO versus Feed Ratio for Mixtures of CH_2Cl_2 and $CHCl_3$

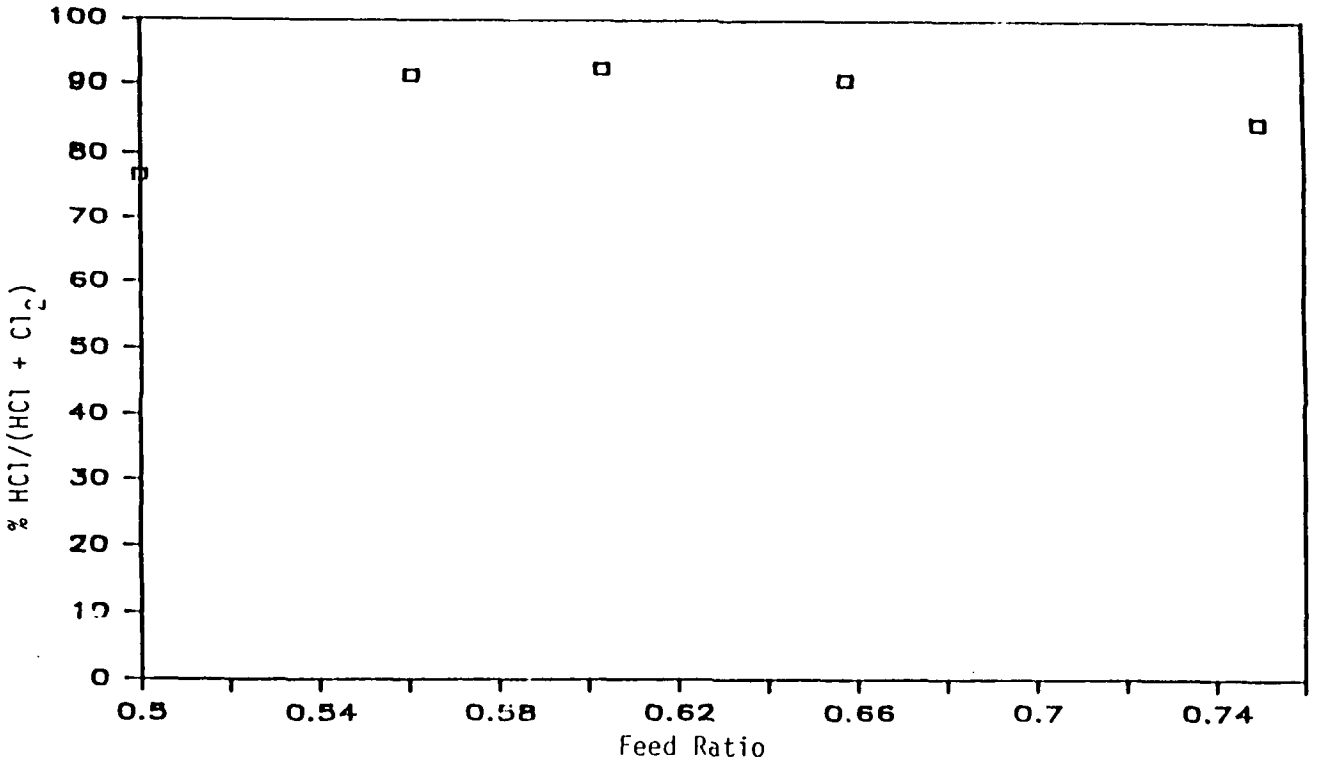

Figure 52. Relative Selectivity of HCl to HCl and Cl_2 Versus Feed Ratio for Mixtures of CH_2Cl_2 and $CHCl_3$

3. CH_2Cl_2 Trials with Varying Residence Times

Longer residence times are expected to show a greater tendency toward conversion of the feed to the products of equilibrium, which are CO_2, HCl, H_2O, and Cl_2. Results of experimental trials with CH_2Cl_2 feed at varying residence times will be discussed here.

Figure 53 shows the conversions for each run at different residence times, ranging from 0.2 seconds (18,000 h^{-1}) to 1.1 seconds (3,300 h^{-1}). Conversions increased from 31 percent to 94 percent over the range of residence times. The fact that conversion was still increasing even at the longest residence time indicated that equilibrium had not yet been reached.

Figure 54 shows the C–Cl formed/reacted ratio at each residence time. Since chlorinated hydrocarbons are not favored thermodynamically at equilibrium, it was expected that this ratio would decrease as residence time was increased, which agrees with Figure 54. Figure 55 shows that the amount of $CHCl_3$ decreased as residence time increased, as predicted. However, Figure 56 shows the amounts of CCl_4 in the product stream to be increasing slightly, reaching its highest point at the longest residence time. Since CCl_4 is the end product of methane chlorination, it appears that a series mechanism, in which CH_2Cl_2 is converted step–wise to $CHCl_3$ and then to CCl_4, is favored. If residence time were increased further, these products would be expected to eventually yield the products of equilibrium, and CCl_4 production would eventually peak and then decline.

Figure 57 shows HCl production for the various residence times. Since HCl is one of the products of equilibrium, it was expected that longer residence times should favor its formation. However, because of scatter in the data, no real trend can be observed.

Figure 58 shows Cl_2 production for the various residence times. Cl_2 is also an equilibrium product, therefore its production should increase as residence time increased. Data are also slightly scattered, but an upward trend for Cl_2 production as residence time was increased does appear to occur.

Figure 59 shows CO_2 production for the different residence times. CO_2 was the final, measured product of equilibrium from chlorinated hydrocarbon destruction. Its production also increased as residence time increased, as expected. At true equilibrium, CO_2 would be the only carbon–containing species observed. Its production increased from around 45 percent to nearly 70 percent of converted atomic

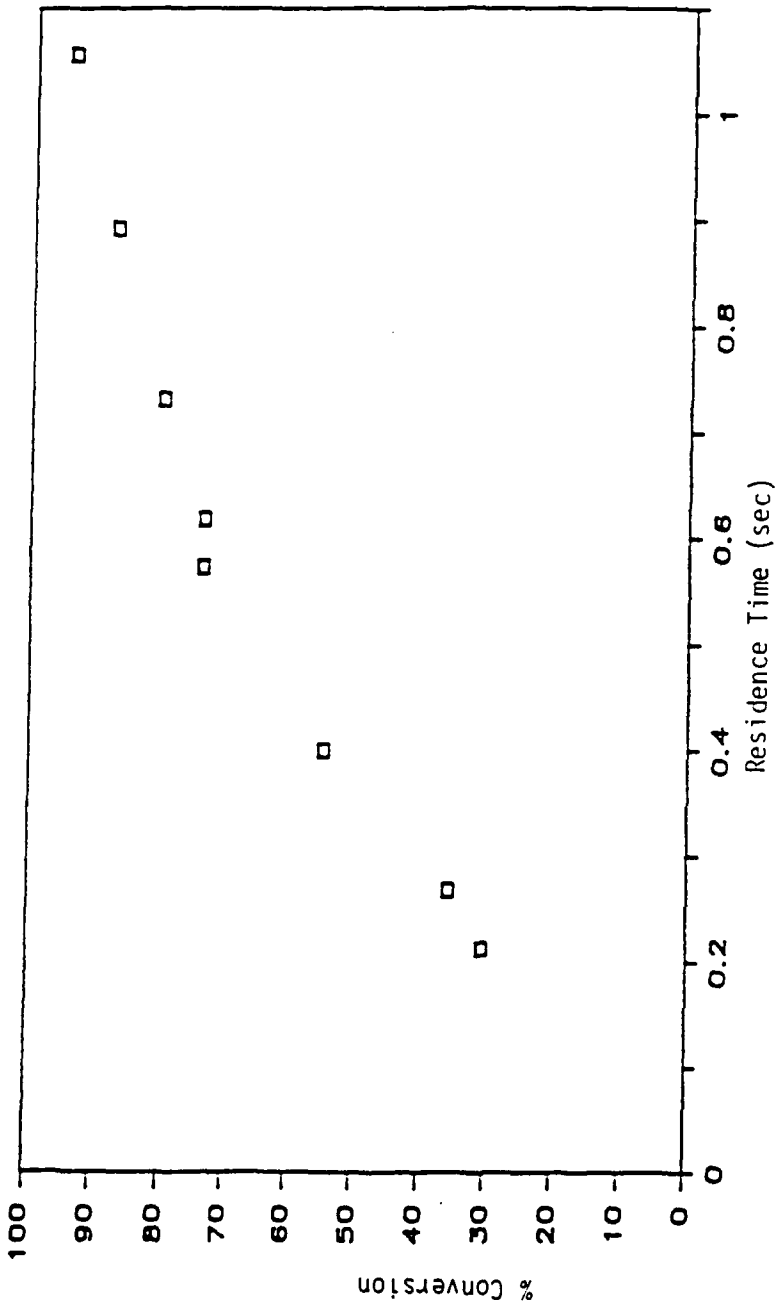

Figure 53. CH_2Cl_2 Conversion versus Residence Time

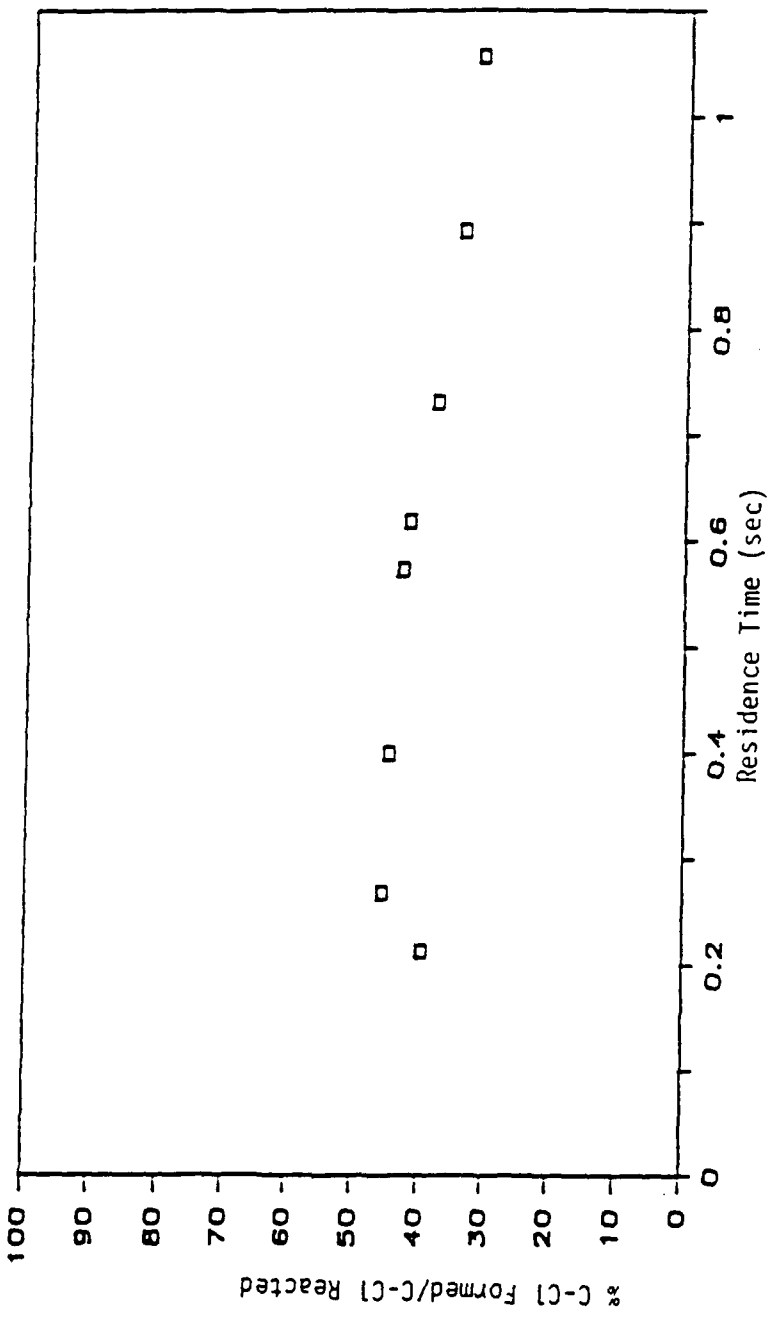

Figure 54. Chlorination Efficiency of CH_2Cl_2 versus Residence Time

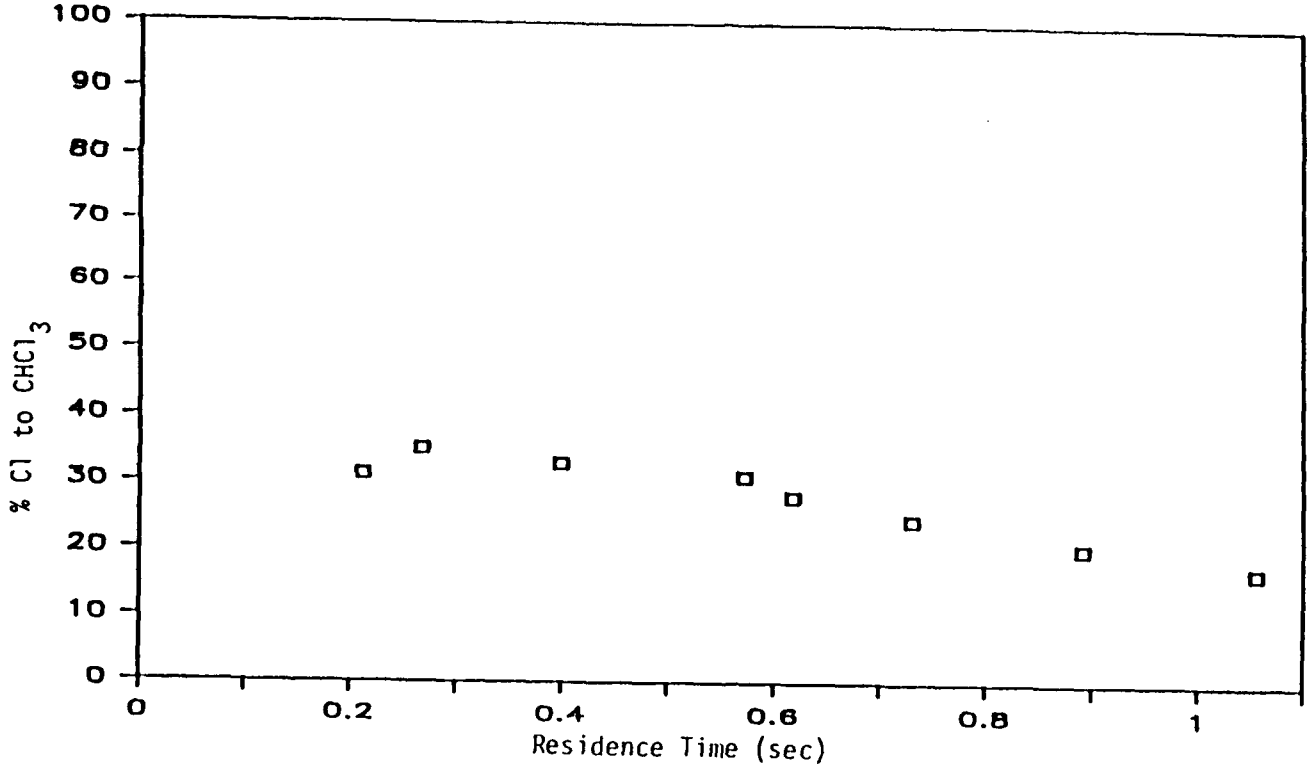

Figure 55. Selectivity of CH_2Cl_2 to $CHCl_3$ versus Residence Time

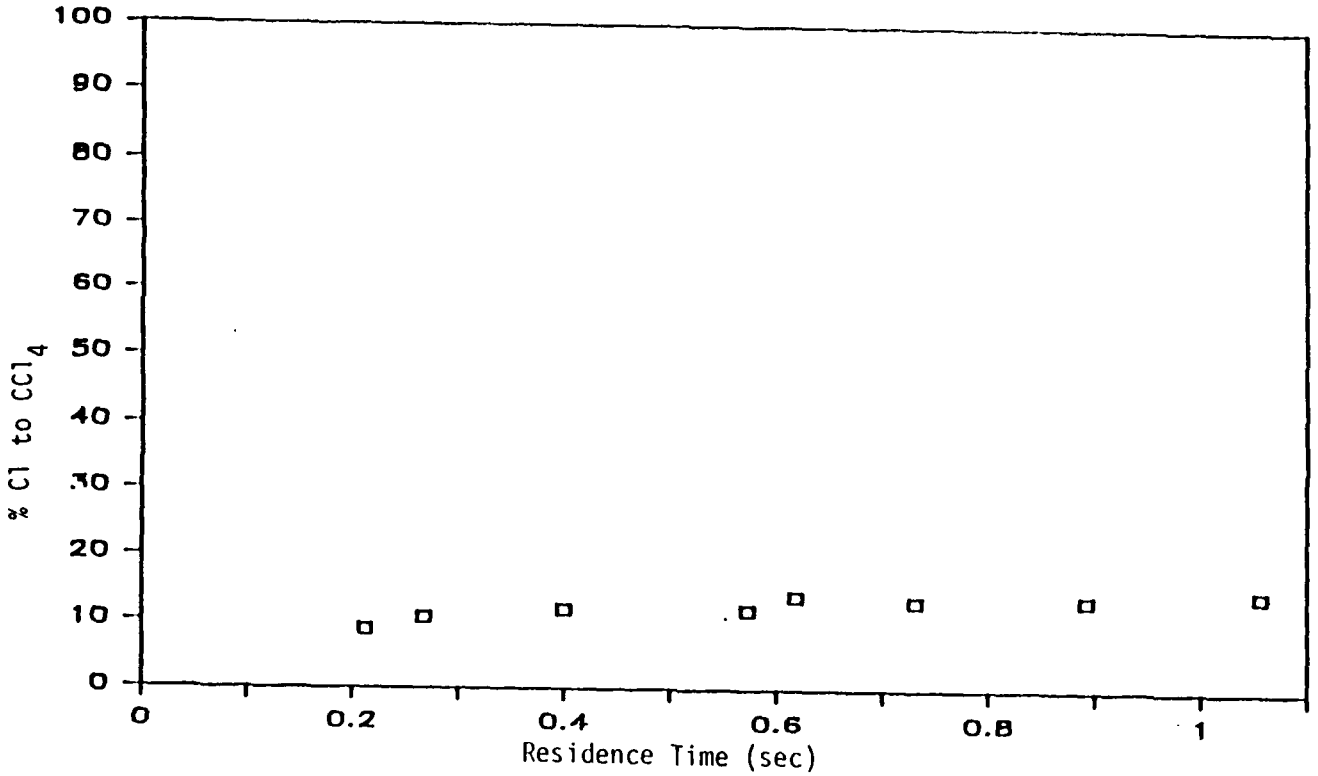

Figure 56. Selectivity of CH_2Cl_2 to CCl_4 versus Residence Time

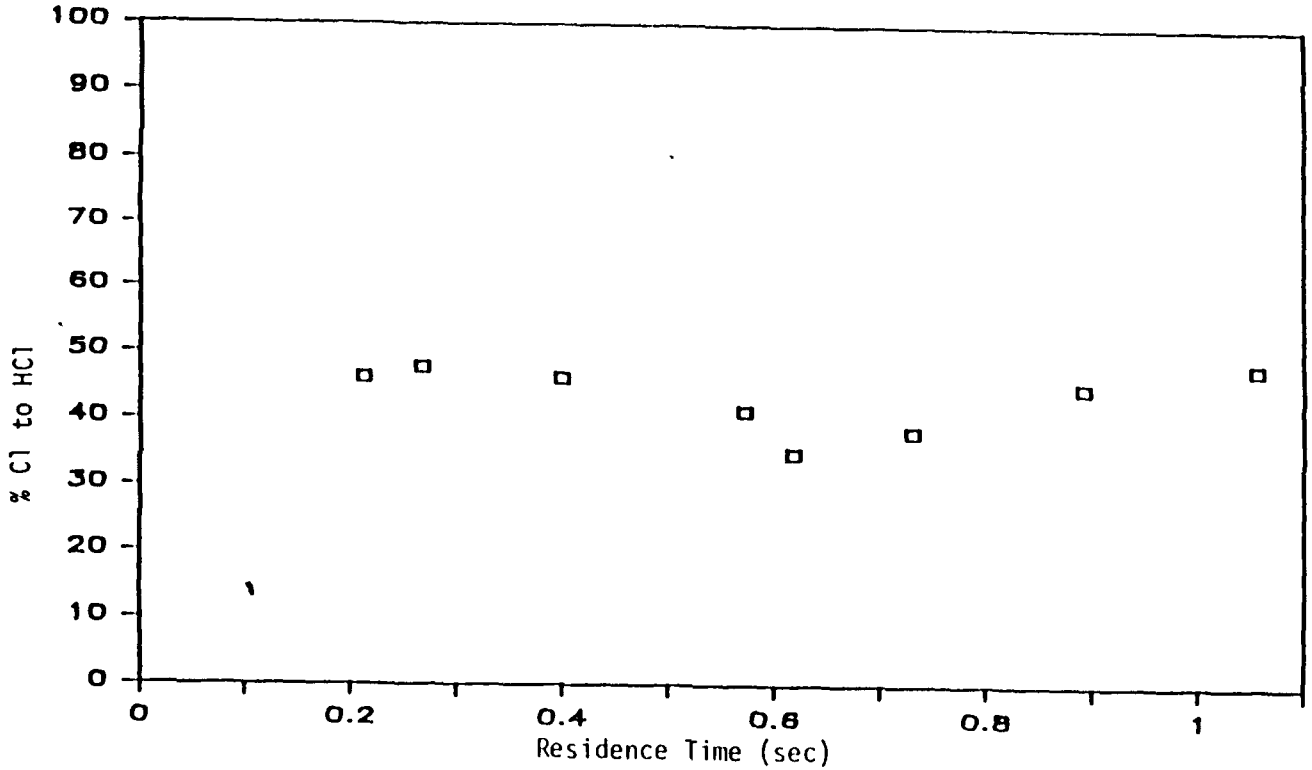

Figure 57. Selectivity of CH_2Cl_2 to HCl versus Residence Time

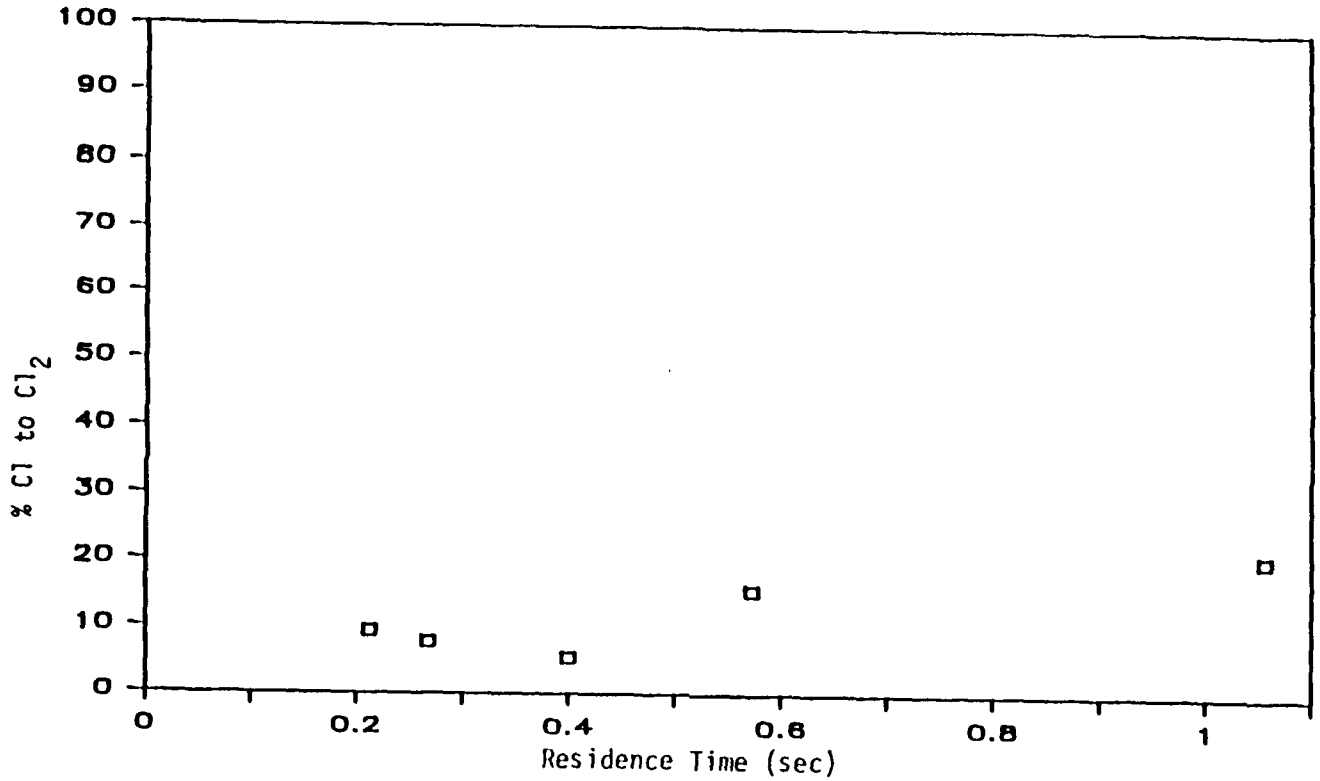

Figure 58. Selectivity of CH_2Cl_2 to Cl_2 versus Residence Time

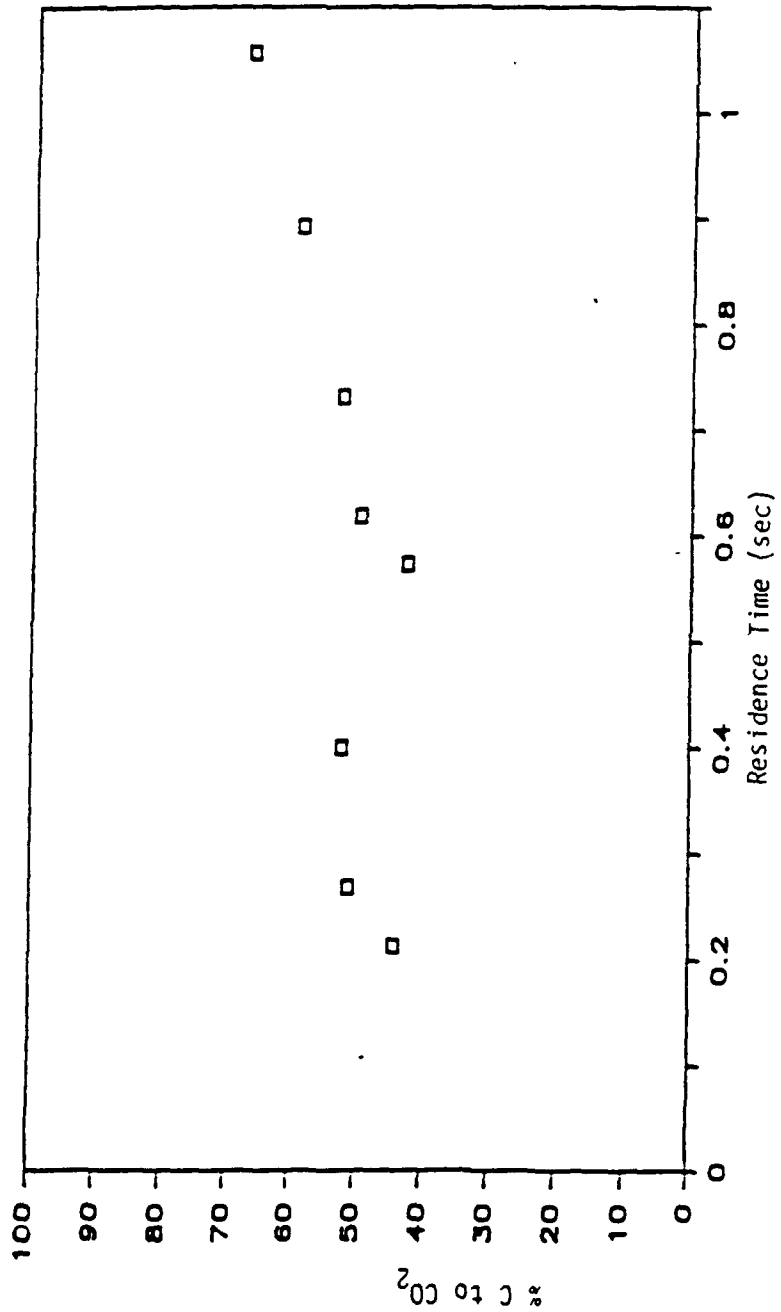

Figure 59. Selectivity of CH_2Cl_2 to CO_2 versus Residence Time

carbon, but the fact that it was still this low confirms that equilibrium conversion had not been closely approached.

Figure 60 shows $COCl_2$ production for different residence times. $COCl_2$ production is very low and it does appear to decrease with increased residence time. This is an expected result since $COCl_2$ is not favored as a product of equilibrium.

Figure 61 shows CO production for different residence times. As CO is not an equilibrium product, its amounts were expected to decrease as residence time increased. Its production does not appear to show any definitive trend, and any changes in its formation do not appear to be as dramatic as those of other non-equilibrium products (such as $CHCl_3$ and $COCl_2$).

4. Catalyst Stability Performance Trials

Throughout the course of the experimental trials, a total of 15 runs using only CH_2Cl_2 feed were made in order to check catalyst stability over time. These CH_2Cl_2 runs occurred periodically, allowing the data to be plotted versus catalyst on-stream time. The on-stream time is defined as the time during which a chlorinated hydrocarbon was used as a reactant. The catalyst was eventually used for nearly 80 hours of on-stream time during 57 individual experiments.

Figure 62 shows catalyst stability, based on CH_2Cl_2 conversion, versus the catalyst on-stream time. Generally, catalyst stability appeared satisfactory, with conversion averaging around 50 percent throughout the total on-stream time.

The points at about 8, 45, and 55 hours all show lower than normal conversion without an appreciable difference in selectivity from trials performed near them. All of these runs were first runs for that day. At the beginning of the day, the reactor was heated up with a nitrogen purge to obtain consistent catalyst characteristics. Air flow was begun 30 minutes before any reactant flowed through the reactor, but this may not have been sufficient time for the catalyst surface to become fully oxygenated, thus causing the low conversion levels observed in these runs.

The last three points on the graph indicate a slight decline in conversion. The last two points were taken after trials using HCl and Cl_2, which may have damaged the catalyst. Further, no significant changes in the appearance of the catalyst were noted. Other trends in terms of selectivity of the catalyst over time were fairly constant, indicating the overall stability of performance of the catalyst.

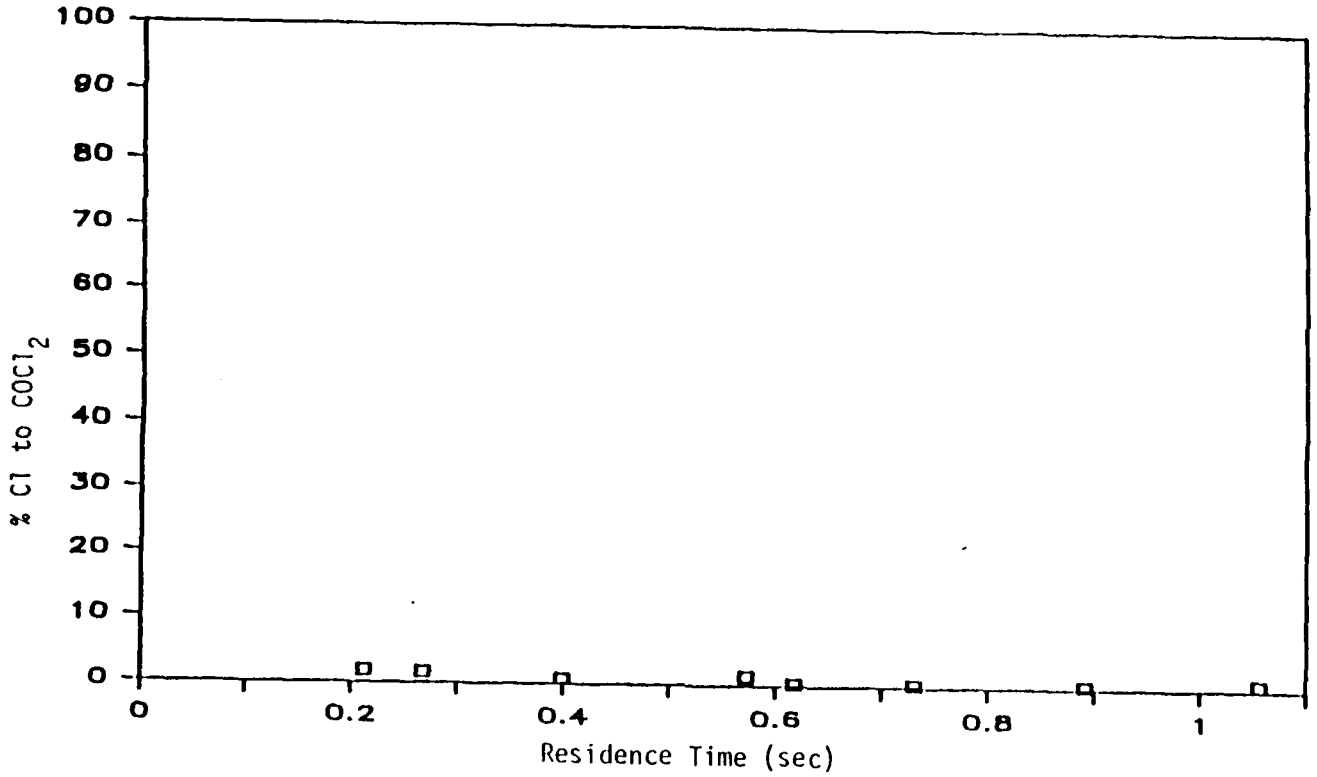

Figure 60. Selectivity of CH_2Cl_2 to $COCl_2$ versus Residence Time

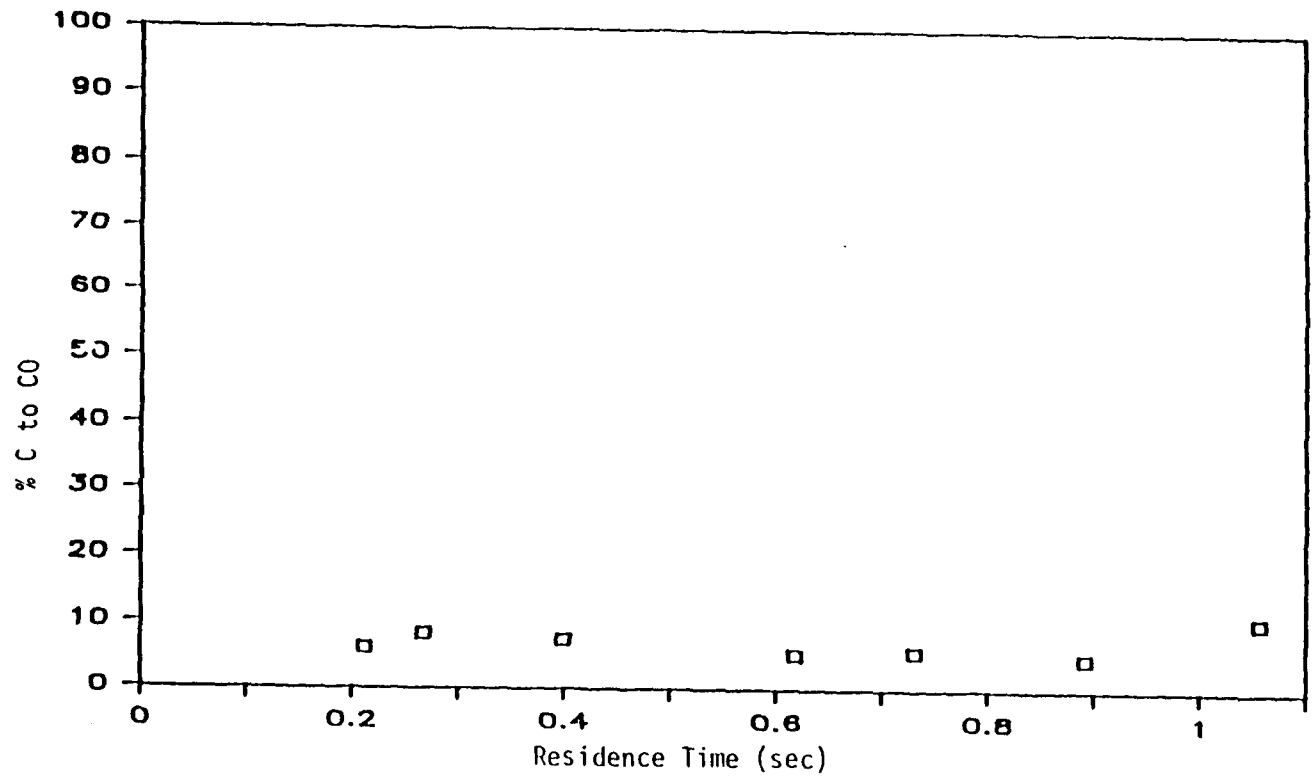

Figure 61. Selectivity of CH_2Cl_2 to CO versus Residence Time

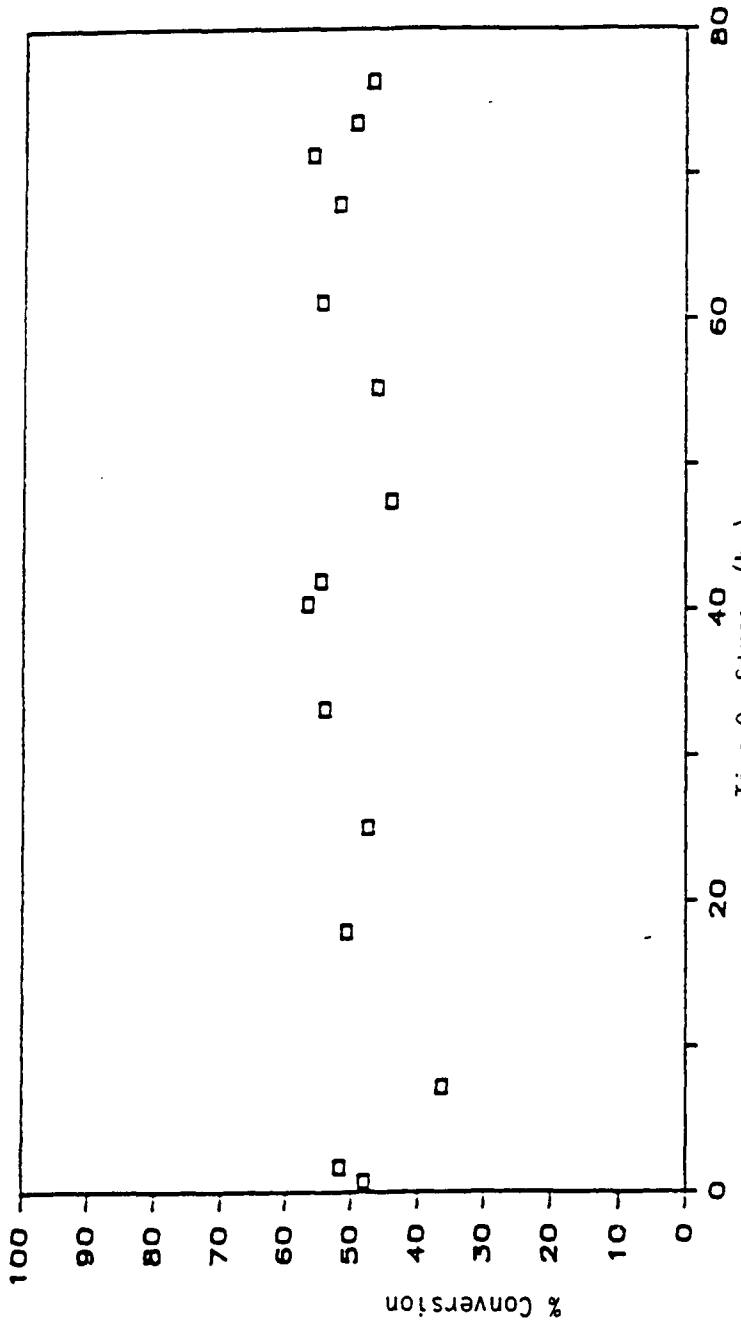

Figure 62. Conversion of CH_2Cl_2 versus Catalyst Time On-Stream

5. Lattice and Adsorbed Oxygen Experiments

The lattice oxygen experiment was performed by first allowing only nitrogen to flow through the reactor to drive off any adsorbed oxygen from the catalyst surface, as well as any oxygen present in the reaction system. After 30 minutes of nitrogen purge at 500°C, CH_2Cl_2 feed was started. Reactor samples were withdrawn at 2–4 minute intervals and injected into the GC/MS. The reaction temperature was maintained at 500°C throughout the experiment.

The lattice-plus-adsorbed oxygen experiment (hereafter called adsorbed oxygen experiment) was run in a similar manner except for one important difference. Instead of a nitrogen purge, air was run through the reactor for 30 minutes at 500°C. At that time, the air was shut off and nitrogen flow was started. After one minute, CH_2Cl_2 flow was begun followed by sampling for GC/MS analysis at 2–4 minute intervals.

For these experiments, instantaneous Cl_2 and CO concentrations could not measured because the sampling interval (10 minutes) would have been similar to the time required for MSA measurements, thus defeating the transient nature of the results. For the same reason, HCl analysis was not attempted. CCl_4 and $COCl_2$ were searched for, but not detected. The only products detected and measured in both experiments were CO_2 and $CHCl_3$.

Figure 63 shows the amount of CO_2 detected versus time for both the lattice and adsorbed oxygen experiments. No significant increase in CO_2 level occurred for the lattice oxygen experiment except at very short times where small amounts of adsorbed oxygen were probably available. In contrast, a relatively high amount of CO_2 was initially detected for the absorbed oxygen experiment, which then gradually decreased and leveled off after about 20 minutes.

Figure 64 shows the amount of $CHCl_3$ detected versus time for both the lattice oxygen and adsorbed oxygen experiments. A very slight increase in $CHCl_3$ was noted during the initial time on-stream for the lattice oxygen experiment, whereas a significantly larger increase in $CHCl_3$ for the adsorbed oxygen experiment was noted. $CHCl_3$ production reached its peak after 5 minutes for the lattice oxygen experiment, whereas the more prominent peak for the adsorbed oxygen experiment was noted after 10 minutes. The $CHCl_3$ formed in the adsorbed oxygen experiment leveled off at just over 20 minutes, in agreement with the CO_2 trend.

Because $CHCl_3$ cannot be formed from CH_2Cl_2 without HCl or Cl_2, it cannot form initially, as confirmed by these experiments. It took nearly 10 minutes for $CHCl_3$ to catch up

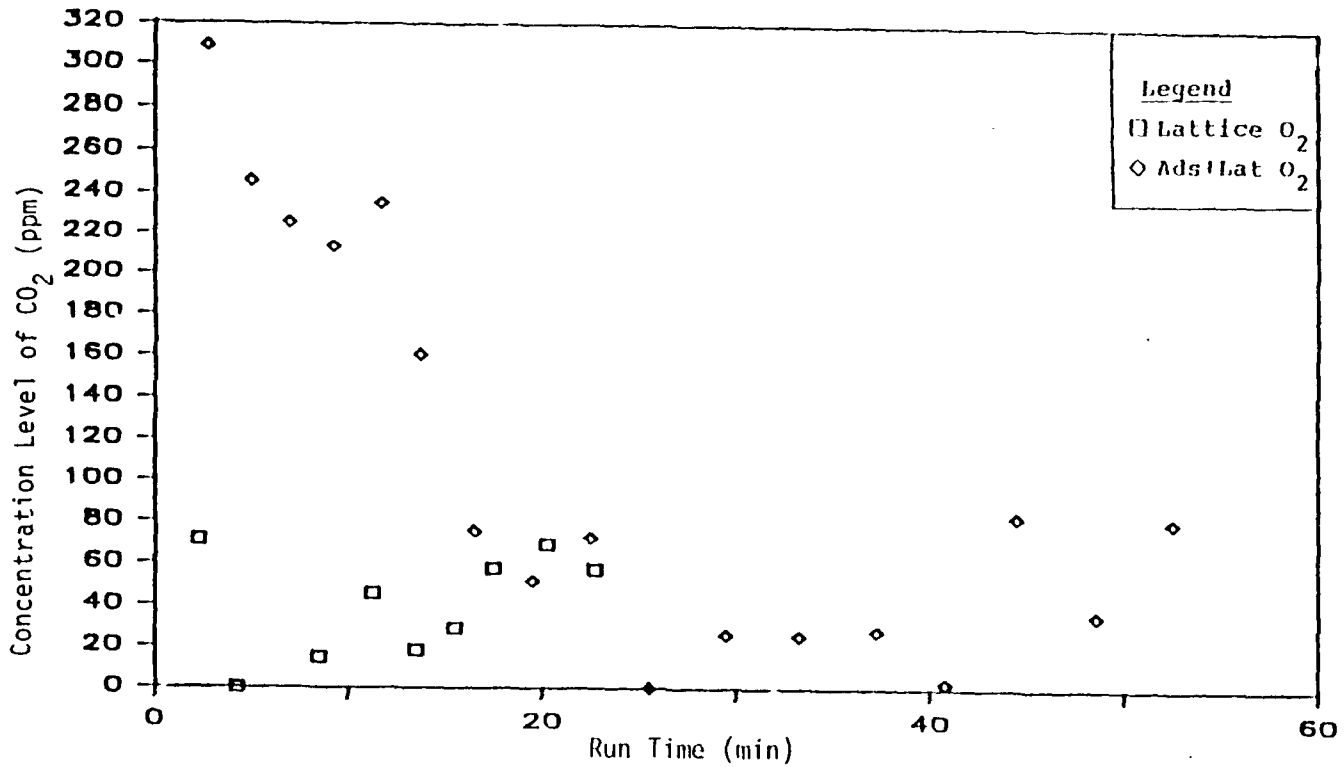

Figure 63. Concentration Level of CO_2 for the Destruction of CH_2Cl_2 using Lattice or Absorbed Oxygen

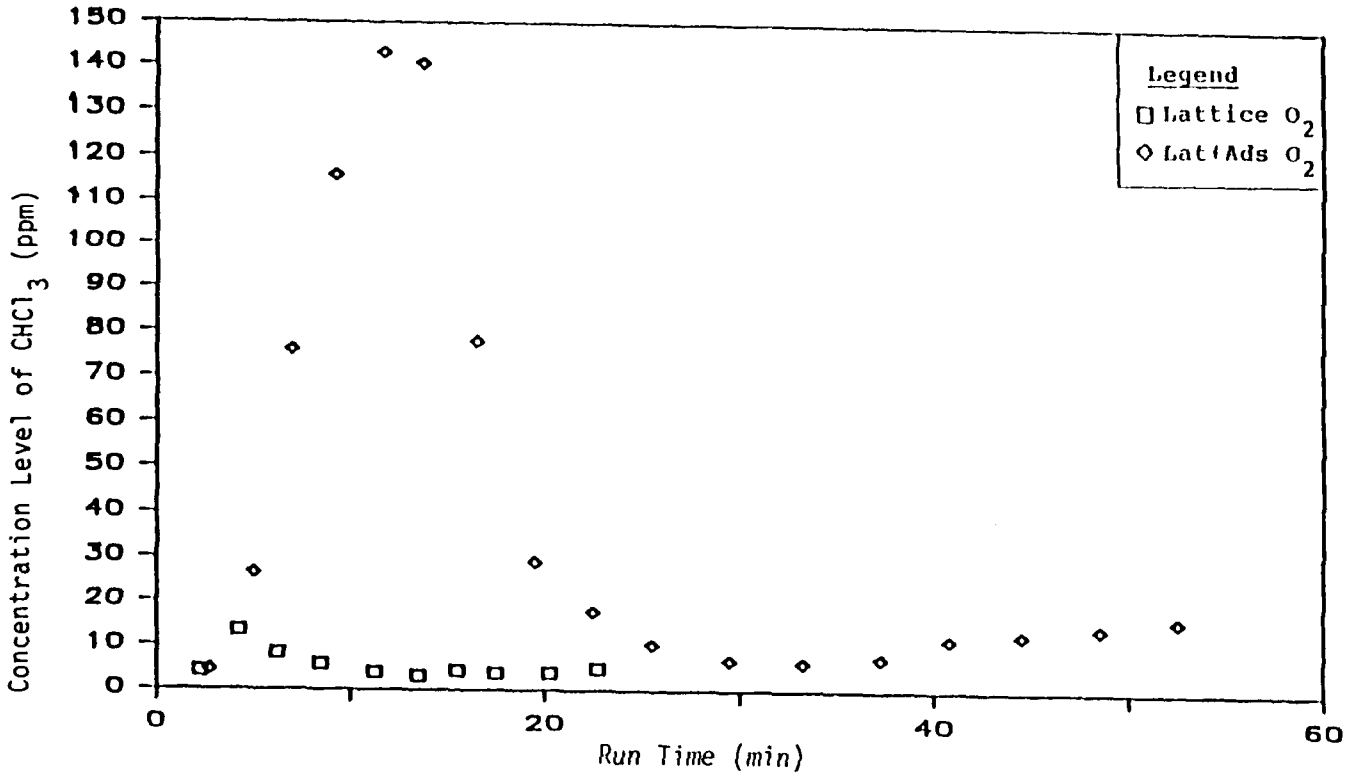

Figure 64. Concentration Level of $CHCl_3$ for the Destruction of CH_2Cl_2 using Lattice or Adsorbed Oxygen

with CO_2 formation, after which their relative formation ratio remained constant. By roughly integrating the areas of the $CHCl_3$ and CO_2 outputs for the adsorbed oxygen experiment, it was estimated that the relative formation in moles of CO_2 to $CHCl_3$ was about 1.6. This is fairly close to their relative formation in a normal steady-state run. This agrees with Spivey (Reference 45), who states that, even in oxygen deficient conditions, the selectivity of a catalyst toward a reactant will be unchanged as long as the reactions are the same order in O_2 concentration. The implications are that the individual reactions involved are probably zero order on O_2, since the large excess of O_2 available does not change significantly in concentration.

The initial rate at which $CHCl_3$ was formed for each experiment was very similar, although $CHCl_3$ formation for the lattice oxygen experiment tailed off very quickly. It appears that lattice and adsorbed oxygen act similarly for catalytic oxidation of CH_2Cl_2. However, adsorbed oxygen is present in greater quantities on the surface and is not as strongly bound as lattice oxygen, and therefore yields greater production of CO_2 and $CHCl_3$ (and probably other products as well). This indicates that KCl/V_2O_5 is acting as an electrophilic catalyst with adsorption of oxygen as a probable first step. Even though V_2O_5 is considered an n-type catalyst, Spivey (Reference 45) noted that V_2O_5 generally acts as an electrophilic catalyst in a manner similar to a p-type catalyst. Surface coverage by oxygen was estimated by assuming only adsorbed oxygen was reacted to form $CHCl_3$ and CO_2, in the stoichiometric ratio of 1 mole O_2 reacted/mole CO_2 formed, and 0.5 moles O_2 reacted/mole $CHCl_3$ formed. This allowed calculation of the moles of oxygen reacted. The fractional surface coverage could be calculated from this based on the surface area of the catalyst tube (as measured by BET) and the area of coverage by an oxygen molecule (determined to be 14.1 $A^{\circ 2}$ by Lowell and Shields (Reference 46)). The oxygen coverage value of 13 percent for the KCl/V_2O_5 catalyst determined by this method was much greater than the maximum value of 1.5 percent at 250°C as cited by Rey, et al. (Reference 47) for pure V_2O_5. This indicates that adsorption of oxygen into the KCl/V_2O_5 catalyst melt may be occurring, although this contradicts Shakirov, et al. (Reference 48), who found no observable chemisorbed oxygen in V_2O_5 melts involving KCl. The greater surface coverage may also suggest that the KCl/V_2O_5 sites are more strongly attractive to O_2 than pure V_2O_5.

After the adsorbed oxygen experiment, formation of a green deposit was noted on the cooled section of the Pyrex® tube at the outlet of the catalyst tube. Both VCl_2 and $VOCl_2$ are green and may well have been formed and partly volatilized during the experiment, considering that the percentage of

catalyst on the support dropped from an initial 0.75 percent to 0.68 percent after all of the experiments were completed. The formation of this substance may have been caused by Cl_2 adsorbing on the catalyst when it was in an oxygen starved condition. It is presumed that Cl_2 caused the deposit to form since prolonged exposure to HCl caused no noticeable deposit to form. Therefore, it seems that Cl_2 resistance for a catalyst (although not quantified in the present experiments) is as important a criterion to examine as HCl resistance. From a practical standpoint, it is important that the KCl/V_2O_5 catalyst never reach an oxygen starved condition to avoid loss of catalyst by chlorination and subsequent volatilization.

6. CH_2Cl_2 Trials with Added HCl or Cl_2

Results of experiments conducted using CH_2Cl_2 feed with addition of HCl or Cl_2 will be discussed. These experiments were conducted in order to help determine which of the suspected chlorinating agents were most prominent. Table 6 shows Selectivity and conversion data for the three types of feeds (CH_2Cl_2, CH_2Cl_2 with HCl, and CH_2Cl_2 with Cl_2).

TABLE 6. CONVERSION AND SELECTIVITY DATA FOR CH_2Cl_2 TRIALS WITH AND WITHOUT HCl OR Cl_2 ADDITION

Feed	% Conversion	Selectivities	
		% C to $CHCl_3$	% C to CCl_4
CH_2Cl_2	48.4	24.9	5.8
CH_2Cl_2/HCl	51.7	24.6	5.4
CH_2Cl_2/Cl_2	70.8	50.7	14.4

Feed	Selectivities		
	% Cl to HCl	% Cl to Cl_2	% C to $COCl_2$
CH_2Cl_2	40.6	0.5	0.8
CH_2Cl_2/HCl	34.8	0.2	0.8
CH_2Cl_2/Cl_2	25.8	0.8	0.7

Feed	Selectivities		
	% C to CO	% C to CO_2	% $CO_2/(CO_2+CO)$
CH_2Cl_2	4.4	44.8	90.9
CH_2Cl_2/HCl	5.6	47.0	89.3
CH_2Cl_2/Cl_2	2.4	31.2	92.9

The selectivities to $CHCl_3$, CCl_4, and $COCl_2$ are based on converted atomic carbon instead of converted atomic chlorine as reported in earlier sections. This is because HCl and Cl_2 have no influence on the carbon balance, allowing better observation of their effects on selectivity if that selectivity is based on converted atomic carbon.

Conversion data for the three different feeds show that addition of 1500 ppm of HCl has little influence on conversion of CH_2Cl_2, whereas addition of 2000 ppm Cl_2 increases conversion from 50 percent to 71 percent. The reasons for this apparent increase will be explained later in this section.

Selectivity to $CHCl_3$ did not change significantly when HCl was added to the feed, but selectivity to $CHCl_3$ doubled when Cl_2 was added to the feed. A similar trend is noted for CCl_4, which more than doubles in selectivity when Cl_2 is added, whereas little change is noted for HCl addition. These data show that formation of chlorinated hydrocarbons by direct chlorination with Cl_2 is highly favored, leading to higher conversion of CH_2Cl_2. It appears that the Cl_2 chlorinated the catalyst which led to enhanced chlorination of the feed.

Selectivity to HCl shows a contradiction. One would expect that selectivity to HCl would be highest for the HCl addition experiment. This is not shown by the data, since HCl selectivity was highest for CH_2Cl_2 alone. This may merely reflect an error in the measurement of HCl into the reactor. As mentioned earlier, HCl measurement is very prone to error since only one value is taken for each run.

Selectivities to Cl_2 were very low, probably because of a faulty pump used to pull vapor samples through the MSA tubes. This problem occurred very late in the experimental program and affects only the Cl_2 data reported in this part. Little difference in Cl_2 amounts was noted for all of the feeds, although the Cl_2 feed shows the highest amount of Cl_2 in the products.

Selectivity to $COCl_2$ does not appear to be influenced by the changes in HCl or Cl_2 content. Although more HCl would be expected to show a tendency toward formation of more $COCl_2$, the difference would be very little due to the unfavorable thermodynamics of $COCl_2$ formation.

Selectivities to CO do seem to have a slight dependence on feed composition. Production of CO is lowest for Cl_2 addition, primarily because more of the carbon is ending up in chlorinated hydrocarbons. Conversely, the run with HCl addition shows the highest amount of CO.

Selectivities to CO_2 are nearly equal for CH_2Cl_2 feed and CH_2Cl_2 with HCl feed. When Cl_2 was added to the feed, CO_2 production dropped sharply because more of the available carbon was being used for the production of chlorinated hydrocarbons.

Selectivities of CO_2 versus CO_2 plus CO are all fairly similar, at around 90 percent, although the run with HCl addition is slightly lower. As found by Bakshi, et al. (Reference 49), HCl inhibited the conversion of CO to CO_2 on a $KCl/CuCl_2$ catalyst. Chang et al. (Reference 43) reported Cl_2 as an inhibitor of CO oxidation. As seen in Table 6, the data for relative selectivity of CO_2 to CO_2 plus CO do not appear to support the claims of either Bakshi or Chang. However, Bakshi and Chang both used $KCl/CuCl_2$ catalysts in their studies which suggests that the differences between their results and the data in Table 6 may be related to differences between their catalysts and the KCl/V_2O_5 catalyst used for this study.

SECTION VI

CONCLUSIONS

Development of viable catalysts for destruction of chlorinated hydrocarbons requires that three major criteria be met: high conversion at moderate temperature, selective conversion to benign products, and extended lifetime for the catalyst and support at reactor conditions.

It is now understood that at least four primary reaction paths are involved in the heterogeneous decomposition of chlorinated hydrocarbons, when air and water vapor are present:

1. Deep oxidation to form desirable products such as CO_2, HCl, Cl_2 and H_2O
2. Oxychlorination to form undesirable higher chlorinated products
3. Direct chlorination to form undesirable higher chlorinated products
4. The Deacon process whereby HCl and O_2 are reversibly converted to Cl_2 and H_2O

It is doubtful that any catalyst can be developed which operates totally in a deep oxidation mode for the variety of chlorinated organics in question. Nevertheless, this research has demonstrated order of magnitude performance differences in product selectivities, implying that optimization of catalyst and support is extremely worthwhile. It is concluded that both Cr_2O_3 and KCl/V_2O_5 are primarily deep oxidation systems, remaining primarily in the oxide form at reactor conditions. Conversely KCl/CuO shows more oxychlorination and direct chlorination behavior while remaining in the chloride form at reactor conditions.

Mechanisms for these conversions are not always predictable, as may be concluded from the unexpected formation of significant C_2-chlorinated products during $CHCl_3$ oxidation. In contrast, no detectable C_2-chlorinated products were found when CH_2Cl_2 or CCl_4 were fed to the reactor. Additional experimental work is necessary to understand and control these selectivity problems, as well as the process of deactivation.

For all three primary catalysts, addition of water vapor to the feed generally caused a moderate loss (10–40 percent) in activity, but also produced improvement in the fraction of deep oxidation products obtained. These results are in line with theoretical predictions.

Catalytic oxidation of chlorinated VOC mixtures was briefly studied using the $CHCl_3/CH_2Cl_2$ system. From the results it was concluded that competitive chemisorption of reactants can significantly alter individual VOC activities. It was also concluded that chemisorption of different VOCs on adjacent surface sites can bring about changes in catalyst selectivity, including formation of addition-type products.

RFERENCES

1. Senser, D.W. and Cundy, V.A., "The Combustion Characteristics of Selected Chlorinated Methanes in a Flat Flame Environment," Chem. Eng. Commun., vol 40, pp. 153–168, 1986.

2. Senser, D.W., Cundy, V.A. and Morse, J.S., "Chemical Species and Temperature Profiles of Laminar Dichloromethane–Methane–Air Flames. 1. Variation of Chlorine/Hydrogen Loading," Combust. Sci. and Tech., vol 51, pp. 209–233, 1987.

3. Senser, D.W., Cundy, V.A. and Morse, J.S., "Practical Incinerator Implications from a Fundamental Flat Flame Study of Dichloromethane Combustion," J. Air Poll. Control Assoc., vol 36(7), pp. 824–828, July 1986.

4. Gupta, A.K., "Combustion of Chlorinated Hydrocarbons," Chem. Eng. Commun., vol 41, pp. 1–21, 1986.

5. Bose, D. and Senkan, S.M., "On the Combustion of Chlorinated Hydrocarbons. 1. Trichloroethylene," Combust. Sci. and Tech., vol 35, pp. 187–202, 1983.

6. Chang, W.D., Karra, S.B. and Senkan, S.M., "A Detailed Mechanism for the High Temperature Oxidation of C_2HCl_3," Combust. Sci. and Tech., vol 49, pp. 107–121, 1986.

7. Senkan, S.M., "On the Combustion of Chlorinated Hydrocarbons: II. Detailed Chemical Kinetic Modeling of the Intermediate Zone of the Two Stage Trichloroethylene–Oxygen–Nitrogen Flames," Combust. Sci. and Tech., vol 38(3–4), pp. 197–204, 14 March 1988.

8. Musick, J.K. and Williams, F.W., "Catalytic Decomposition of Halogenated Hydrocarbons Over Hopcalite Catalyst," Ind. Eng. Chem., Prod. Res. Develop., vol 13(3), pp. 175–179, 1974.

9. Bond, G.C. and Sadeghi, N., "Catalysed Destruction of Chlorinated Hydrocarbons," J. Appl. Chem. Biotech., vol 25, pp. 241–248, 1975.

10. Pope, D., Walker, D.S. and Moss, R.L., "Oxidation of Trace Organics on Co_3O_4 Catalysts," Atm. Environ., vol 10, pp. 951–956, 1976.

11. Pope, D., Walker, D.S. and Moss, R.L., "Evaluation of Platinum–Honeycomb Catalysts for the Destuctive Oxidation of Low Concentrations of Odorous Compounds in Air," Atm. Environ. , vol 12, pp. 1921–1927, 1978.

12. Johnston, E.L., "Low Temperature Catalytic Oxidation of Chlorinated Compounds to Recover Chlorine Values Using Chromium-Impregnated Supported Catalysts," U.S. Patent No. 3,989,807, 2 August 1976.

13. Lavanish, J.M. and Sare, E.J., "Catalytic Oxidation of C_2-C_4 Halogenated Hydrocarbons," U.S. Patent No. 4,039,623, 2 August 1977.

14. Sare, E.J. and Lavanish, J.M., "Catalytic Oxidation of C_2-C_4 Halogenated Hydrocarbons," U. S. Patent No. 4,065,543, 27 December 1977.

15. Manning, M.P., "Fluid Bed Catalytic Oxidation: An Underdeveloped Hazardous Waste Disposal Technology," Haz. Waste, vol 1(1), pp. 41-65, January 1984.

16. Weldon, J. and Senkan, S.M., "Catalytic Oxidation of CH_3Cl by Cr_2O_3," Combust. Sci. and Tech., vol 47, pp. 229-237, 1986.

17. Senser, D.W., Morse, J.S. and Cundy, V.A., "PICs - A Consequence of Stable Intermediate Formation During Hazardous Waste Incineration (Dichloromethane)," Haz. Waste and Haz. Materials, vol 2(4), pp. 473-486, 1985.

18. Kenney, C.N., "Molten Salt Catalysis of Gas Reactions," Catal. Rev.-Sci. Eng., vol 11(2), pp. 197-224, February 1975.

19. Villadsen, J. and Livbjerg, H., "Supported Liquid-Phase Catalysts," Catal. Rev.-Sci. Eng., vol 17(2), pp. 203-272 1978.

20. Zipelli, C., Bart, J.C.J., Petrini, G., Galvagno, S. and Cimino, C., "Study of $CuCl_2$ Supported on SiO_2 and Al_2O_3," Z. Anorg. Allg. Chem., vol 502, pp. 199-208, 1983.

21. Aglulin, A.G., Bakshi, Yu.M. and Gel'bshtein, A.I., "Kinetics of the Reaction of the Oxidational Chlorination of Methane with its Catalysis by the System $CuCl_2$-KCl-Carrier," Kinetica i Kataliz, vol 17(3), pp. 670-676, May-June 1976.

22. Bakshi, Yu.M., Aglulin, A.G., Dmitrieva, M.D. and Gel'bshtein, A.I., "Kinetics of the Oxychlorination of Chloromethanes and their Destructive Oxidation on a Supported $CuCl_2$-KCl Catalyst," Kinetica i Kataliz, vol 18(6), pp. 1472-1480, November-December 1977.

23. Muganlinskii, F.F., Guseinzade, E.M. and Mamedov, B.B., "Some Features in the Oxychlorination Process of Chlorohydrocarbons," Oxidation Communications, vol 7(3-4), pp. 235-248, March-April 1984.

24. Stull, D.R. and Prophet, H., JANAF Thermochemical Tables, 2nd ed., NSRDSK-NBS 37, U.S. Government Printing Office, Washington, D.C., 1971.

25. Smith, J.M. and Van Ness, H.C., Introduction to Chemical Engineering Thermodynamics, 3rd ed., pp. 376-438, McGraw-Hill, New York, 1975.

26. Yang, M., Karra, S.B. and Senkan S.M. "Equilibrium Analysis of Combustion/Incineration," Haz. Waste and Haz. Materials, vol 4(1), pp. 55-68, January 1987.

27. Golodets, G.I., Heterogeneous Catalytic Reactions Involving Molecular Oxygen, vol 15, pp. 388-395, Elsevier Sc. Publ., Amsterdam, 1983.

28. Shakhovtseva, G.A., Vasil'eva, N.B., Avetisov, A.K. and Gel'bshtein, A.I., "Kinetics and Mechanisms of the Catalytic Oxidation of Hydrogen Chloride," Kinetika i Kataliz, vol 11(6), pp. 1469-1475, November-December 1970.

29. Shakhovtseva, G.A., Vasil'eva, N.B., Avetisov, A.K. and Gel'bshtein, A.I., "Kinetics and Mechanisms of the Oxidation of Hydrogen Chloride II," Kinetika i Kataliz, vol 12(1), pp. 244-247, January-February 1971.

30. Solomonik, I.G., Kurlyandskaya, I.I., Danyushevskii, V.Ya. and Yakerson, V.I., "Catalytic Systems for Oxidative Chlorination of Hydrocarbons. Communication 1. Thermal Analysis of Copper Chloride Salts and the Catalysts Based on Them," Izv. Acad. Nauk SSSR, Ser. Khim, vol 10, pp. 2175-2180, October 1984.

31. Solomonik, I.G., Kurlyandskaya, I.I., Danyushevskii, V.Ya. and Yakerson, V.I., "Catalytic Systems for Oxidative Chlorination of Hydrocarbons. Communication 2. Study of the Reaction in the Copper-Containing Salt Component-Carrier System by the Method of Thermal Analysis," Izv. Acad. Nauk SSSR, Ser. Khim., vol 10, pp. 2180-2185, October 1984.

32. International Critical Tables, vol 3, pp. 208, McGraw-Hill, New York, 1928.

33. Fontana, C.M., Gordin, E., Kidder, G.A. and Meredith, C.S., "Chlorination of Methane With Copper Chloride Melts. Ternary System Cuprous Chloride–Cupric Chloride–Potassium Chloride and Its Equilibrium Chlorine Pressures," Ind. Eng. Chem., vol 4(2), pp. 363–368, February 1952.

34. Balzhiser, R.E., Samuels, M.R. and Eliassen, J.D, Chemical Engineering Thermodynamics, pp. 434–443, Prentice–Hall Inc., New Jersey, 1972.

35. Sachtler, W.M.H. and Helle, J.N., "Thermodynamic Investigation of Deacon–type Catalysts," Chemisorption and Catalysis, Elsevier Sci. Publ., London, 1970.

36. Perry, R.H. and Chilton, C.H., Chemical Engineer's Handbook, 5th ed, pp. 3/62–63, McGraw–Hill Kogakusha Ltd., Tokyo, 1973.

37. Saraf, A., "Thermal Stability and Activity of Mixed Copper/KCl Catalysts", M.S. Thesis, University of Akron, January 1989.

38. Johnson, A.J., Meyer, F.G., Hunter, D.I., and Lombardi, E.F. Incineration of PCBs Using a Fluidized Bed Incinerator, RFP—3271, Rockwell International, Golden, CO, September 1981.

39. Hunter, W.K., Hardison, L.C. and Dowd, E.J., "Catalytic Fume Incineration," U.S. Patent No. 4,330,513, 18 May 1982.

40. Fergusson, J.E., "Halide Chemistry of Chromium, Molybdenum and Tungsten" Halogen Chemistry, vol 3, Academic Press, New York, 1967.

41. Paraskevov, V.G., Pimenov, I.F., Treger, Yu.A. and Dasaeva, G.S., "Kinetics and Mechanisms of the Oxychlorination of Trichloroethylene," Kinetika i Kataliz, vol 24(4), pp. 1007– 1009, July–August 1983.

42. Werner, J., Kirk–Othmer Encyclopedia of Chemical Technol., vol 3, pp. 773–774, Interscience Publishers, New York, 1949.

43. Chang, W.D., Karra, S.B. and Senkan, S.M., "Molecular Beam Mass Spectroscopic Study of Trichloroethylene Flames," Environ. Sci. Tech., vol 20(12), pp. 1243–1248, December 1986.

44. Ashton, D.P. and Ryan, T.A., "The Catalytic Oxychlorination of Carbon Monoxide to Phosgene," Applied Catalysis, vol 12, pp. 263–282, 1984.

45. Spivey, J.J., "Complete Catalytic Oxidation of Volatile Organics," I&EC Research, vol 26, pp. 2165–2180, 1987.

46. Lowell, S. and Shields, J.E., Powder Surface Area and Porosity, 2nd ed., pp. 43, Chapman and Hall, New York, 1984.

47. Rey, L., Gambaro, L.A. and Thomas, H.J., "Oxygen Chemisorption of V_2O_5," J. of Catalysis, vol 87, pp. 520–523, 1984.

48. Shakirov, I.V., Chekryshkin, Yu.S. and Abanin, V.I., "Correlation Between the Chemical Composition of V_2O_5–Based Melts, The Desorption of Oxygen, and the Catalytic Activity," Kinetika i Kataliz, vol 26(2), pp. 356–362, March–April 1985.

49. Bakshi, P.S., Ackerman, D.G., and Scinta, L.L., Destruction and Disposal of PCBs by Thermal and Nonthermal Methods, Noyes Data Corporation, Park Ridge, New Jersey, 1983.

(The reverse of this page is blank.)